

**Aus dem Institut für Virologie
des Fachbereichs Veterinärmedizin
der Freien Universität Berlin**

**Novel insights into the roles of phospholipids and small GTPases in
equine herpesvirus molecular pathogenesis**

**Inaugural-Dissertation
zur Erlangung des Grades eines
PhD of Biomedical Sciences
an der
Freien Universität Berlin**

**vorgelegt von
Oleksandr Kolyvushko
Tierarzt aus Tscherkassy, Ukraine**

**Berlin 2021
Journal-Nr.: 4264**

Gedruckt mit Genehmigung des Fachbereichs Veterinärmedizin
der Freien Universität Berlin

Dekan: Univ.-Prof. Dr. Uwe Rösler

Erster Gutachter: Univ.-Prof. Dr. Klaus Osterrieder

Zweiter Gutachter: PD Dr. Thorsten Wolff

Dritter Gutachter: PD Dr. Michael Veit

Deskriptoren (nach CAB-Thesaurus): phospholipids, equid herpesviruses, interaction,
liposomes, pathogenesis, flow cytometry, immunofluorescence

Tag der Promotion: 24.08.2021

Table of contents

Contents

List of Figures.....	5
Abbreviations.....	6
Chapter 1	1
Introduction	1
1.1 Overview of virus entry.....	1
1.2 Taxonomy of Herpesviruses.....	3
1.3 Binding and signaling	3
1.4 Small GTPases	4
1.5 Lipids.....	7
1.6 Aims of the study.....	8
1.7 References.....	9
Chapter 2	16
Differentially-Charged Liposomes Interact with Alphaherpesviruses and Interfere with Virus Entry	16
2.1 Abstract.....	16
2.2 Importance	17
2.3 Introduction	17
2.4 Results	17
2.4.1 DOTAP and PS liposomes inhibit viral infection	17
2.4.2 Interaction of viral particles with phospholipids.	18
2.5 Discussion.....	19
2.6 Materials and Methods	21
2.7 Author Contributions.....	23
2.8 Funding	23
2.9 Acknowledgments	23
2.10 Conflicts of Interest.....	23
2.11 References.....	24
Chapter 3	25
Equine alphaherpesviruses require activation of the small GTPases Rac1 and Cdc42 for intracellular transport.....	25
3.1 Abstract.....	25
3.2 Introduction	26
3.3 Materials and Methods	26
3.3.1 Cells and Viruses	26
3.3.2 Inhibitors	27
3.3.3 Cytotoxicity assay.....	27
3.3.4 Flow Cytometry	27

3.3.5	Plaque assay.....	28
3.3.6	Virus localization and immunofluorescence	28
3.3.7	Ratiometric fluorescence resonance energy transfer (FRET)	28
3.3.8	Immunoblotting.....	29
3.3.9	Cell-to-cell fusion.....	29
3.3.10	Statistical Analysis.....	29
3.4	Results	31
3.4.1	Cdc42 and Rac1 Inhibitors Reduce EHV-1 and EHV-4 Infection	31
3.4.2	Small GTPases Facilitate Infection and Cell-to-Cell Spread	32
3.4.3	EHV-1 Activates Small GTPases Rac1 and Cdc42	33
3.4.4	Tracking of Virus Transport in Cells.....	34
3.4.5	Rac1 and Cdc42 Activation Is Required for EHV-1-Induced Tubulin Acetylation	36
3.4.6	EHV-1-Induced Cell-to-Cell Fusion Is Dependent on Rac1 and Cdc42 Activation	37
3.5	Discussion.....	38
3.6	Author Contributions.....	40
3.7	Funding	40
3.8	Acknowledgments	40
3.9	Conflicts of Interest.....	40
3.10	References.....	40
Chapter 4	45
4.1	General discussion.....	45
4.2	Importance of phospholipids in EHV-1 entry.....	45
4.3	EHV-1 inhibition with charged lipids.....	45
4.4	Role of Rac1 and Cdc42 in EHV-1 infection	46
4.5	Small GTPases activation is independent from integrin interaction.....	46
4.6	Role of small GTPases in EHV-1 transport.....	46
4.7	Role of small GTPases in EHV-4 infection.....	46
4.8	Final remarks and outlook	48
4.9	Reference.....	49

List of Figures

Figure 1.1. Virus entry and types endocytic entry	2
Figure 2.1. Phospholipids inhibit EHV-1 infection	18
Figure 2.2. Virus interaction with phospholipids	19
Figure 3.1. Cytotoxicity and inhibition of virus infection using GTPase inhibitors.	32
Figure 3.2. EHV-1 infection and cell-to-cell spread is influenced by small GTPases.	33
Figure 3.3. Small GTPase activation with ratiometric FRET in response to EHV-1 infection.	34
Figure 3.4. Effects of small GTPase inhibitors on virus transport.	36
Figure 3.5. Tubulin acetylation by EHV-1 requires virus-activated GTPases.....	37
Figure 3.6. Small GTPases influence cell-to-cell fusion after infection.	38

Abbreviations

AAV-2	Adeno-Associated Virus Type 2
Cdc42	Cell division control protein 42 homolog
<i>c-kras</i>	Cellular Kirsten rat sarcoma gene
CSPG	Chondroitin sulfate proteoglycans
DOTAP	N-[1-(2,3-Dioleoyloxy) propyl]-N,N,N-trimethylammonium)
ED	Equine dermal
EEA-1	Early endosome antigen 1
EHV-1	Equine herpesvirus type 1
EHV-4	Equine herpesvirus type 4
FACS	Fluorescence activated cell sorting
FAK	Focal adhesion kinase
FRET	Fluorescence resonance energy transfer
GAPs	GTPase-activating protein
gB	Glycoprotein B
gC	Glycoprotein C
GDI	Gdp dissociation inhibitor
GDP	Guanosine diphosphate
GEFs	Guanine exchange factors
gH	Glycoprotein H
gH	Glycoprotein H
gL	Glycoprotein L
GTP	Guanosine triphosphate
GUV	Giant unilamellar vesicles
HIV-1	Human immunodeficiency virus type 1
<i>hras</i>	Harvey rat sarcoma gene
HS	Heparan sulfate
HSPG	Heparan sulfate proteoglycans
HSV-1	Herpes simplex virus type 1
HSV-2	Herpes simplex virus type 2
IMDM	Iscove's modified Dulbecco's medium
ITO	Indium tin oxide
<i>kras</i>	Kirsten rat sarcoma gene
KSHV	Kaposi's sarcoma-associated herpesvirus
LAMP-1	Lysosomal-associated membrane protein 1
LUV	Large unilamellar vesicles
MHC-1	Major histocompatibility complex class 1
MLVs	Multilamellar vesicles
MOI	Multiplicity of infection
MSV	Murine sarcoma virus
MT	Microtubules
NE	Nuclear envelope
NPC	Nuclear pore complex
PC	Phosphatidylcholine
PE	Polyethylenimine
PI3K	Phosphoinositide 3-kinases
PIP5K	Phosphatidylinositol-4-phosphate5-kinases
PLC	Phospholipase C
PLSCR-1	Phospholipid Scramblase 1
PS	Phosphatidylserine
Rac1	Ras-related C3 botulinum toxin substrate 1

RhoA	Ras homolog family member A
ROCK1	Rho-associated, coiled-coil-containing protein kinase 1
SPR	Surface plasmon resonance
<i>v-kras</i>	Viral Kirsten rat sarcoma gene

Chapter 1

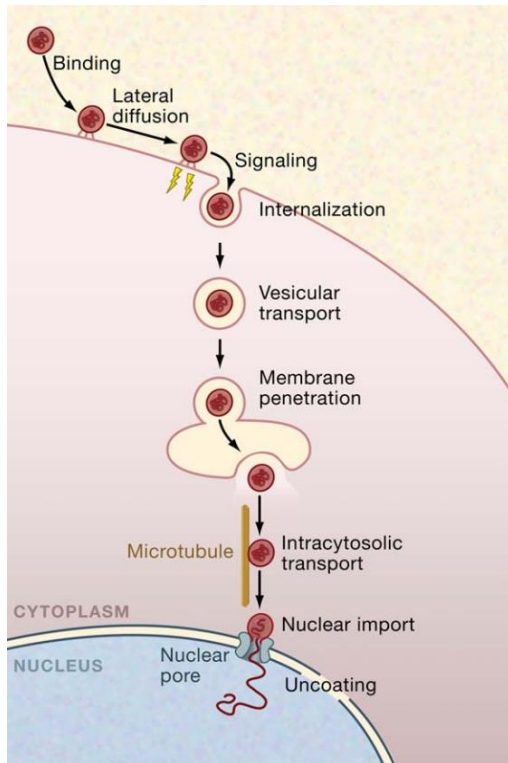
Introduction

1.1 Overview of virus entry

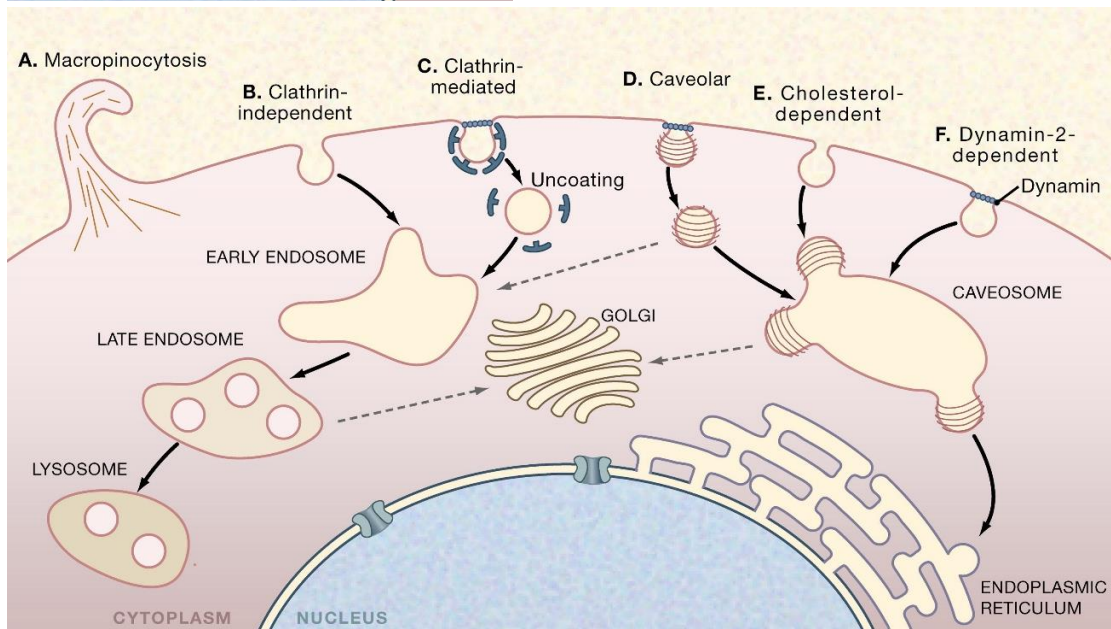
Viruses are obligatory intracellular parasites whose evolutionary strategy relies on the host cell's ability to accept and replicate the incoming virus genomes and transmit viral progeny to other cells. Since viral particles lack motility or any metabolic activity outside of the host cell, viruses have evolved to hijack and exploit host cell machinery for an infectious process. Viruses induce the cell's machinery to facilitate crossing of barriers, such as cellular and nuclear membranes, as well as other parts of the infection process.

Infection of the cell with a free virus typically starts with the attachment step, is relatively nonspecific, and often relies on charged attachment factors, components of the glycocalyx, and surface molecules such as heparan sulfate or other carbohydrate structures [1–7]. After lateral migration on the cell surface, the virus can interact with specific cellular receptor(s) to promote entry by initiating signaling cascades that will result in virus penetration. Viruses have been described to utilize a variety of cell surface molecules as attachment factors or entry receptors such as proteoglycans, heparan sulfates, surface proteins, and adhesion factors. Virus-cell interactions are often carried out through numerous copies of receptor molecules. Such interactions compensate for low affinity with individual receptors and allows for clustering of the receptor molecules on the cell surface. This relocation of surface proteins can serve as a start of the subsequent signaling cascade. Virus-induced signaling can have far reaching downstream responses. For example in the case of Kaposi's sarcoma-associated herpesvirus (human herpesvirus 8) whose binding of gB with $\alpha 3\beta 1$ integrin activates focal adhesion kinase (FAK) and Src kinases, phosphatidylinositol 3-kinases (PI3-Kinase), and consequently RhoA GTPases and Dia2; this signaling is required for cytoskeleton remodeling during the virus uptake via endocytosis and viral and tubulin acetylation to promote microtubule stability and enhanced transport [8].

Interaction of the virion with the surface receptors promotes penetration—transfer of the viral genome and structural proteins into the host cell cytoplasm. Viruses have different ways of overcoming the first barrier - the plasma membrane - and being transported towards the replication compartment. Herpesviruses, retroviruses, and paramyxoviruses, can fuse with the plasma membrane, and thus do not require endocytosis for productive infection [9–12].



A)



B)

Figure 1.1. Virus entry and types of endocytic entry. a) Types of virus entry (copied with permission from Marsh 2006). Numerous steps have to be undertaken in order for the virus to overcome cellular barriers and deliver its genetic material to the nucleus. First, the virus has to attach to the cell surface, this is usually done through nonspecific charge mechanisms. The virus then moves laterally on the surface of the cell until it can interact with cellular receptors and, at this step, the virus can activate intracellular signaling to facilitate its own internalization and intracellular transport. b) Types of endocytic mechanisms used for virus entry (copied from Marsh 2006). Clathrin-mediated endocytosis is the most frequently used mechanism for virus entry. Caveolar endocytosis is used by polyomaviruses and depends on caveolin and lipid raft formation. Caveolin-independent lipid raft endocytosis and nonclathrin, noncaveolin mechanisms have similarities to macropinocytosis.

When the capsid of the virus is inside the appropriate host cell, it needs to be transported to the proper compartment for replication to take place. Viruses rely on the cellular transport system to reach the replication or uncoating compartments, since passive diffusion in the context of the animal cell is an ineffective mode of transportation [13–17]. Loss of structural proteins, environmental cues, or conformational changes facilitate the uncoating of the viral genome. For replication of most DNA viruses, the viral genome is imported into the nucleus, or transported to a cytoplasmic viral replication site. For herpesviruses, the viral capsid attaches to the nuclear pore complex (NPC) and extrudes the genome into the nucleus, leaving the empty capsid in contact with the NPC.

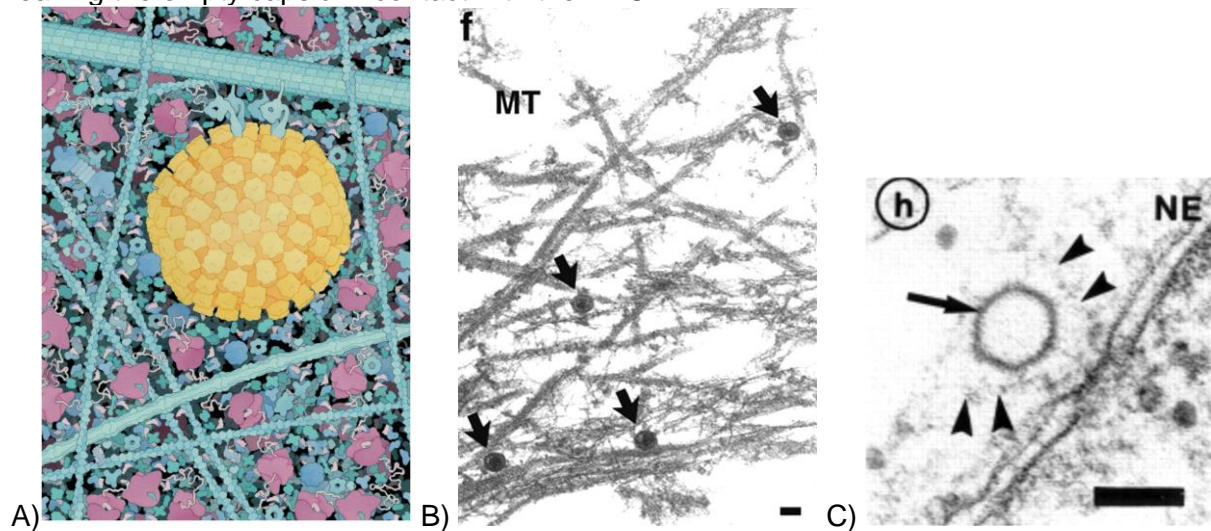


Figure 1.2. Intracellular transport of herpesviruses. a) Drawing representing herpesvirus nucleocapsid transported along the microtubule by the dynein motor proteins (copied with permission from Lyman 2009). b) Electron micrograph of HSV-1 infected Vero cell (1 HPI, MOI = 500) (copied with permission from Sodeik 1997) labeled with primary anti-tubulin rabbit antibodies, and secondary anti-rabbit gold-labeled antibodies. Icosahedral, electronically dense nucleocapsids are visualized alongside the microtubules (MT) (filled arrow). c) Electron micrograph of HSV-1 nucleocapsid (filled arrow) that has lost its electronically dense DNA core at the periphery of the nuclear envelope (NE), surrounding the nucleocapsid is tegument protein (arrow heads) (copied with permission from Sodeik 1997). Bars are 100nm.

1.2 Taxonomy of Herpesviruses

Herpesviridae is a large family of linear double-stranded DNA viruses belonging to order *Herpesvirales*. Members of *Herpesviridae* have been found to infect wide range of vertebrates and invertebrate species. Based on the genomic organization and host range Herpesviruses are divided into three families: *Alloherpesviridae*, *Herpesviridae*, and *Malacoherpesviridae*. Members of the *Herpesviridae* are classified into three subfamilies: *Alpha*-, *Beta*-, and *Gammaherpesvirinae*. Alphaherpesviruses EHV-1 and EHV-4 are members of genus *Varicellovirus* and have a high degree of genetic similarity [18,19].

1.3 Binding and signaling

Viral particles of herpesviruses are complex structures comprised of a lipid-based envelope that contains glycoproteins, tegument, and nucleocapsid. Nucleocapsid is a proteinaceous icosahedral structure that encases linear double-stranded DNA. Attachment of EHV-1 and EHV-4 to cells is a charge-based process facilitated by interactions between surface glycoproteins (gC and gB) and surface heparan sulfate proteoglycans (HSPG)[7,20] similar to other Alphaherpesviruses [21,22]. gC and gB are presumably interacting through their positively charged domains with the negatively charged HS. gD then interacts with MHC-1 and promotes fusion at the plasma membrane [23–25]. In the case of EHV-1, interaction of

gH/gL complex with $\alpha 4\beta 1$ integrin triggers fusion at the plasma membrane [26]. Interaction between EHV-1 gH and $\alpha 4\beta 1$ integrin on the surface of equine epithelial cells induces influx of cytosolic Ca^{2+} and subsequently activates phospholipase C (PLC) and inositol 1,4,5-trisphosphate (InsP3) pathway, and phospholipid scramblase that results in non-directional redistribution of the phospholipids comprising plasma membrane, ultimately leading to phosphatidylserine (PS) exposure on the outer leaflet of the plasma membrane [27]. The ability to induce influx of cytosolic Ca^{2+} is further localized to specific integrin-binding domain in EHV-1 gH, thus EHV-1 gHS440A [28] (with mutation in the integrin binding motif) is not able to induce Ca^{2+} release and prevents fusion of the virus with the plasma membrane.

1.4 Small GTPases

Small GTPases are signaling proteins that can exist in GTP (activated) or GDP (not activated) bound states [29]. Activation status of the small GTPases changes their conformation and consequently their range of interaction with other proteins in the cell, thus giving them the ability to transfer signals specific to the activation status [30]. Biochemically, the function of small GTPases is to metabolize GTP into GDP, an action facilitated by GAPs (GTPase-activating protein). GEFs (Guanine exchange factors) on the other hand facilitate the release of GDP and binding to GTP [31].

The story of the discovery of small GTPases started in the 1960s, with the discovery of oncogenic viruses in mice, Harvey MSV (murine sarcoma virus) and Kirsten MSV [32]. These two viruses were found to contain sequences similar to cellular sequences [33,34] designated as *cellular hras* or *cellular kras*. K-MSV and H-MSV contained *hras* and *kras* (Kirsten rat sarcoma) genes, also known as transforming protein p21 due to its molecular weight [33,34], and found to possess guanine nucleotide-binding activity [35]. In 1982 multiple p21 homologues genes were found in the human genome, high homology between *c-kras*, *v-kras*, and the human analog implied important biological functions of these genes [36]. In 1983 expression of *kras* was shown in cells chemically transformed with 3-methylcholanthrene [37], further suggesting that *hras* plays role in oncogenesis. The difference between normal and oncogenic *kras* encoded p21 protein was localized to the 12th amino acid position when sequences of *kras* were compared from carcinomas of different origin to non-carcinogenic sequence [38]. An indication of the importance of GTPase activity of RAS proteins had come with a 1984 study comparing rates of GTP hydrolysis between p21 protein cloned from normal cells, and a tumorigenic variant of p21 [Val12] [39]. The oncogene had significantly lower GTPase hydrolysis rates, suggesting that GTP hydrolysis is what prevents the growth-promoting effects of p21 proteins [39]. Later, with the advance of structural analysis, the mechanism in which such mutation acts was discovered; mutation at position 12 prevents interaction with the arginine finger of the GAP that is required for the cleavage between β - and γ -phosphates of GTP [40], thus reducing GTPase function of the p21 protein. The first GTPase-activating proteins (GAPs), proteins that accelerate hydrolysis of GTP by small GTPases, were being identified and cloned in 1987 and 1988 [41,42]. At the same time, there was growing body of evidence that mutations in *kras* were associated with oncogenesis in humans [43,44]. With the solving of the Ras structure and a greater understanding of GTP hydrolysis [45,46], discovery of ras-GEFs [47], identification of interaction partners such as PI3K [48] and Raf-1 [49], and the realization that KRAS was essential not only for tumor maintenance [50] but also for embryonic development [51,52], came the realization of the huge variety of roles that small GTPase KRAS plays. Today, the Ras superfamily of small GTPases includes over 150 known proteins in humans, and homologues are found in insects (*Drosophila*), roundworms (*C. elegans*), yeasts (*S. cerevisiae* and *S. pombe*), *Dictyostelium*, and plants [53]. The Ras superfamily is divided into 5 subfamilies based on sequence. They all share conserved G box GDP/GTP-binding motif at the amino-terminus: G1, GXXXXGKS/T; G2, T; G3, DXXGQ/H/T; G4, T/NKXD; and G5, C/SAK/L/T, and together these elements contribute to a conserved structure with a molecular weight around 20 kDa [54]. Small GTPases have high affinity for GTP and GDP binding, and low GTP/GDP exchange and GDP hydrolysis activities. The regulatory function of GAPs and GEFs is required to facilitate exchange of GDP to GTP or GTP hydrolysis [54]. Additionally, small GTPases can undergo

post-translational modifications such as farnesylation or palmitoylation due to sequences that are recognized by farnesyltransferase and geranylgeranyltransferase type I which are present at the carboxyl-terminus. Post-translational modifications are important for membrane attachment and subcellular localization of the GTPases [55]. Rho GTPases are regulated by GDI, GEF, and GAP [31,55]. GDI interacts with GDP bound GTPases, masking the prenyl that is responsible for membrane attachment, thus increasing cytoplasmic accumulation of GTPases[31,55]. The Rho (Ras homologous) family of small GTPases regulate actin reorganization, cell cycle, gene expression, cell polarity, morphology, movement, intracellular transport, cell-cell interactions, membrane remodeling, as well as endo- and exocytosis [29,56–60].

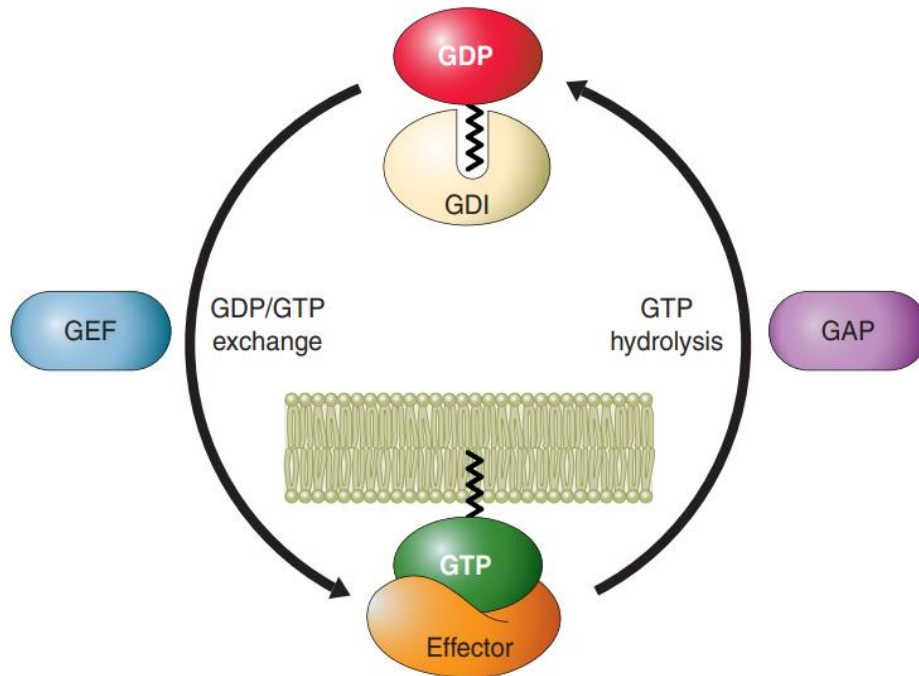


Figure 1.3. Regulation of GDP/GTP switch by GEFs, GAPs, and GDIs. (Copied with permission from Cherflis and Zeghouf 2013). Small GTPase shown in red when GDP bound, GDI (guanine dissociation inhibitor) keeps the complex stable, upon interaction with GEF GDP is exchanged for GTP, which allows interaction with effector molecules. In order to hydrolyze GTP, small GTPase needs to interact with GAP.

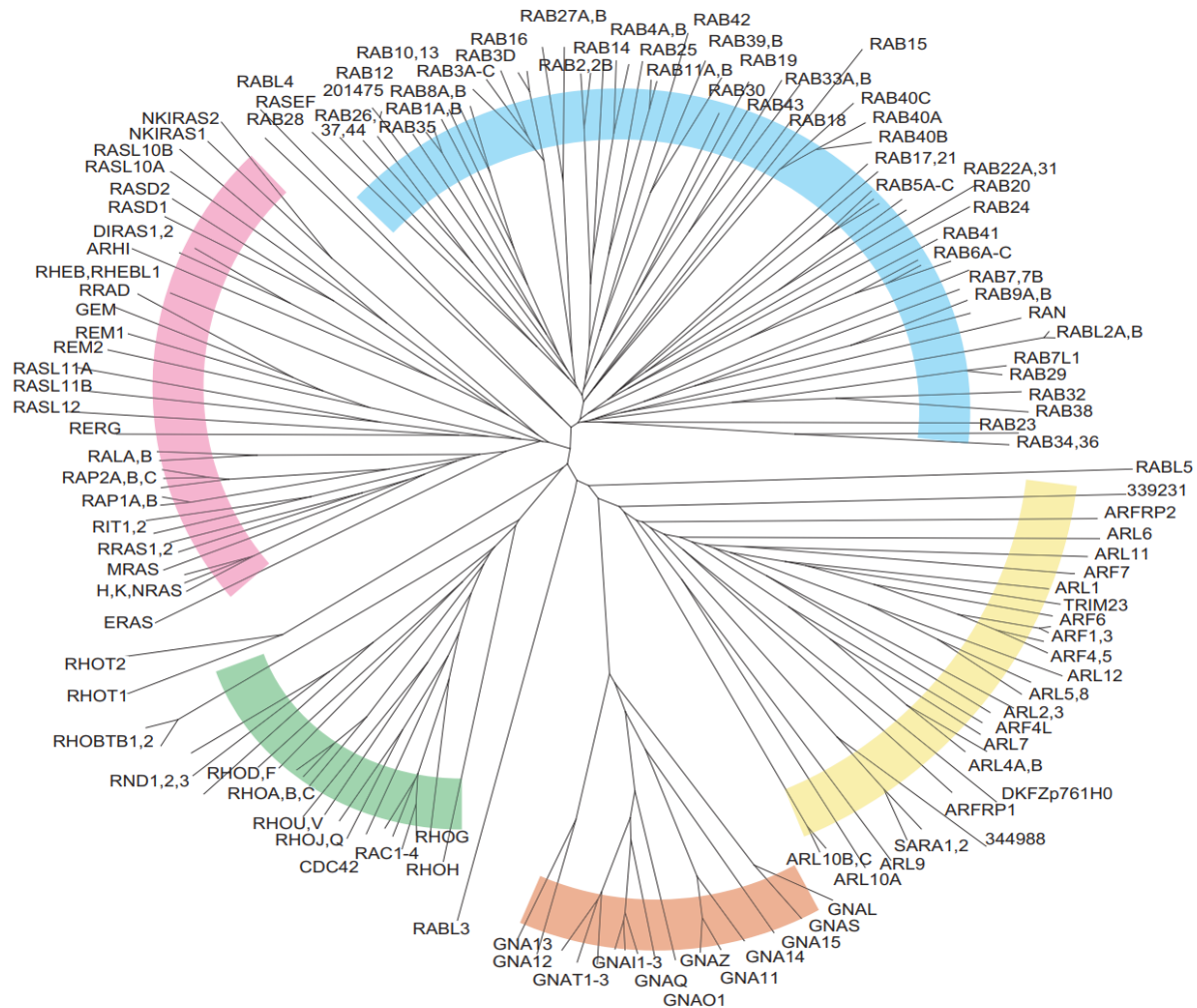


Figure 1.4 Diversity of Ras superfamily GTPases Unrooted tree of human Ras superfamily member (copied with permission from Colicelli 2004). Branches grouped by subfamilies and designated by colored arcs: Ras -red, Rho -green, Ga -orange, Arf -yellow and Rab -blue. Role of the small GTPases from Rho subfamily, in particular Cdc42, Rac1, RhoA as well as HRas from Ras subfamily will be examined in the current work.

Small GTPases have been described to play a role in viral-induced signaling [61–66]. For example, it was shown that in infection with dengue virus, Rac1 activation levels are reduced at the start of the infection and inactivation of Rac1 is essential for the entry of the dengue virus in ECV304 and EAhy926 cells, since Rac1 is a negative regulator of clathrin-dependent endocytosis used by dengue virus. Early dengue virus infection is negatively regulated by the expression of Rac1V12 a dominant negative form of Rac1. While in later stages of infection Rac1 is upregulated, expression of dengue virus E protein is sufficient to induce activation of small GTPase Rac1 and promote actin reorganization [65,66]. Furthermore, E protein colocalizes with cellular actin during infection and when E protein is expressed by transfection [65,66]. Interestingly, in HMEC-1 cells Dengue virus activates both Rac1 and Cdc42 upon virus binding, resulting in formation of filopodia and facilitating cell entry. Disruption of Rac1 and Cdc42 signaling cascades via expression of dominant negative mutants of the small GTPases hinders actin reorganization [67,68]. It was further discovered that the signaling cascade required for effective Dengue virus replication that involves actin reorganization and Rock1, Rac1, Cdc42 is regulated via the PI3K/Akt [69]. Small GTPase signaling in dengue virus infection remains to be examined further and presents an interesting case where Dengue virus manipulates cellular GTPases in a time-dependent manner to better suit different phases of the replication cycle.

Small GTPases also play a role in the case of the gene and vaccine vector, Adeno-Associated Virus Type 2 (AAV-2). AAV-2 attaches to heparan sulfate on the surface of host cells [70], and uses $\alpha V\beta 5$ integrin as a coreceptor [71]. AAV-2 interaction with $\alpha V\beta 5$ integrin is required activation of Rac1 that is needed for virus endocytosis. If the $\alpha V\beta 5$ integrin is blocked by antibodies, or if the activation of Rac1 is prevented by the expression of the dominant negative mutant, viral endocytosis is blocked. AAV-2-induced activation of the PI3K pathway was found to temporally coincide with the activation of Rac1 [72]. Expression of dominant negative Rac1 prevented PI3K activation, suggesting that for AAV-2 it is Rac1 that is responsible for activation of PI3K [72]. Activation of PI3K is required for the nuclear transport of AAV-2 along the microtubules, but not for endocytosis [72]. The particular examples of cell signaling in AAV-2 and dengue virus infection highlight the complex and reciprocal nature of signaling networks.

For influenza A virus, the small GTPase RhoA is activated downstream from virus-induced Ca^{2+} [61], and promotes oscillations in cytoplasmic Ca^{2+} concentration, and mediates signaling through PLC and PIP5K, which are required for both clathrin-mediated and clathrin-independent endocytosis [61,73].

1.5 Lipids

Lipids are the main structural component of biological membranes. The property of lipids to spontaneously form bilayers due to their amphiphilic nature is important for models explaining the formation of protocell membranes. Lipids are recognized to have functions ranging from structural functions, to energy storage and signaling [74,75]. In eukaryotic cells lipids compartmentalize the intracellular space and are the interface of the cell with the extracellular space. Thus, lipid membranes are one of the first barriers infectious agents need to overcome during an infection [76]. The plasma membrane performs numerous functions, being the interface between the intra- and extracellular space, receptors on the plasma membrane coordinate uptake and internalization of solid particles and fluids through mechanism of endocytosis [75,77]. Enveloped viruses have evolved mechanisms to utilize and interact with plasma membrane. For example, a number of viruses have special membrane-fusing proteins [11,12,78–80] or they can modify the plasma membrane of the host cell in order to avoid immune response [81–83].

The virus envelope typically originates from the existing membranes of the host cell and due to the functional importance of the outer lipid layer, enveloped viruses are generally more susceptible to environmental factors such as heat, detergents, and desiccation [84]. On the other hand among enveloped viruses there are more viral families that infect non cell-walled hosts, while nonenveloped virus families are more prevalent in hosts whose cells are surrounded by a cell wall [84], suggesting that there is an evolutionary advantage to having an envelope in the infection of animals. Enveloped viruses require cell fusion to enter a host cell. Cell-to-cell fusion is a process where viral proteins facilitate thermodynamically favorable processes of membrane fusion by overcoming the hydration barrier responsible for the repulsive force that becomes stronger with the closing in the distance between the surfaces of the two membranes [85,86]. Viral proteins responsible for fusion typically only become fusogenically active under strict conditions, to minimize premature fusion within the host cell if virus production is already taking place or fusion with the non-susceptible cell types, since fusion proteins can only facilitate one fusion event during which they undergo irreversible conformational changes [87]. There are 3 structural classes of fusion proteins [88]. Class I has influenza virus hemagglutinin or Paramyxovirus F protein as models and is characterized by a perpendicular orientation where the protein protrudes from the membrane surface membrane as a spike, commonly with the N-terminus on the outside where the fusion peptide is located [89]. The majority of its secondary structures consist of α -helices that form trimers, and the changes to fusogenic form are activated by the low pH [89]. Semliki Forest virus E1/E2 and Tick-borne encephalitis virus E1 proteins are examples of class II fusion proteins. Unlike class I proteins, class II proteins are located parallelly, close to the viral membrane's surface, and the majority of their secondary structures are β -sheets that oligomerizes in to dimer [4]. Both

class I and II fusion proteins require proteolytic processing of the fusion protein in the case of class I and of accessory proteins in class II [87]. The class III fusion protein is commonly represented by gB of HSV-1, Varicella zoster virus G protein, and Ebolavirus GP [90]. The main distinction of class III fusion proteins is that they don't require proteolytic processing or priming prior to fusion [91–94]. Some authors classify proteins of nonenveloped reoviruses fusion-associated small transmembrane (FAST) [90] into a fourth class of viral fusion proteins, class IV, as they are sufficient to cause cell to cell fusion, even though class IV is not essential for the infection cycle [95].

Current models of the behavior of plasma membrane lipids predict that in addition to freely diffusing through the membrane surface, they can also cluster into lipid rafts which are important for apoptosis [76,96–98]. In general, apoptosis involves PS exposure on the apoptotic cell that engages the PS receptor on a phagocyte, leading to endocytosis of the PS-presenting cell. The phagocyte processes the engulfed cell and produces anti-inflammatory cytokines to dampen innate immune responses [99,100]. Liposomes are a commonly used model to study effects of the phospholipids. Liposomes can be formed artificially with the desired size and composition of phospholipids. Liposomes could have an effect on viral infection through various routes. For example, PS liposomes were shown to promote HIV-1 entry through integration of PS into the membrane of the host cells and restructuring of the prefusion complex [101]. Liposomes could serve as vehicle to carry decoy interaction targets, for example, polyethylenimine (PE) inhibition of HSV-2 infection was significantly increased when PE was mixed with the liposomes that have no effect on viral infection when used alone [102]. Liposomes can nonspecifically interfere with viral infection through adherence to the cell surface, and thus limiting binding sites for the virus [103].

1.6 Aims of the study

Previous studies have shown that for EHV-1 fusion of the viral envelope with the plasma membrane, interaction of EHV-1 gH with cellular $\alpha 4\beta 1$ integrins is required. The interaction between gH and $\alpha 4\beta 1$ results in rapid influx of cytosolic Ca^{2+} and PS scrambling [27]. Alteration of the plasma membrane composition can play a role in facilitating fusion at the plasma membrane, while increases in cytosolic Ca^{2+} has been described as the event triggering signal transduction involving small GTPases [57,61,96,104,105]. The exact role and effects of signaling downstream from the gH- $\alpha 4\beta 1$ interaction are unknown. In this research my focus was to examine the role that small GTPases play in the EHV-1 infection, and how PS or other lipids can interact with EHV-1 and facilitate virus entry through comparisons between EHV-1 and EHV-4 infections.

1.7 References

1. Rodrigues, R.; Danskog, K.; Överby, A.K.; Arnberg, N. Characterizing the Cellular Attachment Receptor for Langkat Virus. *PLOS ONE* **2019**, *14*, e0217359, doi:10.1371/journal.pone.0217359.
2. Ugolini, S.; Mondor, I.; Sattentau, Q.J. HIV-1 Attachment: Another Look. *Trends Microbiol.* **1999**, *7*, 144–149, doi:10.1016/s0966-842x(99)01474-2.
3. Vlasak, M.; Goesler, I.; Blaas, D. Human Rhinovirus Type 89 Variants Use Heparan Sulfate Proteoglycan for Cell Attachment. *J. Virol.* **2005**, *79*, 5963–5970, doi:10.1128/JVI.79.10.5963-5970.2005.
4. Fields, B.N.; Knipe, D.M.; Howley, P.M.; Griffin, D.E. *Fields Virology*; Lippincott Williams & Wilkins: Philadelphia, 2001; ISBN 978-0-7817-1832-5.
5. Di Lorenzo, C.; Angus, A.G.N.; Patel, A.H. Hepatitis C Virus Evasion Mechanisms from Neutralizing Antibodies. *Viruses* **2011**, *3*, 2280–2300, doi:10.3390/v3112280.
6. Mondor, I.; Ugolini, S.; Sattentau, Q.J. Human Immunodeficiency Virus Type 1 Attachment to HeLa CD4 Cells Is CD4 Independent and Gp120 Dependent and Requires Cell Surface Heparans. *J. Virol.* **1998**, *72*, 3623–3634, doi:10.1128/JVI.72.5.3623-3634.1998.
7. Osterrieder, N. Construction and Characterization of an Equine Herpesvirus 1 Glycoprotein C Negative Mutant. *Virus Res.* **1999**, *59*, 165–177, doi:10.1016/S0168-1702(98)00134-8.
8. Chandran, B. Early Events in Kaposi's Sarcoma-Associated Herpesvirus Infection of Target Cells. *J. Virol.* **2010**, *84*, 2188–2199, doi:10.1128/JVI.01334-09.
9. Xiong, X.; Zhao, Y.; Zhuge, S.; Zhou, H.; Cui, Y. Small Interfering RNA-Mediated Inhibition of Respiratory Syncytial Virus Infections in Hela Cells. *Int. J. Clin. Exp. Med.* **2019**, *12*, 12264–12270.
10. Nicola, A.V.; Hou, J.; Major, E.O.; Straus, S.E. Herpes Simplex Virus Type 1 Enters Human Epidermal Keratinocytes, but Not Neurons, via a PH-Dependent Endocytic Pathway. *J. Virol.* **2005**, *79*, 7609–7616, doi:10.1128/JVI.79.12.7609-7616.2005.
11. Ward, A.E.; Dryden, K.A.; Tamm, L.K.; Ganser-Pornillos, B.K. Catching HIV in the Act of Fusion: Insight from Cryo-Et Intermediates of HIV Membrane Fusion. *Biophys. J.* **2019**, *116*, 180a.
12. Moss, B. Membrane Fusion during Poxvirus Entry. *Semin. Cell Dev. Biol.* **2016**, *60*, 89–96, doi:10.1016/j.semcdb.2016.07.015.
13. Theerawatanasirikul, S.; Phecharat, N.; Prawetongsopon, C.; Chaicumpa, W.; Lekcharoensuk, P. Dynein Light Chain DYNLL1 Subunit Facilitates Porcine Circovirus Type 2 Intracellular Transports along Microtubules. *Arch. Virol.* **2017**, *162*, 677–686, doi:10.1007/s00705-016-3140-0.
14. Döhner, K.; Nagel, C.-H.; Sodeik, B. Viral Stop-and-Go along Microtubules: Taking a Ride with Dynein and Kinesins. *Trends Microbiol.* **2005**, *13*, 320–327, doi:10.1016/j.tim.2005.05.010.
15. Wen, L.; Zheng, Z.-H.; Liu, A.-A.; Lv, C.; Zhang, L.-J.; Ao, J.; Zhang, Z.-L.; Wang, H.-Z.; Lin, Y.; Pang, D.-W. Tracking Single Baculovirus Retrograde Transportation in Host Cell via Quantum Dot-Labeling of Virus Internal Component. *J. Nanobiotechnology* **2017**, *15*, 37, doi:10.1186/s12951-017-0270-9.
16. Greber, U.F.; Way, M. A Superhighway to Virus Infection. *Cell* **2006**, *124*, 741–754, doi:10.1016/j.cell.2006.02.018.
17. Lyman, M.G.; Enquist, L.W. Herpesvirus Interactions with the Host Cytoskeleton. *J. Virol.* **2009**, *83*, 2058–2066, doi:10.1128/JVI.01718-08.
18. Davison, A.J.; Eberle, R.; Ehlers, B.; Hayward, G.S.; McGeoch, D.J.; Minson, A.C.; Pellett, P.E.; Roizman, B.; Studdert, M.J.; Thiry, E. The Order Herpesvirales. *Arch. Virol.* **2009**, *154*,

- 171–177, doi:10.1007/s00705-008-0278-4.
19. Ma, G.; Azab, W.; Osterrieder, N. Equine Herpesviruses Type 1 (EHV-1) and 4 (EHV-4)—Masters of Co-Evolution and a Constant Threat to Equids and Beyond. *Vet. Microbiol.* **2013**, *167*, 123–134, doi:10.1016/j.vetmic.2013.06.018.
 20. Azab, W.; Tsujimura, K.; Maeda, K.; Kobayashi, K.; Mohamed, Y.M.; Kato, K.; Matsumura, T.; Akashi, H. Glycoprotein C of Equine Herpesvirus 4 Plays a Role in Viral Binding to Cell Surface Heparan Sulfate. *Virus Res.* **2010**, *151*, 1–9, doi:10.1016/j.virusres.2010.03.003.
 21. Banfield, B.W.; Leduc, Y.; Esford, L.; Schubert, K.; Tufaro, F. Sequential Isolation of Proteoglycan Synthesis Mutants by Using Herpes Simplex Virus as a Selective Agent: Evidence for a Proteoglycan-Independent Virus Entry Pathway. *J. Virol.* **1995**, *69*, 3290–3298.
 22. Spear, P.G.; Longnecker, R. Herpesvirus Entry: An Update. *J. Virol.* **2003**, *77*, 10179–10185, doi:10.1128/JVI.77.19.10179-10185.2003.
 23. Kurtz, B.M.; Singletary, L.B.; Kelly, S.D.; Frampton, A.R. Equus Caballus Major Histocompatibility Complex Class I Is an Entry Receptor for Equine Herpesvirus Type 1. *J. Virol.* **2010**, *84*, 9027–9034, doi:10.1128/JVI.00287-10.
 24. Sasaki, M.; Hasebe, R.; Makino, Y.; Suzuki, T.; Fukushi, H.; Okamoto, M.; Matsuda, K.; Taniyama, H.; Sawa, H.; Kimura, T. Equine Major Histocompatibility Complex Class I Molecules Act as Entry Receptors That Bind to Equine Herpesvirus-1 Glycoprotein D. *Genes Cells* **2011**, *16*, 343–357, doi:10.1111/j.1365-2443.2011.01491.x.
 25. Azab, W.; Harman, R.; Miller, D.; Tallmadge, R.; Frampton, A.R.; Antczak, D.F.; Osterrieder, N. Equid Herpesvirus Type 4 Uses a Restricted Set of Equine Major Histocompatibility Complex Class I Proteins as Entry Receptors. *J. Gen. Virol.* **2014**, *95*, 1554–1563, doi:10.1099/vir.0.066407-0.
 26. Azab, W.; Lehmann, M.J.; Osterrieder, N. Glycoprotein H and A4 β 1 Integrins Determine the Entry Pathway of Alphaherpesviruses. *J. Virol.* **2013**, *87*, 5937–5948, doi:10.1128/JVI.03522-12.
 27. Azab, W.; Gramatica, A.; Herrmann, A.; Osterrieder, N. Binding of Alphaherpesvirus Glycoprotein H to Surface A4 β 1-Integrins Activates Calcium-Signaling Pathways and Induces Phosphatidylserine Exposure on the Plasma Membrane. *mBio* **2015**, *6*, e01552-15, doi:10.1128/mBio.01552-15.
 28. Azab, W.; Zajic, L.; Osterrieder, N. The Role of Glycoprotein H of Equine Herpesviruses 1 and 4 (EHV-1 and EHV-4) in Cellular Host Range and Integrin Binding. *Vet. Res.* **2012**, *43*, 61, doi:10.1186/1297-9716-43-61.
 29. Nobes, C.D.; Hall, A. Rho GTPases Control Polarity, Protrusion, and Adhesion during Cell Movement. *J. Cell Biol.* **1999**, *144*, 1235–1244, doi:10.1083/jcb.144.6.1235.
 30. Kötting, C.; Gerwert, K. The Dynamics of the Catalytic Site in Small GTPases, Variations on a Common Motif. *FEBS Lett.* **2013**, *587*, 2025–2027, doi:10.1016/j.febslet.2013.05.021.
 31. Cherfils, J.; Zeghouf, M. Regulation of Small GTPases by GEFs, GAPs, and GDIs. *Physiol. Rev.* **2013**, *93*, 269–309, doi:10.1152/physrev.00003.2012.
 32. Harvey, J.J. AN UNIDENTIFIED VIRUS WHICH CAUSES THE RAPID PRODUCTION OF TUMOURS IN MICE. *Nature* **1964**, *204*, 1104–1105, doi:10.1038/2041104b0.
 33. Willingham, M.C.; Pastan, I.; Shih, T.Y.; Scolnick, E.M. Localization of the Src Gene Product of the Harvey Strain of MSV to Plasma Membrane of Transformed Cells by Electron Microscopic Immunocytochemistry. *Cell* **1980**, *19*, 1005–1014, doi:10.1016/0092-8674(80)90091-4.
 34. Shih, T.Y.; Weeks, M.O.; Young, H.A.; Scholnick, E.M. Identification of a Sarcoma Virus-Coded Phosphoprotein in Nonproducer Cells Transformed by Kirsten or Harvey Murine Sarcoma

- Virus. *Virology* **1979**, *96*, 64–79, doi:10.1016/0042-6822(79)90173-9.
35. Scolnick, E.M.; Papageorge, A.G.; Shih, T.Y. Guanine Nucleotide-Binding Activity as an Assay for Src Protein of Rat-Derived Murine Sarcoma Viruses. *Proc. Natl. Acad. Sci.* **1979**, *76*, 5355–5359, doi:10.1073/pnas.76.10.5355.
 36. Chang, E.H.; Gonda, M.A.; Ellis, R.W.; Scolnick, E.M.; Lowy, D.R. Human Genome Contains Four Genes Homologous to Transforming Genes of Harvey and Kirsten Murine Sarcoma Viruses. *Proc. Natl. Acad. Sci. U. S. A.* **1982**, *79*, 4848–4852.
 37. Parada, L.F.; Weinberg, R.A. Presence of a Kirsten Murine Sarcoma Virus Ras Oncogene in Cells Transformed by 3-Methylcholanthrene. *Mol. Cell. Biol.* **1983**, *3*, 2298–2301.
 38. Santos, E.; Martin-Zanca, D.; Reddy, E.P.; Pierotti, M.A.; Della Porta, G.; Barbacid, M. Malignant Activation of a K-Ras Oncogene in Lung Carcinoma but Not in Normal Tissue of the Same Patient. *Science* **1984**, *223*, 661–664, doi:10.1126/science.6695174.
 39. Gibbs, J.B.; Sigal, I.S.; Poe, M.; Scolnick, E.M. Intrinsic GTPase Activity Distinguishes Normal and Oncogenic Ras P21 Molecules. *Proc. Natl. Acad. Sci. U. S. A.* **1984**, *81*, 5704–5708, doi:10.1073/pnas.81.18.5704.
 40. Scheffzek, K.; Ahmadian, M.R.; Kabsch, W.; Wiesmüller, L.; Lautwein, A.; Schmitz, F.; Wittinghofer, A. The Ras-RasGAP Complex: Structural Basis for GTPase Activation and Its Loss in Oncogenic Ras Mutants. *Science* **1997**, *277*, 333–339, doi:10.1126/science.277.5324.333.
 41. Trahey, M.; Wong, G.; Halenbeck, R.; Rubinfeld, B.; Martin, G.A.; Ladner, M.; Long, C.M.; Crosier, W.J.; Watt, K.; Kohts, K. Molecular Cloning of Two Types of GAP Complementary DNA from Human Placenta. *Science* **1988**, *242*, 1697–1700, doi:10.1126/science.3201259.
 42. Trahey, M.; McCormick, F. A Cytoplasmic Protein Stimulates Normal N-Ras P21 GTPase, but Does Not Affect Oncogenic Mutants. *Science* **1987**, *238*, 542–545, doi:10.1126/science.2821624.
 43. Bos, J.L.; Fearon, E.R.; Hamilton, S.R.; Verlaan-de Vries, M.; van Boom, J.H.; van der Eb, A.J.; Vogelstein, B. Prevalence of Ras Gene Mutations in Human Colorectal Cancers. *Nature* **1987**, *327*, 293–297, doi:10.1038/327293a0.
 44. Ras Oncogenes in Human Cancer: A Review | Cancer Research Available online: <https://cancerres.aacrjournals.org/content/49/17/4682.short> (accessed on 12 June 2020).
 45. de Vos, A.M.; Tong, L.; Milburn, M.V.; Matias, P.M.; Jancarik, J.; Noguchi, S.; Nishimura, S.; Miura, K.; Ohtsuka, E.; Kim, S.H. Three-Dimensional Structure of an Oncogene Protein: Catalytic Domain of Human c-H-Ras P21. *Science* **1988**, *239*, 888–893, doi:10.1126/science.2448879.
 46. Schlichting, I.; Almo, S.C.; Rapp, G.; Wilson, K.; Petratos, K.; Lentfer, A.; Wittinghofer, A.; Kabsch, W.; Pai, E.F.; Petsko, G.A.; et al. Time-Resolved X-Ray Crystallographic Study of the Conformational Change in Ha-Ras P21 Protein on GTP Hydrolysis. *Nature* **1990**, *345*, 309–315, doi:10.1038/345309a0.
 47. Downward, J.; Riehl, R.; Wu, L.; Weinberg, R.A. Identification of a Nucleotide Exchange-Promoting Activity for P21ras. *Proc. Natl. Acad. Sci. U. S. A.* **1990**, *87*, 5998–6002, doi:10.1073/pnas.87.15.5998.
 48. Rodriguez-Viciano, P.; Warne, P.H.; Dhand, R.; Vanhaesebroeck, B.; Gout, I.; Fry, M.J.; Waterfield, M.D.; Downward, J. Phosphatidylinositol-3-OH Kinase Direct Target of Ras. *Nature* **1994**, *370*, 527–532, doi:10.1038/370527a0.
 49. Warne, P.H.; Vician, P.R.; Downward, J. Direct Interaction of Ras and the Amino-Terminal Region of Raf-1 in Vitro. *Nature* **1993**, *364*, 352–355, doi:10.1038/364352a0.
 50. Chin, L.; Tam, A.; Pomerantz, J.; Wong, M.; Holash, J.; Bardeesy, N.; Shen, Q.; O'Hagan, R.; Pantginis, J.; Zhou, H.; et al. Essential Role for Oncogenic Ras in Tumour

- Maintenance. *Nature* **1999**, *400*, 468–472, doi:10.1038/22788.
51. Johnson, L.; Greenbaum, D.; Cichowski, K.; Mercer, K.; Murphy, E.; Schmitt, E.; Bronson, R.T.; Umanoff, H.; Edelman, W.; Kucherlapati, R.; et al. K-Ras Is an Essential Gene in the Mouse with Partial Functional Overlap with N-Ras. *Genes Dev.* **1997**, *11*, 2468–2481.
 52. Koera, K.; Nakamura, K.; Nakao, K.; Miyoshi, J.; Toyoshima, K.; Hatta, T.; Otani, H.; Aiba, A.; Katsuki, M. K-Ras Is Essential for the Development of the Mouse Embryo. *Oncogene* **1997**, *15*, 1151–1159, doi:10.1038/sj.onc.1201284.
 53. Colicelli, J. Human RAS Superfamily Proteins and Related GTPases. *Sci. STKE* **2004**, *2004*, re13–re13, doi:10.1126/stke.2502004re13.
 54. Bourne, H.R.; Sanders, D.A.; McCormick, F. The GTPase Superfamily: Conserved Structure and Molecular Mechanism. *Nature* **1991**, *349*, 117–127, doi:10.1038/349117a0.
 55. Seabra, M.C.; Wasmeier, C. Controlling the Location and Activation of Rab GTPases. *Curr. Opin. Cell Biol.* **2004**, *16*, 451–457, doi:10.1016/j.ceb.2004.06.014.
 56. Bishop, A.L.; Hall, A. Rho GTPases and Their Effector Proteins. *Biochem. J.* **2000**, *348 Pt 2*, 241–255.
 57. Hall, A. Rho GTPases and the Control of Cell Behaviour. *Biochem. Soc. Trans.* **2005**, *33*, 891–895, doi:10.1042/BST0330891.
 58. Ridley, A.J. Rho Family Proteins: Coordinating Cell Responses. *Trends Cell Biol.* **2001**, *11*, 471–477, doi:10.1016/s0962-8924(01)02153-5.
 59. Haga, R.B.; Ridley, A.J. Rho GTPases: Regulation and Roles in Cancer Cell Biology. *Small GTPases* **2016**, *7*, 207–221, doi:10.1080/21541248.2016.1232583.
 60. Etienne-Manneville, S.; Hall, A. Rho GTPases in Cell Biology. *Nature* **2002**, *420*, 629–635, doi:10.1038/nature01148.
 61. Fujioka, Y.; Tsuda, M.; Nanbo, A.; Hattori, T.; Sasaki, J.; Sasaki, T.; Miyazaki, T.; Ohba, Y. A Ca²⁺-Dependent Signalling Circuit Regulates Influenza A Virus Internalization and Infection. *Nat. Commun.* **2013**, *4*, 1–13, doi:10.1038/ncomms3763.
 62. Hoppe, S.; Schelhaas, M.; Jaeger, V.; Liebig, T.; Petermann, P.; Knebel-Mörsdorf, D. Early Herpes Simplex Virus Type 1 Infection Is Dependent on Regulated Rac1/Cdc42 Signalling in Epithelial MDCKII Cells. *J. Gen. Virol.* **2006**, *87*, 3483–3494, doi:10.1099/vir.0.82231-0.
 63. Zamudio-Meza, H.; Castillo-Alvarez, A.; González-Bonilla, C.; Meza, I. Cross-Talk between Rac1 and Cdc42 GTPases Regulates Formation of Filopodia Required for Dengue Virus Type-2 Entry into HMEC-1 Cells. *J. Gen. Virol.* **2009**, *90*, 2902–2911, doi:10.1099/vir.0.014159-0.
 64. Frampton, A.R.; Uchida, H.; von Einem, J.; Goins, W.F.; Grandi, P.; Cohen, J.B.; Osterrieder, N.; Glorioso, J.C. Equine Herpesvirus Type 1 (EHV-1) Utilizes Microtubules, Dynein, and ROCK1 to Productively Infect Cells. *Vet. Microbiol.* **2010**, *141*, 12–21, doi:10.1016/j.vetmic.2009.07.035.
 65. Wang, J.-L.; Zhang, J.-L.; Chen, W.; Xu, X.-F.; Gao, N.; Fan, D.-Y.; An, J. Roles of Small GTPase Rac1 in the Regulation of Actin Cytoskeleton during Dengue Virus Infection. *PLoS Negl. Trop. Dis.* **2010**, *4*, e809, doi:10.1371/journal.pntd.0000809.
 66. Zhang, J.; Wu, N.; Gao, N.; Yan, W.; Sheng, Z.; Fan, D.; An, J. Small G Rac1 Is Involved in Replication Cycle of Dengue Serotype 2 Virus in EAhy926 Cells via the Regulation of Actin Cytoskeleton. *Sci. China Life Sci.* **2016**, *59*, 487–494, doi:10.1007/s11427-016-5042-5.
 67. Fernandes, J.J.; Atreya, K.B.; Desai, K.M.; Hall, R.E.; Patel, M.D.; Desai, A.A.; Benham, A.E.; Mable, J.L.; Straessle, J.L. A Dominant Negative Form of Rac1 Affects Myogenesis of Adult Thoracic Muscles in *Drosophila*. *Dev. Biol.* **2005**, *285*, 11–27, doi:10.1016/j.ydbio.2005.05.040.
 68. Akeda, Y.; Kodama, T.; Kashimoto, T.; Cantarelli, V.; Horiguchi, Y.; Nagayama, K.; Iida, T.; Honda, T. Dominant-Negative Rho, Rac, and

- Cdc42 Facilitate the Invasion Process of *Vibrio Parahaemolyticus* into Caco-2 Cells. *Infect. Immun.* **2002**, *70*, 970–973, doi:10.1128/IAI.70.2.970-973.2002.
69. Cuartas-López, A.M.; Hernández-Cuellar, C.E.; Gallego-Gómez, J.C. Disentangling the Role of PI3K/Akt, Rho GTPase and the Actin Cytoskeleton on Dengue Virus Infection. *Virus Res.* **2018**, *256*, 153–165, doi:10.1016/j.virusres.2018.08.013.
 70. Johnson, F.B.; Fenn, L.B.; Owens, T.J.; Faucheux, L.J.; Blackburn, S.D. Attachment of Bovine Parvovirus to Sialic Acids on Bovine Cell Membranes. *J. Gen. Virol.* **2004**, *85*, 2199–2207, doi:10.1099/vir.0.79899-0.
 71. Summerford, C.; Bartlett, J.S.; Samulski, R.J. AVβ5 Integrin: A Co-Receptor for Adeno-Associated Virus Type 2 Infection. *Nat. Med.* **1999**, *5*, 78–82, doi:10.1038/4768.
 72. Sanlioglu, S.; Benson, P.K.; Yang, J.; Atkinson, E.M.; Reynolds, T.; Engelhardt, J.F. Endocytosis and Nuclear Trafficking of Adeno-Associated Virus Type 2 Are Controlled by Rac1 and Phosphatidylinositol-3 Kinase Activation. *J. Virol.* **2000**, *74*, 9184–9196, doi:10.1128/JVI.74.19.9184-9196.2000.
 73. Ueda, M.; Daidoji, T.; Du, A.; Yang, C.-S.; Ibrahim, M.S.; Ikuta, K.; Nakaya, T. Highly Pathogenic H5N1 Avian Influenza Virus Induces Extracellular Ca²⁺ Influx, Leading to Apoptosis in Avian Cells. *J. Virol.* **2010**, *84*, 3068–3078, doi:10.1128/JVI.01923-09.
 74. Vanhaesebroeck, B.; Stephens, L.; Hawkins, P. PI3K Signalling: The Path to Discovery and Understanding. *Nat. Rev. Mol. Cell Biol.* **2012**, *13*, 195–203, doi:10.1038/nrm3290.
 75. Alberts, B.; Johnson, A.; Lewis, J.; Raff, M.; Roberts, K.; Walter, P. *Molecular Biology of the Cell*, 4th ed.; Garland Science, 2002; ISBN 978-0-8153-3218-3.
 76. van Meer, G.; Voelker, D.R.; Feigenson, G.W. Membrane Lipids: Where They Are and How They Behave. *Nat. Rev. Mol. Cell Biol.* **2008**, *9*, 112–124, doi:10.1038/nrm2330.
 77. Doherty, G.J.; McMahon, H.T. Mechanisms of Endocytosis. *Annu. Rev. Biochem.* **2009**, *78*, 857–902, doi:10.1146/annurev.biochem.78.0813.07.110540.
 78. Chen, E.H.; Olson, E.N. Unveiling the Mechanisms of Cell-Cell Fusion. *Science* **2005**, *308*, 369–373, doi:10.1126/science.1104799.
 79. Eitzen, G. Actin Remodeling to Facilitate Membrane Fusion. *Biochim. Biophys. Acta BBA - Mol. Cell Res.* **2003**, *1641*, 175–181, doi:10.1016/S0167-4889(03)00087-9.
 80. Zhang, C.; Zhu, S.; Wei, L.; Yan, X.; Wang, J.; Quan, R.; She, R.; Hu, F.; Liu, J. Recombinant Flagellin-Porcine Circovirus Type 2 Cap Fusion Protein Promotes Protective Immune Responses in Mice. *PLoS ONE* **2015**, *10*, e0129617, doi:10.1371/journal.pone.0129617.
 81. Mercer, J. Viral Apoptotic Mimicry Party: P.S. Bring Your Own Gas6. *Cell Host Microbe* **2011**, *9*, 255–257, doi:10.1016/j.chom.2011.04.002.
 82. de Freitas Balanco, J.M.; Costa Moreira, M.E.; Bonomo, A.; Bozza, P.T.; Amarante-Mendes, G.; Pirmez, C.; Barcinski, M.A. Apoptotic Mimicry by an Obligate Intracellular Parasite Downregulates Macrophage Microbicidal Activity. *Curr. Biol.* **2001**, *11*, 1870–1873, doi:10.1016/S0960-9822(01)00563-2.
 83. Amara, A.; Mercer, J. Viral Apoptotic Mimicry. *Nat. Rev. Microbiol.* **2015**, *13*, 461–469, doi:10.1038/nrmicro3469.
 84. Buchmann, J.P.; Holmes, E.C. Cell Walls and the Convergent Evolution of the Viral Envelope. *Microbiol. Mol. Biol. Rev.* **2015**, *79*, 403–418, doi:10.1128/MMBR.00017-15.
 85. Zimmerberg, J.; Chernomordik, L.V. Membrane Fusion. *Adv. Drug Deliv. Rev.* **1999**, *38*, 197–205, doi:10.1016/S0169-409X(99)00029-0.
 86. Leikin, S.L.; Kozlov, M.M.; Chernomordik, L.V.; Markin, V.S.; Chizmadzhev, Y.A. Membrane Fusion: Overcoming of the Hydration Barrier and Local Restructuring. *J. Theor.*

- Biol.* **1987**, *129*, 411–425, doi:10.1016/S0022-5193(87)80021-8.
87. White, J.M.; Whittaker, G.R. Fusion of Enveloped Viruses in Endosomes. *Traffic* **2016**, *17*, 593–614, doi:10.1111/tra.12389.
 88. Harrison, S.C. Viral Membrane Fusion. *Nat. Struct. Mol. Biol.* **2008**, *15*, 690–698, doi:10.1038/nsmb.1456.
 89. Harrison, S.C. Viral Membrane Fusion. *Virology* **2015**, *479–480*, 498–507, doi:10.1016/j.virol.2015.03.043.
 90. Shmulevitz, M.; Duncan, R. A New Class of Fusion-Associated Small Transmembrane (FAST) Proteins Encoded by the Non-Enveloped Fusogenic Reoviruses. *EMBO J.* **2000**, *19*, 902–912, doi:10.1093/emboj/19.5.902.
 91. Weed, D.J.; Nicola, A.V. Herpes Simplex Virus Membrane Fusion. *Adv. Anat. Embryol. Cell Biol.* **2017**, *223*, 29–47, doi:10.1007/978-3-319-53168-7_2.
 92. Cole, N.L.; Grose, C. Membrane Fusion Mediated by Herpesvirus Glycoproteins: The Paradigm of Varicella-Zoster Virus. *Rev. Med. Virol.* **2003**, *13*, 207–222, doi:10.1002/rmv.377.
 93. Markosyan, R.M.; Miao, C.; Zheng, Y.-M.; Melikyan, G.B.; Liu, S.-L.; Cohen, F.S. Induction of Cell-Cell Fusion by Ebola Virus Glycoprotein: Low PH Is Not a Trigger. *PLOS Pathog.* **2016**, *12*, e1005373, doi:10.1371/journal.ppat.1005373.
 94. Bornholdt, Z.A.; Ndungo, E.; Fusco, M.L.; Bale, S.; Flyak, A.I.; Crowe, J.E.; Chandran, K.; Saphire, E.O. Host-Primed Ebola Virus GP Exposes a Hydrophobic NPC1 Receptor-Binding Pocket, Revealing a Target for Broadly Neutralizing Antibodies. *mBio* **2016**, *7*, doi:10.1128/mBio.02154-15.
 95. Podbilewicz, B. Virus and Cell Fusion Mechanisms. *Annu. Rev. Cell Dev. Biol.* **2014**, *30*, 111–139, doi:10.1146/annurev-cellbio-101512-122422.
 96. Raghu, H.; Sharma-Walia, N.; Veettil, M.V.; Sadagopan, S.; Caballero, A.; Sivakumar, R.; Varga, L.; Bottero, V.; Chandran, B. Lipid Rafts of Primary Endothelial Cells Are Essential for Kaposi's Sarcoma-Associated Herpesvirus/Human Herpesvirus 8-Induced Phosphatidylinositol 3-Kinase and RhoA-GTPases Critical for Microtubule Dynamics and Nuclear Delivery of Viral DNA but Dispensable for Binding and Entry. *J. Virol.* **2007**, *81*, 7941–7959, doi:10.1128/JVI.02848-06.
 97. Lingwood, D.; Simons, K. Lipid Rafts As a Membrane-Organizing Principle. *Science* **2010**, *327*, 46–50, doi:10.1126/science.1174621.
 98. Simons, K.; Toomre, D. Lipid Rafts and Signal Transduction. *Nat. Rev. Mol. Cell Biol.* **2000**, *1*, 31–39, doi:10.1038/35036052.
 99. Erwig, L.-P.; Henson, P.M. Clearance of Apoptotic Cells by Phagocytes. *Cell Death Differ.* **2008**, *15*, 243–250, doi:10.1038/sj.cdd.4402184.
 100. Wood, W.; Turmaine, M.; Weber, R.; Camp, V.; Maki, R.A.; McKercher, S.R.; Martin, P. Mesenchymal Cells Engulf and Clear Apoptotic Footplate Cells in Macrophageless PU.1 Null Mouse Embryos. *Development* **2000**, *127*, 5245–5252.
 101. Zaitseva, E.; Zaitsev, E.; Melikov, K.; Arakelyan, A.; Marin, M.; Villasmil, R.; Margolis, L.B.; Melikyan, G.B.; Chernomordik, L.V. Fusion Stage of HIV-1 Entry Depends on Virus-Induced Cell Surface Exposure of Phosphatidylserine. *Cell Host Microbe* **2017**, *22*, 99-110.e7, doi:10.1016/j.chom.2017.06.012.
 102. Maitani, Y.; Ishigaki, K.; Nakazawa, Y.; Aragane, D.; Akimoto, T.; Iwamizu, M.; Kai, T.; Hayashi, K. Polyethylenimine Combined with Liposomes and with Decreased Numbers of Primary Amine Residues Strongly Enhanced Therapeutic Antiviral Efficiency against Herpes Simplex Virus Type 2 in a Mouse Model. *J. Controlled Release* **2013**, *166*, 139–146, doi:10.1016/j.jconrel.2012.12.027.
 103. Tahara, K.; Kobayashi, M.; Yoshida, S.; Onodera, R.; Inoue, N.; Takeuchi, H. Effects of Cationic Liposomes with Stearylamine against Virus Infection. *Int. J. Pharm.* **2018**,

- 543, 311–317,
doi:10.1016/j.ijpharm.2018.04.001.
104. Ellis, S.; Mellor, H. The Novel Rho-Family GTPase Rif Regulates Coordinated Actin-Based Membrane Rearrangements. *Curr. Biol.* **2000**, *10*, 1387–1390, doi:10.1016/S0960-9822(00)00777-6.
105. Jin, M.; Guan, C.; Jiang, Y.; Chen, G.; Zhao, C.; Cui, K.; Song, Y.; Wu, C.; Poo, M.; Yuan, X. Ca²⁺-Dependent Regulation of Rho GTPases Triggers Turning of Nerve Growth Cones. *J. Neurosci.* **2005**, *25*, 2338–2347, doi:10.1523/JNEUROSCI.4889-04.2005.
106. Kreuger, J.; Spillmann, D.; Li, J.; Lindahl, U. Interactions between Heparan Sulfate and Proteins: The Concept of Specificity. *J. Cell Biol.* **2006**, *174*, 323–327, doi:10.1083/jcb.200604035.
107. Eskandarynasab, M.; Doustimotlagh, A.H.; Takzaree, N.; Etemad-Moghadam, S.; Alaeddini, M.; Dehpour, A.R.; Goudarzi, R.; Partoazar, A. Phosphatidylserine Nanoliposomes Inhibit Glucocorticoid-Induced Osteoporosis: A Potential Combination Therapy with Alendronate. *Life Sci.* **2020**, *257*, 118033, doi:10.1016/j.lfs.2020.118033.
108. Fan, D.; Bucana, C.D.; O'Brian, C.A.; Zwelling, L.A.; Seid, C.; Fidler, I.J. Enhancement of Murine Tumor Cell Sensitivity to Adriamycin by Presentation of the Drug in Phosphatidylcholine-Phosphatidylserine Liposomes. *Cancer Res.* **1990**, *50*, 3619–3626.
109. Tomizawa, H.; Aramaki, Y.; Fujii, Y.; Kara, T.; Suzuki, N.; Yachi, K.; Kikuchi, H.; Tsuchiya, S. Uptake of Phosphatidylserine Liposomes by Rat Peyer's Patches Following Intraluminal Administration. *Pharm. Res.* **1993**, *10*, 549–552, doi:10.1023/A:1018945902276.
110. Veetil, M.V.; Sharma-Walia, N.; Sadagopan, S.; Raghu, H.; Sivakumar, R.; Naranatt, P.P.; Chandran, B. RhoA-GTPase Facilitates Entry of Kaposi's Sarcoma-Associated Herpesvirus into Adherent Target Cells in a Src-Dependent Manner. *J. Virol.* **2006**, *80*, 11432–11446, doi:10.1128/JVI.01342-06.
111. Kumar, D.; Lassar, A.B. The Transcriptional Activity of Sox9 in Chondrocytes Is Regulated by RhoA Signaling and Actin Polymerization. *Mol. Cell. Biol.* **2009**, *29*, 4262–4273, doi:10.1128/MCB.01779-08.
112. Anderson, B.R.; Karikó, K.; Weissman, D. Nucleofection Induces Transient EIF2 α Phosphorylation by GCN2 and PERK. *Gene Ther.* **2013**, *20*, 136–142, doi:10.1038/gt.2012.5.
113. McMahon, C.; Baier, A.S.; Pascolutti, R.; Wegrecki, M.; Zheng, S.; Ong, J.X.; Erlandson, S.C.; Hilger, D.; Rasmussen, S.G.F.; Ring, A.M.; et al. Yeast Surface Display Platform for Rapid Discovery of Conformationally Selective Nanobodies. *Nat. Struct. Mol. Biol.* **2018**, *25*, 289–296, doi:10.1038/s41594-018-0028-6.
114. Yang, S.; Guo, C.; Li, Y.; Guo, J.; Xiao, J.; Qing, Z.; Li, J.; Yang, R. A Ratiometric Two-Photon Fluorescent Cysteine Probe with Well-Resolved Dual Emissions Based on Intramolecular Charge Transfer-Mediated Two-Photon-FRET Integration Mechanism. *ACS Sens.* **2018**, *3*, 2415–2422, doi:10.1021/acssensors.8b00919.
115. Shcherbakova, D.M.; Cox Cammer, N.; Huisman, T.M.; Verkhusha, V.V.; Hodgson, L. Direct Multiplex Imaging and Optogenetics of Rho GTPases Enabled by Near-Infrared FRET. *Nat. Chem. Biol.* **2018**, *14*, 591–600, doi:10.1038/s41589-018-0044-1.

Chapter 2

Differentially-Charged Liposomes Interact with Alphaherpesviruses and Interfere with Virus Entry

Oleksandr Kolyvushko ¹, Juliane Latzke ¹, Ismail Dahmani ², Nikolaus Osterrieder ¹,
Salvatore Chiantia ² and Walid Azab ¹

¹ Institut für Virologie, Robert von Ostertag-Haus, Zentrum für Infektionsmedizin, Freie Universität Berlin, Robert-von-Ostertag-Street 7-13, 14163 Berlin, Germany; olek@zedat.fu-berlin.de (O.K.); j.latzke@fu-berlin.de (J.L.); no.34@fu-berlin.de (N.O.)

² Institute of Biochemistry and Biology, University of Potsdam, Karl-Liebknecht-Street 24-25, 14476 Potsdam, Germany; dahsmail@gmail.com (I.D.); chiantia@uni-potsdam.de (S.C.)

Pathogens **2020**, *9*(5), 359

<https://doi.org/10.3390/pathogens9050359>

2.1 Abstract

Exposure of phosphatidylserine (PS) in the outer leaflet of the plasma membrane is induced by infection with several members of the Alphaherpesvirinae subfamily. There is evidence that PS is used by the equine herpesvirus type 1 (EHV-1) during entry, but the exact role of PS and other phospholipids in the entry process remains unknown. Here, we investigated the interaction of differently charged phospholipids with virus particles and determined their influence on infection. Our data show that liposomes containing negatively charged PS or positively charged DOTAP [N-[1-(2,3-Dioleoyloxy)propyl]-N,N,N-trimethylammonium] inhibited EHV-1 infection, while neutral phosphatidylcholine (PC) had no effect. Inhibition of infection with PS was transient, decreased with time, and was dose dependent. Our findings indicate that both cationic and anionic phospholipids can interact with the virus and reduce infectivity, while, presumably, acting through different mechanisms. Charged phospholipids were found to have antiviral effects and can may be used to inhibit EHV-1 infection.

2.2 Importance

Cell entry is one of the first steps in virus infection of the target cell. Equid herpesvirus type 1 (EHV-1) is an important pathogen affecting equids worldwide. EHV-1 binding to cellular receptors involves activation of phospholipid scramblase and subsequent exposure of the PS on the outer leaflet of the plasma membrane. Application of phospholipids can change the outcome of infection, and understanding the mechanism and factors involved in this step may lead to improved control of infection.

2.3 Introduction

Phospholipids have been shown to be necessary for enveloped viruses to promote infection. Phosphatidylserine (PS) is used as a receptor by different viruses [1,2]. Recently, it was shown that PS exposure on cell surface occurs shortly after equine herpesvirus type 1 (EHV-1) contacts the cell [3]. Similar findings for another alphaherpesvirus, herpes simplex virus type 1 (HSV-1), were reported [4]. Exogenous PS and the anionic lipid phosphatidylglycerol facilitate cell-to-cell fusion of cells expressing human immunodeficiency virus 1 (HIV-1) proteins. This led to the conclusion that specific interactions can occur between virus particles and cellular phospholipids [5]. Here, we investigated the role of PS as well as other phospholipids during virus infection. Furthermore, we assessed the specificity of the interaction between EHV-1 and differentially charged phospholipids. To this end, we used small unilamellar vesicles (SUV) composed of exogenous lipids that have different charges: (i) negatively charged PS; (ii) positively charged DOTAP [N-[1-(2,3-Dioleoyloxy)propyl]-N,N,N-trimethylammonium]); or (iii) neutral phosphatidylcholine (PC). We investigated the interaction between virus particles and the different phospholipids by means of surface plasmon resonance (SPR) and visualized virus interaction with giant unilamellar vesicles (GUV) or large unilamellar vesicles (LUV) via confocal microscopy.

2.4 Results

2.4.1 DOTAP and PS liposomes inhibit viral infection

Three types of lipids were tested: positively charged DOTAP, negatively charged PS, and neutral PC. Equine dermal (ED) cells were treated with SUVs containing PS, PC or DOTAP:PC (1:1) at a concentration of 200 μ M or 300 μ M for 3 hours prior to infection with EHV-1. ED cells infected without previous SUV treatment were used as a control. Positively and negatively charged DOTAP and PS lipids significantly inhibited EHV-1 infection (Figure 1A). In contrast, neutral PC SUVs had no effect on virus infection. At a concentration of 300 μ M of all lipid preparations, none of the SUVs significantly affected cell viability after a 24 hour incubation period (Figure 1C).

In another experiment, ED cells were incubated with 300 μ M PS SUVs for different times (0, 1, 2, or 3 hours) and then infected with EHV-1 for 24 hours. At all time points, virus infection was significantly inhibited in the presence of PS (Figure 1B). The dataset termed "3H transient" represents the treatment of ED cells with 300 μ M PS SUVs for 3 hours, before the SUVs were removed by 3 consecutive washes with PBS and addition of EHV-1 to the cells at an MOI of 0.1. Interestingly, there was no inhibition of virus infection in the absence of PS, indicating that the inhibitory effect of PS is transient and only effective if PS liposomes are present at the time of virus exposure (Figure 1B). Longer incubation of cells with PS rescued EHV-1 infectivity, although at significantly lower levels when compared with that in non-treated cells (Figure 1B). It is worth mentioning that EHV-4, a close relative to EHV-1, was also inhibited in a similar fashion (data not shown).

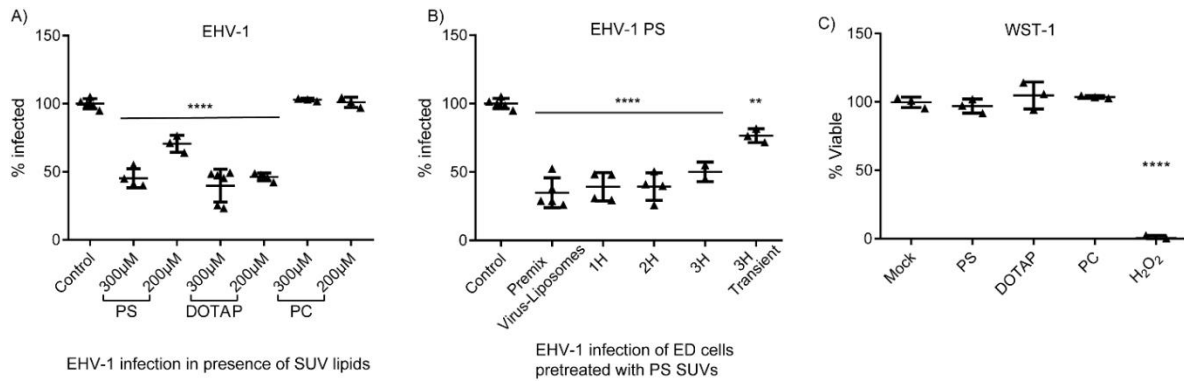


Figure 2.1. Phospholipids inhibit EHV-1 infection. (A) Effects of lipid concentration on EHV-1 infection. ED cells were treated with 200 μM or 300 μM of SUVs (PS, DOTAP:PC 1:1, or PC SUVs) for 3 hours and infected with EHV-1 at an MOI of 0.1. GFP expression at 24 hours post infection was measured by FACS. (B) ED cells were treated with 300 μM of PS SUVs for different times (0; Premix Virus-Liposomes, 1, 2, or 3 hours) and then infected with EHV-1 at MOI of 0.1. GFP expression at 24 hours post infection was measured by FACS. Control: cells infected with viruses without previous treatment with lipids. 3H Transient: SUVs were removed by washing the cells 3 times with PBS before infection. (C) Cell viability assay, cells were treated with SUVs composed of PS, DOTAP:PC (1:1) or PC lipids for 24 hours. Mock-treated cells and cells treated with H₂O₂ (30%) were used as the 100% and 0% viability controls, respectively. No significant differences between treatment groups and mock control were found. $p < 0.05$, Kolmogorov-Smirnov normality test followed by One Way ANOVA with Dunnett's multiple comparison test. Asterisks indicate a significant difference of lipid-treated to the control non-treated cells.

2.4.2 Interaction of viral particles with phospholipids.

Fluorescently (Cy 5.5 PE)-labeled LUVs composed of three different lipids (PS, PC, or DOTAP:PC 1:1) were mixed with EHV-1-RFP at an MOI of 5 and added to ED cells. The cells were incubated for 1 hour on ice to allow virus binding without internalization. Cells were fixed with 4% PFA and visualized with a confocal microscope. Viral particles (all of the 103 virus particles counted blindly on 10 cells) were found to significantly colocalized with DOTAP LUVs when compared to PS LUVs (P value < 0.00001 ; Fisher's exact test). Colocalization was much less frequently observed with PS (27 out of 105 virus particles counted blindly in 13 cells) or PC (4 out of 108 virus particles counted blindly in 17 cells) LUVs (Figure 2A).

Under cell-free conditions, fluorescent confocal microscopy was used to quantify the specific binding between RFP-labeled EHV-1 and GUVs of different composition: PC, PC:PS (1:1) or DOTAP:PC (1:1) (Figure 2B); GUVs composed entirely of DOTAP or PS could not be obtained at high enough yield. Mean fluorescence intensity was measured in 15-21 vesicles for each lipid composition in two independent experiments. Our data showed that EHV-1 bound more tightly to DOTAP:PC (1:1) GUVs when compared to PS:PC (1:1) and PC GUVs (Figure 2B and C). Additionally, surface plasmon resonance (SPR) was used to detect binding dynamics of viral particles to PS, PC or DOTAP lipids (Figure 2D). A lipid monolayer was formed, and purified virus was injected until an equilibrium was reached. In the case of PC, binding was very low (ca. 400 ± 100 RU, $n=2$) and equilibrium was reached after around 10 min. Binding of the virus to PS monolayers was intermediate (ca. $3,500 \pm 800$ RU, $n=4$), but should only be considered an estimate, since no clear equilibrium was observed even after 40 minutes. Binding to DOTAP reached an equilibrium within the injection time and was quantified at approximately $7,000 \pm 500$ RU ($n=2$).

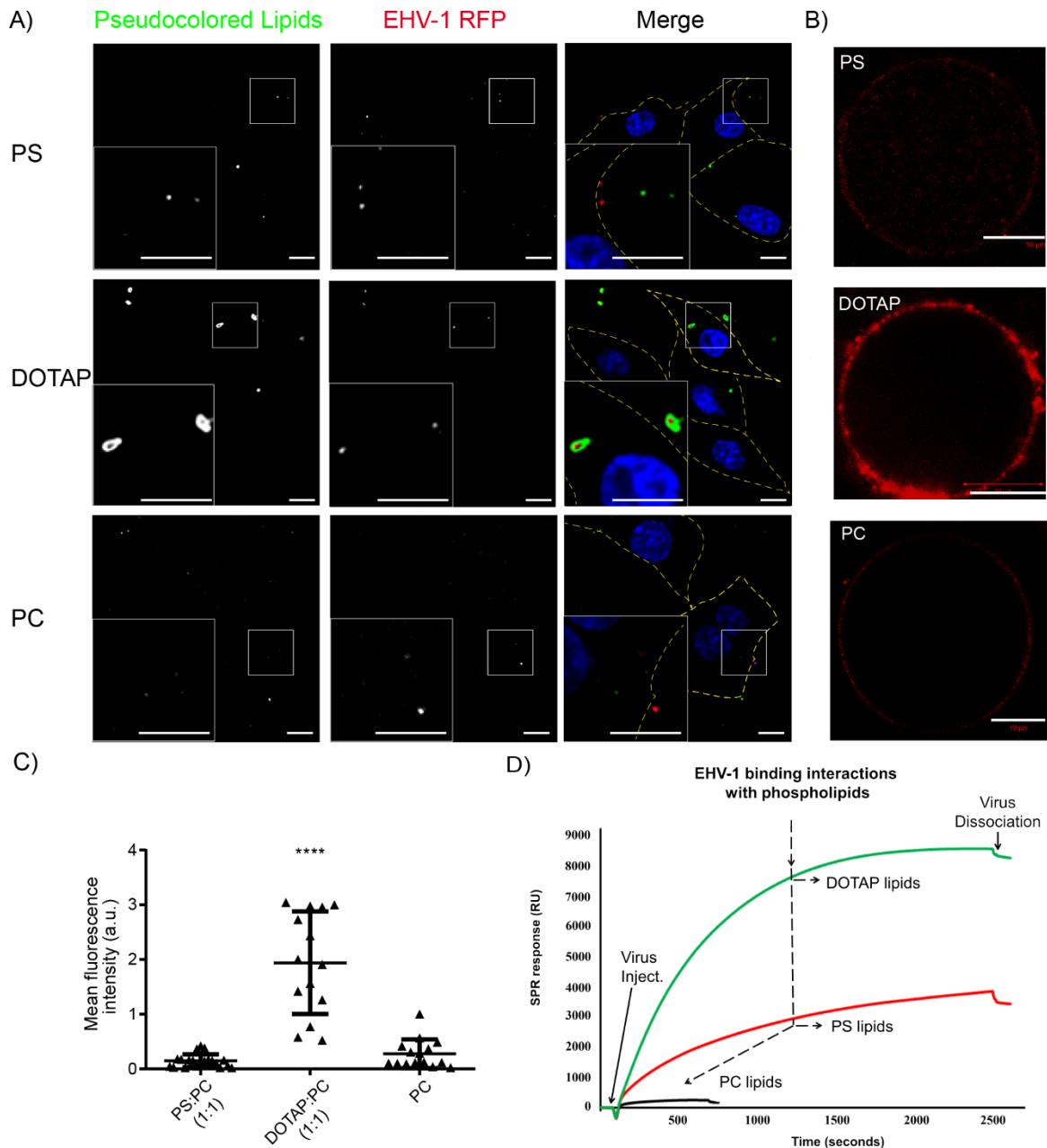


Figure 2.2. Virus interaction with phospholipids. (A) EHV-1-RFP (MOI = 5) was mixed with fluorescently labeled large unilamellar vesicles (LUVs) of PS, PC or DOTAP:PC (1:1). The mixture was applied to ED cells that were incubated for 1 hour on ice. Green: pseudocolored fluorescently labeled LUVs; Red: RFP-labeled viruses; Blue: DAPI stained nucleus. Merge panels: dotted lines represent the boundaries of cells. Scale bar = 10 μm . (B) Binding of EHV-1-RFP to GUVs. Pictures of GUVs made of PS:PC (1:1), DOTAP:PC (1:1), PC with bound RFP-labeled virus. Scale bars indicate 10 μm . (C) Quantification of the average signal in 15-21 GUVs from two independent experiments for each lipid compositions: PC, PC:PS (1:1) or DOTAP:PC (1:1). ****p < 0.0001 (One Way ANOVA with Dunnet's test was used to correct for multiple comparisons). (D) Surface plasmon resonance (SPR) analysis of EHV-1 interactions with model membrane composed of neutral, cationic or anionic phospholipids. Representative sensorgrams after curve alignment show the virus association to the immobilized lipid monolayer composed of DOTAP 100 mol%, PC 100 mol% or PS 100 mol%. RU: corrected SPR response unit.

2.5 Discussion

We report here that PS and DOTAP inhibit the infection of ED cells by EHV-1. The inhibition is immediate, reversible, and dose-dependent. Previously, we showed that EHV-1

facilitates scramblase-dependent exposure of PS on the outer leaflet of the plasma membrane, suggesting that there is a specific, yet unknown, role for PS in fusion with the plasma membrane [3]. Thus, we surmised that integration of external PS would promote fusion and enhance the infection process [5]. Contrary to our expectations, we found that EHV-1 infection was reduced in the presence of PS.

The hypothesis that PS liposomes are blocking the infection after integration into the plasma membrane of the target cell, as was described for HIV before [5], was not supported by our data, because (i) there was no significant change in virus inhibition with increase in duration of incubation times; (ii) significant inhibition was observed immediately after addition (0 hour time point); (iii) removal of PS liposomes prior to infection rescued virus infection. From our results we concluded that the mechanism of virus entry, although appearing similar, is distinct between HIV and herpesviruses.

Higher concentration of PS resulted in more pronounced reduction of infection. EHV-1 induces localized PS exposure during the early stages of infection [3] and, presumably, viral particles have the capacity to bind to PS to facilitate membrane fusion. Possibly, addition of external PS may transiently bind to the viral particles and thus reduce infectivity. When media containing PS was removed, cells regained susceptibility to infection independently of previous exposure to PS. We surmise that free PS liposomes in media are interfering specifically with the process of virus-cell interaction (binding) with EHV-1. It is likely that EHV-1 envelope glycoproteins, like those of other viruses, feature a phospholipid (PS)-binding domain that enables virus binding to different phospholipids of the plasma membrane to facilitate entry [3,6,7]. Addition of exogenous PS can interact with herpesviral glycoproteins, particularly gH/gL and gB, and block virus entry as was described for other viruses [6]. On the other hand, it is possible that PS is redistributing the charges on the cell surface in a fashion that makes the initial contact between virus particles and cell surface proteoglycans containing heparan sulfate less likely, thus reducing the probability of virus entry. However, the exact mechanism of how PS is blocking the infection needs to be investigated.

Our confocal microscopy and SPR data both confirmed that PS interact with EHV-1. Although the microscopy data did not show strong interaction between PS and virus particles, the SPR data indicated a stronger interaction as compared to neutral liposomes (PC). It became clear in our study that SPR analysis is more sensitive than microscopic examination. It can detect binding of small amounts of phospholipids from exosomes, cell debris or other impurities from the virus purification process that could interact with virus particles, but remains undetected by confocal microscopy. This approach is complementary to confocal microscopy, which is more specific since it relies on labeled viral and lipid particles.

Our data provides evidence of virus interaction with DOTAP, as is the case with PS. Both the SPR and confocal microscopy results showed that interaction of EHV-1 with the cationic DOTAP is stronger than that with PS, whereas there is no interaction with PC. Positively charged DOTAP also had an inhibitory effect on EHV-1 infection. However, unlike in the case of PS lipids, the strong interaction between DOTAP and virus particles (Figure 2) can be explained by the negative charge of the virus particle that can attract cationic DOTAP vesicles. The strong liposome-virus interaction in turn leads to a reduction of infection through preventing virus from interacting with its cognate cellular receptors. The electrostatic interaction (of DOTAP with EHV-1) is in-line with the data describing that herpesviruses possess a negative overall charge [8], probably due to anionic lipids present in the envelope and to the protein's net charges and glycans, which carry charged carboxy- or sulfate groups. Zwitterionic lipid PC, on the other hand, showed no binding with EHV-1, and had no effect on infection.

Strong inhibitory effect of DOTAP and PS that was observed in-vitro, could point further investigation into the biophysical interaction between virus and the cell and would improve our understanding of infection process. Furthermore, as phospholipids are important for the entry of several viruses, they might have a great potential as antiviral agents.

2.6 Materials and Methods

2.6.1 Viruses and Cells

Equine herpesvirus type 1 strain RacL11 EHV-1-RFP [9] with a red fluorescent protein (RFP) fused to the small capsid protein VP26 [3] was used in this study. The virus further expresses the enhanced green fluorescent protein (eGFP) for efficient identification of infected cells. The virus was grown on primary equine dermal (ED) cells (CCLV-RIE 1222, Federal Research Institute for Animal health, Germany) as described before [3]. The cells were propagated in Isocove's Liquid Medium with stable glutamine (Pan - Biotech GmbH) supplemented with 20% fetal calf serum (Pan - Biotech GmbH), 0.5% penicillin (Roth), 0.5% streptomycin (Alfa Aesar), 1% sodium pyruvate 100 mM (Pan - Biotech GmbH) and 1% nonessential amino acids (Merck KGaA). For microscopy experiments, virus was purified by ultracentrifugation over a 30% sucrose solution followed by sucrose step gradient ultracentrifugation exactly as described before [10].

2.6.2 Phospholipids

Phosphatidylserine (PS; 1,2-dioleoyl-sn-glycero-3-phospho-L-serine; number: 840035), phosphatidylcholine (PC; 1,2-dioleoyl-sn-glycero-3-phosphocholine; number: 850375), and DOTAP (1,2-dioleoyl-3-trimethylammonium-propane; number: 890890) were purchased from Avanti Polar Lipids, USA. Multilamellar vesicles (MLVs) were prepared at concentration of 1 mM. Lipid stock was dissolved in ultrapure chloroform (Sigma Aldrich, Germany) in a glass vial. The solvent was evaporated under gentle flow of nitrogen and lipids were kept in a desiccator with calcium chloride overnight. The dry lipid film was resuspended in phosphate-buffered saline (PBS) with at least 2 hours of shaking at 200 rpm at room temperature. The resulting opaque 1 mM MLV solution was stored at -80°C. Large unilamellar vesicles (LUVs) were generated via extrusion through a polycarbonate membrane with 0.1 µm pore size. The extruder setup consisted of two syringes and the extruder itself, all held together by a holding block (Avanti Polar Lipids, USA). Extrusion was performed at a constant temperature of 37°C, and LUVs were stored at 4°C for up to 3 days. The mixture of MLVs was passed through the membrane 31 times to ensure homogeneous LUV size. Small unilamellar vesicles (SUVs) were produced through ultrasonication of MLVs in 1.5 ml tubes at room temperature, with ultrasonic frequency: 35 kHz, ultrasonic peak output: 320 W, in a Sonorex Super RK100 (Bandelin, Germany). Ultrasonication was carried out in two 15-minutes steps, with vortexing in between. SUVs and LUVs used throughout this study were composed of either 100 mol% PS, 100 mol% PC or 1:1 DOTAP:PC. All SUVs and LUVs were labeled via addition of DHPE, Oregon Green™ 488 (1,2-Dihexadecanoyl-sn-Glycero-3-Phosphoethanolamine, Thermo Fisher Scientific, USA-IL, Rockford) and 18:0 Cy5.5 PE1,2-distearoyl-sn-glycero-3-phosphoethanolamine-N-(Cyanine 5.5) (Avanti Polar Lipids, USA). During the preparation process, a final concentration of 0.01 to 0.05 mol% was used for both fluorescent lipids. All lipid preparations were tested for their possible cytotoxic effects on cells using WST-1 cell proliferation assay kit (Cayman chemical, USA) [11,12].

Giant unilamellar vesicles (GUVs) were produced through electroformation [13]. Briefly, a lipid solution in organic solvent with the desired lipid components was dried on indium tin oxide (ITO) coated glass slides. After evaporation of the solvent, a swelling solution of 150 mM sucrose was carefully added. The two ITO slides were separated by a 3-mm thick Teflon spacer. An alternating current (AC) with a 10 Hz sine wave, and electric potential difference of 0.5 V was applied for the first 30 minutes, following by 1.0 V for 30 minutes and 1.6 V for 30 minutes. The resulting GUVs were assessed via confocal microscopy. In order to increase the yield of the electroformation process, PS-containing GUVs were prepared with a composition of 1:1 PS:PC (rather than 100% PS, as used for SUVs or LUVs).

2.6.3 Flow cytometry

Approximately 30,000 cells were treated with freshly prepared SUVs of the appropriate lipids (PS, PC, or DOTAP:PC 1:1; 300 µM), and incubated for different periods (0, 1, 2, and 3 hours) at 37°C and 5% CO₂. Afterwards, cells were infected in the presence of SUVs with EHV-

1 at a multiplicity of infection (MOI) of 0.1. At the 0 time point (Premix Virus-Liposomes), lipids were mixed with viruses and immediately added to the cells. Mock-treated cells (i.e. cells without addition of lipids) were infected with EHV-1 and used as positive controls. In another experiment, cells were incubated with different concentrations, 200 μ M or 300 μ M, of lipids (PS, PC, or DOTAP:PC 1:1) for 3 hours before infection with EHV-1 (MOI = 0.1). Twenty-four hours post infection, 10,000 cells were analyzed using CytoFLEX S (Beckman Coulter, Germany). The subset of GFP positive cells among viable population was considered infected. The percent of GFP-positive cells in the mock-treated group was set to 100%.

2.6.4 Surface plasmon resonance

This experiment was performed on a SPR GE Biacore J Biomolecular Interaction Analyser instrument (Uppsala, Sweden) using a lipid-coated HPP sensor chip (XanTec bioanalytics GmbH) prepared according to the protocol provided by the chip vendor. All solutions were freshly prepared, degassed, and filtered through 0.22 μ m-pore filters and measurements were performed at 24 °C in PBS (pH 7.4). Prior to use, the surface of the HPP chip was cleaned by an injection of the nonionic detergent N-octyl β -d-glucopyranoside (100 μ l, 40 mM) at low flow setting. PS (100 mol%), PC (100 mol%) and DOTAP (100 mol%) liposomes (1 mM) were injected as required over the surface of the HPP sensor chip for 60 minutes. Note that DOTAP and PS liposomes did not contain PC, for all SPR experiments, in order to avoid uncertainties regarding the actual final composition of the lipid monolayer. One of the two available chip channels (flow cells) was incubated in all experiment with PS vesicles. The second channel was treated with either PC or DOTAP vesicles. Then, NaOH (200 μ l, 20 mM) was injected several times until producing a stable baseline with a signal ranging from 2500 to 3200 resonance units (RU), compatible with the presence of a stable lipid monolayer in both channels. EHV-1 was injected simultaneously over the lipid monolayers in both channels and virus binding was monitored for up to 40 minutes, to provide sufficient time for the association phase to reach saturation equilibrium levels (Req) [14]. The dissociation phase was monitored for 5 minutes. Each lipid composition was analyzed in independent duplicates (n=2 for DOTAP and PC, n=4 for PS).

2.6.5 Microscopy

Confocal laser scanning microscopy was conducted with Nikon Eclipse Ti Visitron microscope (Visitron Systems GmbH, Germany) to visualize the colocalization of LUVs with RFP-labeled viruses. A 100x oil immersion objective was used in combination with an EMCCD camera and the VisiVIEW imaging software (Visitron Systems GmbH, Germany). Twenty-four hours before the experiment, 2,000 ED cells were plated in a μ -Slide 8-well (ibidi, USA). On the day of experiment, cells were incubated with a mixture of EHV-1-RFP (MOI of 5) and fluorescently labeled LUVs of PS, PC, or DOTAP:PC 1:1 (300 μ M) for 1 hour on ice. Cells were fixed with 4% paraformaldehyde (PFA), visualized under the microscope, and virus particles (RFP-labeled) were counted as colocalized if the visible portion of the point spread function of the signals were overlapping. The experiment was conducted blindly three independent times.

GUVs were observed with a Zeiss LSM780 system (Carl Zeiss, Oberkochen, Germany) using a 40x, 1.2 numerical aperture water-immersion objective. A fresh suspension of GUVs (either PS:PC 1:1, PC, or DOTAP:PC 1:1) was released from the ITO slide and transferred to imaging chambers. EHV-1-RFP virus was added to allow the interaction with the GUVs. The mixture was incubated at room temperature for at least 20 min prior to imaging. Fluorescence intensities values corresponding to the EHV-1-RFP bound to the GUVs membrane were quantified using Zen Black Software (Carl Zeiss). The vesicles were outlined manually (drawing two circles delimiting the membrane).

2.6.6 Statistical analysis

Experiments were performed in triplicate, unless specified otherwise. Image analysis was performed in a blinded fashion. One-way ANOVA was performed using GraphPad Prism (GraphPad Software, USA). The mean of each treatment groups was compared to the mean of the control group. The Dunnett's test was used to correct for multiple comparisons. Fisher's

exact test was used to compare colocalization of virus particles with DOTAP compared to PS. Values of $p < 0.05$ are considered significant.

2.7 Author Contributions

Conceptualization, W.A. and S.C.; methodology, W.A., O.K., J.L. and I.D.; writing—original draft preparation, O.K.; writing—review and editing, W.A, N.O., S.C. and I.D.; visualization, O.K. and I.D.; supervision, W.A., S.C. and N.O; project administration, W.A. and N.O.; funding acquisition, W.A. and N.O. All authors have read and agreed to the published version of the manuscript

2.8 Funding

This work was supported by grants from the Deutsche Forschungsgemeinschaft (DFG AZ 97/3-2) to WA and Morris Animal Foundation (D19EQ-003) to WA and NO, and unrestricted funds made available by Dr. Manfred Semmer to the Equine Herpesvirus Program at Freie Universität Berlin.

2.9 Acknowledgments

We thank Dr. Chris Höfer for her help with liposome preparation.

2.10 Conflicts of Interest

The authors declare no conflict of interest

2.11 References

1. Moller-Tank, S.; Kondratowicz, A.S.; Davey, R.A.; Rennert, P.D.; Maury, W. Role of the Phosphatidylserine Receptor TIM-1 in Enveloped-Virus Entry. *J. Virol.* 2013, 87, 8327–8341.
2. Morizono, K.; Chen, I.S.Y. Role of Phosphatidylserine Receptors in Enveloped Virus Infection. *J. Virol.* 2014, 88, 4275–4290.
3. Azab, W.; Gramatica, A.; Herrmann, A.; Osterrieder, N. Binding of alphaherpesvirus glycoprotein H to surface $\alpha 4\beta 1$ -integrins activates calcium-signaling pathways and induces phosphatidylserine exposure on the plasma membrane. *mBio* 2015, 6, e01552-01515.
4. Cheshenko, N.; Pierce, C.; Herold, B.C. Herpes simplex viruses activate phospholipid scramblase to redistribute phosphatidylserines and Akt to the outer leaflet of the plasma membrane and promote viral entry. *PLOS Pathog.* 2018, 14, e1006766.
5. Zaitseva, E.; Zaitsev, E.; Melikov, K.; Arakelyan, A.; Marin, M.; Villasmil, R.; Margolis, L.B.; Melikyan, G.B.; Chernomordik, L.V. Fusion Stage of HIV-1 Entry Depends on Virus-Induced Cell Surface Exposure of Phosphatidylserine. *Cell Host Microbe* 2017, 22, 99-110.e7.
6. Estepa, A.; Coll, J.M. Phosphatidylserine binding to solid-phase rhabdoviral peptides: a new method to study phospholipid/viral protein interactions. *J. Virol. Methods* 1996, 61, 37–45.
7. Hall, M.P.; Burson, K.K.; Huestis, W.H. Interactions of a vesicular stomatitis virus G protein fragment with phosphatidylserine: NMR and fluorescence studies. *Biochim. Biophys. Acta* 1998, 1415, 101–113.
8. Kreuger, J.; Spillmann, D.; Li, J.; Lindahl, U. Interactions between heparan sulfate and proteins: the concept of specificity. *J. Cell Biol.* 2006, 174, 323–327.
9. Rudolph, J.; O'Callaghan, D.J.; Osterrieder, N. Cloning of the genomes of equine herpesvirus type 1 (EHV-1) strains KyA and racL11 as bacterial artificial chromosomes (BAC). *J. Vet. Med. B Infect. Dis. Vet. Public Health* 2002, 49, 31–36.
10. Sathananthan, B.; Rødahl, E.; Flatmark, T.; Langeland, N.; Haarr, L. Purification of herpes simplex virus type 1 by density gradient centrifugation and estimation of the sedimentation coefficient of the virion. *APMIS* 1997, 105, 238–246.
11. Assay Guidance Manual; Sittampalam, G.S., Coussens, N.P., Brimacombe, K., Grossman, A., Arkin, M., Auld, D., Austin, C., Baell, J., Bejcek, B., Caaveiro, J.M.M., Chung, T.D.Y., Dahlin, J.L., Devanaryan, V., Foley, T.L., Glicksman, M., Hall, M.D., Haas, J.V., Inglese, J., Iversen, P.W., Kahl, S.D., Kales, S.C., Lal-Nag, M., Li, Z., McGee, J., McManus, O., Riss, T., Trask, O.J., Weidner, J.R., Wildey, M.J., Xia, M., Xu, X., Eds.; Eli Lilly & Company and the National Center for Advancing Translational Sciences: Bethesda (MD), 2004;
12. Dey, P.; Bergmann, T.; Cuellar-Camacho, J.L.; Ehrmann, S.; Chowdhury, M.S.; Zhang, M.; Dahmani, I.; Haag, R.; Azab, W. Multivalent Flexible Nanogels Exhibit Broad-Spectrum Antiviral Activity by Blocking Virus Entry. *ACS Nano* 2018, 12, 6429–6442.
13. Angelova, M.I.; Soléau, S.; Méléard, Ph.; Faucon, F.; Bothorel, P. Preparation of giant vesicles by external AC electric fields. Kinetics and applications. In *Proceedings of the Trends in Colloid and Interface Science VI*; Helm, C., Lösche, M., Möhwald, H., Eds.; Steinkopff, 1992; pp. 127–131.
14. Ananthanarayanan, B.; Stahelin, R.V.; Digman, M.A.; Cho, W. Activation Mechanisms of Conventional Protein Kinase C Isoforms Are Determined by the Ligand Affinity and Conformational Flexibility of Their C1 Domains. *J. Biol. Chem.* 2003, 278, 46886–46894.

Chapter 3

Equine alphaherpesviruses require activation of the small GTPases Rac1 and Cdc42 for intracellular transport

Oleksandr Kolyvushko¹, Maximilian A. Kelch¹, Nikolaus Osterrieder¹, Walid Azab¹

¹Institut für Virologie, Robert von Ostertag-Haus, Zentrum für Infektionsmedizin, Freie Universität Berlin, Robert-von-Ostertag-Str. 7-13, 14163 Berlin, Germany

Microorganisms **2020**, *8*(7), 1013
<https://doi.org/10.3390/microorganisms8071013>

3.1 Abstract

Viruses utilize host cell signaling to facilitate productive infection. Equine herpesvirus type 1 (EHV-1) has been shown to activate Ca²⁺ release and phospholipase C upon contact with $\alpha 4\beta 1$ integrins on the cell surface. Signaling molecules, including small GTPases, have been shown to be activated downstream of Ca²⁺ release, and modulate virus entry, membrane remodeling and intracellular transport. In this study, we show that EHV-1 activates the small GTPases Rac1 and Cdc42 during infection. The activation of Rac1 and Cdc42 is necessary for virus-induced acetylation of tubulin, effective viral transport to the nucleus, and cell-to-cell spread. We also show that inhibitors of Rac1 and Cdc42 did not block virus entry, but inhibited overall virus infection. The Rac1 and Cdc42 signaling is presumably orthogonal to Ca²⁺ release, since Rac1 and Cdc42 inhibitors affected the infection of both EHV-1 and EHV-4, which do not bind to integrins.

3.2 Introduction

Cellular functions are governed by complex signaling networks, and regulation is achieved by countless molecules, most of which are proteins [1]. Small GTPases are cellular signaling proteins that hydrolyze GTP and transduce the signal by changing the dynamics of interaction with other cellular proteins in the phosphorylated (GTP) or dephosphorylated (GDP) bound states. The regulation of small GTPases is achieved by several factors, the most important being guanine nucleotide exchange factor (GEFs), GTPase-activating proteins (GAPs), and guanine nucleotide dissociation inhibitors (GDIs) [2]. The role of GEFs is to promote release of GDP and allow the binding of GTP. GDIs play an opposite role, by preventing GDP release from the small GTPase molecule. GAPs are responsible for activation of GTP hydrolysis [3,4]. Additionally, other factors, such as cytoplasmic Ca²⁺, may facilitate the activation of small GTPases, as is the case in lamellipodia formation by platelets [5]. Small GTPases are understood to be in an active state when GTP is bound, and inactive when GDP is bound [4]. The Rho family of small GTPases was first discovered through transcriptomic screens, as they were overexpressed in cancer cells, and later described to play a role in a number of important cellular processes, such as morphological changes, reorganization of the cytoskeleton, cell cycle regulation, growth, motility, and adhesion [3,6]. The dysregulation of small GTPases may lead to disease and cancerous transformation, abnormal patterns of expression or mutations of GEFs; GDIs and GAPs are associated with different cancer types [2,7–9]. Members of Rho family small GTPases, such as Rac1 and Cdc42, were described to play roles in virus infection [10–12].

Viruses have evolved mechanisms to hijack cellular signaling, in order to facilitate infection. The Alphaherpesvirinae subfamily includes many pathogens that are of great importance to animal and human health, including equine herpesviruses 1 and 4 (EHV-1 and EHV-4). Cell entry of the two closely related alphaherpesviruses EHV-1 and EHV-4 exhibits differences, even though MHC class I molecules are the entry receptor for both [13,14]. Following receptor binding that is mediated by glycoprotein D (gD), EHV-1 gH binds to $\alpha 4\beta 1$ -integrin and induces cellular signaling cascades, resulting in virus fusion with the plasma membrane. The disruption of gH- $\alpha 4\beta 1$ -integrin interaction results in the inhibition of signaling cascades and re-routing of the virus to a caveolin/raft-dependent endocytic pathway. On the other hand, EHV-4 cannot interact with cell surface integrins, and enters equine cells through the caveolin/raft-dependent endocytic pathway. In particular, EHV-1 is able to induce signal transduction inside the infected cell that leads to the activation of phospholipase C, the release of inositol triphosphate, Ca²⁺ release from endoplasmic reticulum, after interaction with $\alpha 4\beta 1$ -integrins on the surface of the cells. This signaling cascade is necessary for fusion at the plasma membrane [15]; however, the exact mechanism that facilitates virus entry is still unknown. The investigation of cellular signaling may lead to better understanding of host-pathogen interaction. Small GTPases were described to be activated downstream of Ca²⁺ release, and are involved in cellular processes such as cytoskeleton remodeling, membrane fusion and intracellular transport. These properties make small GTPases a good candidate to further investigate the signaling cascade induced by EHV-1 [16–18]. In the current study, we tested the hypothesis that small GTPases play a role in EHV-1 infection, with assays based on chemical inhibitors of small GTPases, cell-to-cell spread, and FRET biosensor GTPase activation assays. We further identified specific steps of the infection process, at which Rac1 and Cdc42 play a crucial role. We identified that Rac1 and Cdc42 small GTPases activation is required for the intracellular transport of EHV-1 through the acetylation of microtubules.

3.3 Materials and Methods

3.3.1 Cells and Viruses

Equine dermal (ED) cells (CCLV-RIE 1222, Federal Research Institute for Animal Health, Germany) were cultivated in Iscove's modified Dulbecco's medium (IMDM) (Invitrogen, Carlsbad, USA), supplemented with 20% fetal bovine serum (FBS; Pan - Biotech GmbH, Aidenbach, Germany), 100 U/mL penicillin (Roth, Karlsruhe, Germany), 100 μ g/mL streptomycin (Alfa Aesar, Haverhill, USA), 1 mM sodium pyruvate (Pan - Biotech GmbH) and

1x nonessential amino acids (Pan - Biotech GmbH). Human embryonic kidney (293T) cells were cultured in Dulbecco's modified Eagle's medium (DMEM) (Biochrom, Cambridge, UK), and supplemented with 10% FBS (Pan - Biotech GmbH), 100 U/mL penicillin (Roth), and 100 µg/mL streptomycin (Alfa Aesar). Cells were grown at a temperature of 37 °C and a 5% CO₂ atmosphere. EHV-1 strain RacL11 (L11-RFP), expressing red fluorescent protein (RFP), fused to the small capsid protein VP26 [15], EHV-1 gH4 [19]—EHV-1 expressing gH from EHV-4 that cannot bind to α4β1 integrins (L11-gH4), EHV-1 gHS440A [19] that harbors 3 amino acid substitutions in the gH-integrin binding motif that renders the virus unable to bind to α4β1 integrins, and the EHV-4 strain TH20p [20] was used in this study. All viruses express the enhanced green fluorescent protein (eGFP) for the rapid identification of infected cells. Viruses were reconstituted by the transfection of 2 µg of bacterial artificial chromosome (BAC) DNA into 293T cells using polyethylenimine (PEI; 408727, Sigma-Aldrich, St. Louis, MI, USA). Viruses harvested from 293T cells were then passaged on ED cells. For all experiments, only viruses grown on ED cells were used. For UV-inactivation, 150 µL of virus containing media was placed in a 5-cm cell culture dish and exposed to 30 ss at a power setting of 600, using a UV DNA crosslinker at 254 nm and 8 Watt UV tubes (Analytik Jena, Jena, Germany) [21]. Such parameters were sufficient to efficiently inactivate an infectious virus, as determined by back titration.

3.3.2 *Inhibitors*

RhoA Inhibitor I based on a purified C3 Transferase (dissolved in water; Cat. # CT04, Cytoskeleton, Inc.), and a Rho/Rac/Cdc42 Activator I (dissolved in water; Cat. # CN04, Cytoskeleton, Inc.) were used at final concentrations of 2 µg/mL, following the manufacturer's instructions. Rac1-specific inhibitor NSC 23766 (dissolved in water; ab142161, Abcam, Cambridge, UK) and Cdc42 specific inhibitor ML-141 (dissolved in DMSO; ab145603, Abcam) [22] were used at final concentrations of 100 µM and 80 µM, respectively. Stocks of ML-141 were dissolved in DMSO and the final concentration of DMSO in the media was 0.4% [23]. Target cells were serum-starved for 1 h and incubated for 3 h in the presence of inhibitors before further treatment, unless otherwise specified.

3.3.3 *Cytotoxicity assay*

The cytotoxic effects of inhibitors at selected concentrations on ED cells were assessed using the WTS-1 assay (Cayman Chemicals No. 10008883) after 24 and 48 h, as described before [24,25]. In short, cells seeded in a 96-well plate were cultivated for 24 or 48 h at 37 °C under a 5% CO₂ atmosphere in media, with the designated concentration of inhibitors. Negative control consisted of cells without the addition of inhibitors. Cells treated for 30 s with a 30% solution of hydrogen peroxide (Sigma No. H1009) were used as a positive control. Cells were treated for 24 or 48 h with the inhibitors as specified above, before the WTS-1 reagent was added to the media of each well and incubation for 2 more hours. Absorbance at 450 nm was measured for each sample using a microplate reader (BioTek Instruments, Winooski, VT, USA).

3.3.4 *Flow Cytometry*

ED cells were seeded in a 96-well plate, such that, on the day of the experiment, 2.5 × 10⁴ cells were present in each well. On the day of the experiment, media were replaced with media containing one of the chemical inhibitors, the Rho/Rac/Cdc42 Activator I, or regular medium as a negative control. Cells were incubated for 3 h and then placed on ice for 10 min. EHV-1, EHV-1 gH4, or EHV-1 gHS440A were added at a multiplicity of infection (MOI) of 1. Cells were kept with the virus on ice for 1 h, to synchronize the infection, then cells were shifted to 37 °C. After 1 h, cells were treated with ice-cold citrate buffer (pH 3) for 1.5 min, to neutralize unpenetrated viruses [25], followed by 2 h incubation with fresh media that also contained the inhibitors or the activator. At this point (in total: 3 h after the temperature shift) 10,000 cells were analyzed for eGFP expression by flow cytometry (CytoFLEX, Beckman Coulter, Pasadena, USA). Notably, eGFP expression in cells without inhibitor treatment was considered the baseline of infection and set at 100%. Flow cytometry data was analyzed using the FlowJo

software (FlowJo, LLC, Ashland, USA) to ensure gating consistency. Each treatment had 3 technical replicates per plate, and the complete experiment was repeated three independent times.

3.3.5 Plaque assay

ED cells were grown in a 6-well plate (1 × 10⁵ cells per well). ED cells were treated with one of the chemical inhibitors, or mock-treated for 3 h. Cells were then placed on ice for 10 min and EHV-1, EHV-1 gH4, EHV-1 gHS440A, or EHV-4 were added at a titer of 100 PFU (plaque forming unit) per well. Attachment was allowed for 1 h to synchronize the infection. To promote virus penetration, cells were incubated at 37 °C for 60 min before they were subjected to citrate treatment (see above) and overlaid with DMEM containing 0.5% methylcellulose in the presence or absence of the inhibitors. Plaques were counted and diameter was measured in a blinded fashion after 48 h of infection at 37 °C using inverted fluorescent microscope (Zeiss Axiovert 100, Zeiss, Oberkochen, Germany), provided with a monochromatic camera (ZEISS AxioCam 305 mono). All taken images were analyzed with Fiji image analysis software. Fifty or all available (if less than 50) plaques were measured for each of the three independent replicates. If no plaques (but only single infected cells) were found per run, plaque diameter was considered to be equal to zero. Single infected cells were not considered plaques. The average of the plaque diameter of each of the three repeats was used for statistical analysis.

3.3.6 Virus localization and immunofluorescence

To quantify and visualize virus localization, 1 × 10⁴ ED cells were seeded on a coverslip, in a 24-well plate. Cells were treated with each individual inhibitor, or mock-treated for 3 h. Before addition of EHV-1, cells were placed on ice for 10 min and EHV-1 was added at a MOI of 1. Virus attachment was allowed to proceed for 1 h on ice, followed by a temperature shift to 37 °C and incubation for 30 min (virus-membrane localization setup), 3 h (virus-endosome localization setup), or 6 h (virus-nucleus localization setup). After the given incubation time, infected cells were fixed with 4% paraformaldehyde (PFA) and stained in one of the three following ways. (i) To visualize the external leaflet of the plasma membrane, cells fixed at 30 min after infection were stained with lectin-FITC conjugate (16441, Sigma-Aldrich). (ii) To examine virus colocalization with endosomes, ED cells were fixed at 3 h post infection (HPI), permeabilized with permeabilization buffer (2% BSA, 0.2% Triton-X 100 in PBS) for 20 min, and stained for 1 h with polyclonal antibodies against LAMP1, EEA1, or caveolin-1 (ab24170, ab2900, ab2910, Abcam, respectively) diluted 1:200 in antibody-dilution buffer (2% BSA, 0.1% Tween-20 in PBS). Secondary goat anti-rabbit IgG Alexa Fluor 647 (Abcam ab150079) was diluted 1:2000 in antibody-dilution buffer and added to the cells. (iii) DAPI was used to visualize the cell nucleus. The cells were examined with a confocal laser scanning Nikon Eclipse Ti Visitron microscope (Visitron Systems GmbH, Puchheim, Germany). Images were analyzed with VisiVIEW imaging software (Visitron Systems GmbH). Virus particles were counted using ImageJ (NIH), according to the following strategy: (i) for the virus-membrane localization setup, all virus particles on (or very close to) the cell membrane were considered to be localizing with the cell membrane; (ii) for the virus-endosome localization setup, all virus particles were considered to be colocalizing with the endosome or being spatially separated from the endosomal markers; (iii) for the virus-nuclear localization setup, all virus particles localized within the DAPI-stained nucleus were considered to exhibit nuclear localization. All other virus particles that were present in the cells and did not fall within one of the 3-setups were considered to localize to the cytoplasm. One-hundred virus particles were counted and categorized manually in a blinded fashion, for each of the 3 independent replicates of the experiments.

3.3.7 Ratiometric fluorescence resonance energy transfer (FRET)

ED cells were grown in an 8-Well μ -Slide (Ibidi) and transfected with pRaichu-Rac1 or pRaichu-Cdc42 plasmids [26,27], using a Xfect Single Shots transfection reagent (Clontech, Mountain View, CA, USA). At 24-h after transfection, wells were analyzed with an inverted fluorescent microscope (Zeiss) at 488 nm, to find which wells had been successfully

transfected with the biosensors. Media was replaced with live cell imaging media (Gibco 21063029, Life Technologies, Carlsbad, CA, USA) without serum. Cells were placed on ice for 2 h, and then into a climate control chamber (37 °C, 80–90% humidity, and 5% CO₂) of the Leica SP8 CLSM. Cells were allowed to equilibrate to the temperature and CO₂ concentration of the chamber for 30 min. Cells were illuminated with Argon laser combined with AOBs beam splitter and the 63x/1.4 HC PL APO CS2 oil immersion objective was used. The excitation beam was tuned to a wavelength of 433 nm; the reporter wavelength was 457 for the donor (CFP) and 527 for the acceptor (FRET) [26,27]. UV-inactivated EHV-1 was added to cells during imaging at a MOI of 10, within the second minute of imaging. Both reporter and acceptor emissions were recorded simultaneously with two gallium arsenide phosphide photomultiplier (PMT) sensors. Cells were imaged with a frequency of 2 Hz, to reduce phototoxicity. Average intensity for the region of interest (Raichu biosensor expressing ED cell) was measured for each channel and time point, and the ratio of FRET/CFP was calculated and plotted as a moving average of 20 points. The experiment was repeated 3 independent times for each biosensor.

3.3.8 Immunoblotting

Immunoblotting was performed to quantify the proportion of acetylated tubulin [28]. On the day of the experiment, 4 × 10⁵ 293T cells in a 12-well plate were serum-starved for 1 h. Cells were treated with small GTPase inhibitors in DMEM for 3 h in a cell culture incubator. The inhibitor-treated 293T cells were infected with EHV-1 at a MOI of 10, for 1 h and lysed on ice as described before [29]. Paclitaxel (T7191 Sigma-Aldrich), a chemical inducer of microtubule acetylation, was used as a positive control. Briefly, 293T cells were serum-starved for 1 h, overlaid with serum-free DMEM containing Paclitaxel at a final concentration of 10 μM for 1 h, and finally, lysed on ice. Cell lysis was achieved by heating the sample to 98 °C in sodium dodecyl sulfate (SDS) sample loading buffer (1 M Tris-HCl (pH 6.8), 0.8% sodium dodecyl sulfate (SDS), 40% glycerol, 0.2% β-mercaptoethanol, 0.02% bromophenol blue) for 10 min. A 12% SDS-polyacrylamide gel was used to separate the proteins based on their molecular weight. Semi-dry transfer was used to transfer proteins to the polyvinylidene fluoride (PVDF) membrane [30]. Immunoblot analysis was done with monoclonal anti-acetylated tubulin 6-11B-1 antibodies (T7451, Sigma-Aldrich), at a dilution of 1:100. Total tubulin was detected with polyclonal anti-tubulin α antibody (SAB4500087, Sigma-Aldrich) at a 1:500 dilution. Secondary anti-mouse and anti-rabbit HRP (ab97023, ab6721, Abcam, respectively) conjugated antibodies were used at a 1:1000 dilution. Densitometry was done using ImageJ (NIH), by measuring the intensity of all pixels comprising the band of interest [31]; the relative density of the bands from each experiment was recorded.

3.3.9 Cell-to-cell fusion

Ten thousand ED cells were divided into two batches: the first was nucleofected with luciferase-expressing plasmid pT7-EMC-Luc where luciferase is under control of the T7 promoter, while the second was nucleofected with T7-polymerase expressing plasmid pCAGT7 [32]. The nucleofection of ED cells was performed using cell line Nucleofector kit V (Lonza, Basel, Switzerland) [33], following the manufacturer's instructions. After 24 h of incubation at 37 °C, cells that received the luciferase plasmid were infected with EHV-1 at a MOI of 1 for 3 h, and then treated for 3 h with one of the small GTPase inhibitors. The cells were washed with PBS, trypsinized, and mixed with the ED cells nucleofected with the T7 polymerase plasmid. Cells were incubated together for 24 h in the presence or absence of inhibitors. All cells were lysed, and the luciferase activity was quantified using the Luciferase Assay System (E1500, Promega, Madison, United States) and a microplate reader according to the manufacturer's protocol.

3.3.10 Statistical Analysis

Cell viability, plaque assays and flow-cytometry-based studies were analyzed with GraphPad software. A one-way ANOVA analysis was done under the assumption of normal

distribution. All values were compared to the control, and Duntett's correction for multiple comparisons was used. Significance value was set to $p = 0.05$.

3.4 Results

3.4.1 *Cdc42 and Rac1 Inhibitors Reduce EHV-1 and EHV-4 Infection*

We have shown previously that the binding of EHV-1, but not EHV-4, to cell surface $\alpha 4\beta 1$ integrins results in the release of cytosolic Ca^{2+} , which is required for virus fusion with the plasma membrane [15]. The mechanism of how cytosolic Ca^{2+} can facilitate the fusion of the virus envelope with the plasma membrane is still unknown. Activation of small GTPases was described to be downstream of Ca^{2+} release [16,34], and might play a role in virus entry and subsequent transport within the cells. Therefore, we investigated the role of different small GTPase in virus infection. ED cells were treated for 3 h with one of the small GTPase-specific inhibitors NSC 23766 (Rac1 inhibitor), ML-141 (Cdc42 inhibitor), purified C3 transferase (RhoA inhibitor) or the small GTPase Rho/Rac/Cdc42 activator. Cells were then infected in a synchronized manner in the presence or absence of inhibitors or the activator. At three hours post-infection (hpi), cells were analyzed by flow cytometry to determine the progress of infection. In a three-hour infection assay, we observed a significant reduction of EHV-1, which binds to $\alpha 4\beta 1$ integrins, as well as EHV-1 gH4 or EHV-1 gHS440A (these two viruses cannot bind to $\alpha 4\beta 1$ -integrin) infections after treatment of cells with Rac1 and Cdc42 inhibitors. The infection of EHV-1 was significantly reduced in cells treated with Rac1 (~60%) and Cdc42 inhibitors (~40%) (Figure 1B). The inhibitory effect of Rac1 and Cdc42 inhibitors was more pronounced in the case of EHV-1 gH4 and EHV-1 gHS440A, where it resulted in an ~80% (Rac1 inhibitor) and ~95% (Cdc42 inhibitor) reduction of infection. The Rho/Rac/Cdc42 activator and RhoA inhibitors had no effect on EHV-1 infection; however, they significantly reduced the infection (30–60% reduction) of EHV-1 gH4 and EHV-1 gHS440A, the two mutants that cannot bind to integrins [19], (Figure 1C,D). EHV-4 was not suitable for such an assay, due to the slow onset of eGFP expression that needed long incubation times to be expressed at measurable levels. It is worth mentioning that neither the inhibitors nor the activator had any toxic effect on the cells (Figure 1A).

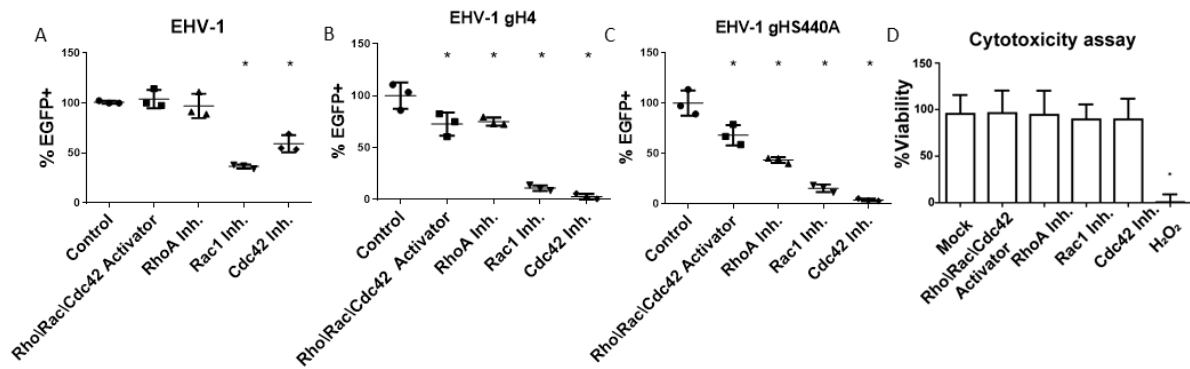


Figure 3.1. Cytotoxicity and inhibition of virus infection using GTPase inhibitors.

Inhibition of equine herpesvirus EHV-1 (A), EHV-1 gH4 (B), or EHV-1 gHS440A; (C) infection in the presence or absence of different inhibitors determined by flow cytometry. Equine dermal (ED) cells were treated for three hours with small GTPase inhibitors or the activator as indicated and infected at a multiplicity of infection (MOI) of 1. eGFP expression was used to determine the percentage of infected cells relative to mock-treated cells. (D) Cytotoxicity assay (WST-1) in ED cells for mock- and hydrogen peroxide-treated cells (as a negative and positive control, respectively) as well as different GTPase inhibitors. Data are presented as means with standard deviation (S.D.) of three independent experiments, and normalized to the mean of mock-treated and infected cells. One-way ANOVA test followed by Dunnett's multiple comparisons test; * $p < 0.05$.

3.4.2 Small GTPases Facilitate Infection and Cell-to-Cell Spread

ED cells were treated with inhibitors for three hours before infection. The virus was allowed to attach to cells for 1 h at 4°C, then the temperature was shifted to 37 °C to facilitate virus entry for another hour. The cells were subjected to citrate treatment to eliminate all non-penetrated virus particles. Later, cells were overlaid with DMEM, containing 0.5% carboxymethyl cellulose in the presence or absence of inhibitors, until analysis at 48 hpi. Treatment of cells with ML-141 (Cdc42 inhibitor) resulted in a significant reduction of EHV-1 plaque formation (less than 3% of plaques; Figure 2 A). On the other hand, Rac1 or RhoA inhibitors or the Rho/Rac/Cdc42 activator had no effect on plaque numbers (Figure 2A). Next, we measured the diameter of plaques produced in the presence of small GTPase inhibitors. The diameter was significantly reduced, and approximately 20% smaller in the presence of RhoA and Rac1 inhibitors, or approximately 90% smaller in the presence of the Cdc42 inhibitor (Figure 2E).

Similar to EHV-1, the number of plaques formed by EHV-1 gH4, EHV-1 gHS440A and EHV-4 was significantly diminished by the Cdc42 inhibitor (Figure 2B-D). RhoA and Rac1 inhibitors significantly reduced plaque numbers for EHV-1 gH4. While not statistically significant, a similar trend was observed for EHV-1 gHS440A and EHV-4 (Figure 2B-D). The diameter of plaques formed by EHV-1 gH4, EHV-1 gHS440A and EHV-4 was significantly smaller in the presence of RhoA and Cdc42 inhibitors (Figure 2F-H). It is noteworthy that, after using Cdc42 inhibitor, in particular, the number of plaques was significantly reduced; however, we were able to analyze the diameter of all available plaques in each replicate (see Materials and Methods). The Rac1 inhibitor resulted in a significant reduction of plaque diameters in EHV-1-derived mutants EHV-1 gH4, EHV-1 gHS440A, but not in EHV-4 (Figure 2F-H).

Absence of the inhibitors from the overlay media did not alter the picture of infection compared to mock-treated cells (all viruses produced plaques that were similar in size and numbers) (Figure 2I, J). This result indicates that the observed inhibition of virus infections requires the presence of inhibitors throughout the infection. We concluded from our data that small GTPases are actively involved in the entry, but also at later steps of the virus infection cycle.

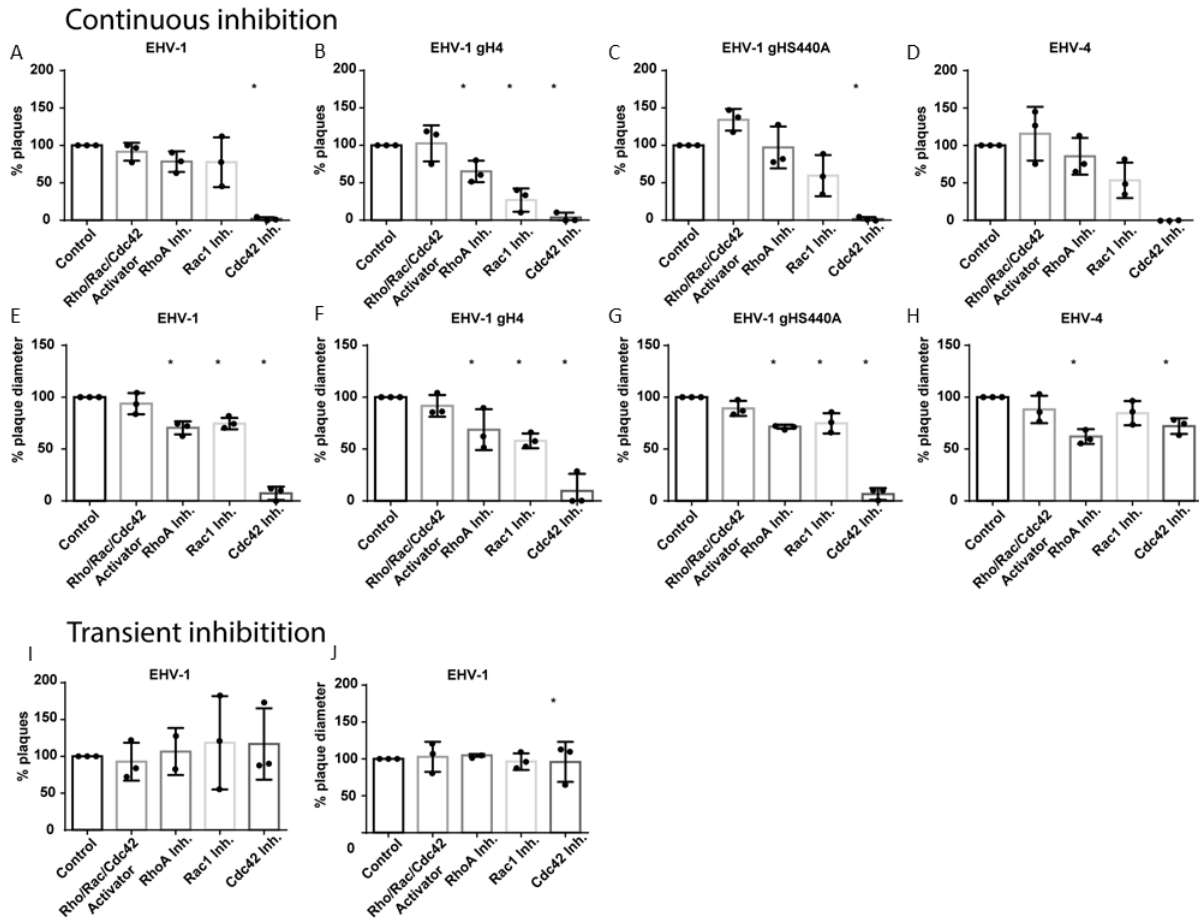


Figure 3.2. EHV-1 infection and cell-to-cell spread is influenced by small GTPases. Plaque reduction assay of EHV-1 (A,E,I,J), EHV-1 gH4 (B,F), EHV-1 gHS440A (C,G) and EHV-4 (D,H) in ED cells following inhibition of small GTPases. ED cells treated for three hours with inhibitors of small GTPases were infected with 100 PFU of the indicated virus for one hour, and then subjected to citrate treatment, overlaid with media that was inhibitor-free (I,J), or contained inhibitor (A-H) for 48 hours. The number of plaques (A-D, I) was counted with an inverted fluorescent microscope and plaque diameters (E-H, J) were measured using ImageJ (NIH). Black circles “*” represent data obtained from each replicate. In case of plaque diameter panels (F-H), each circle represents average plaque diameter of 50 plaques (or all available) in a replicate; when there were no plaques (but only single infected cells) in a replicate, plaque diameter was considered to be zero. Data are presented as means with S.D. of three independent experiments and normalized to the mean of the control (virus infection without treatment). One-way ANOVA test followed by Dunnett’s multiple comparisons test; * $p < 0.05$.

3.4.3 EHV-1 Activates Small GTPases Rac1 and Cdc42

To get a direct measurement of the activation status of the small GTPases Rac1 and Cdc42 during virus infection, a FRET-based system was employed. ED cells were transfected with either the pRaichu-Rac1- or pRaichu-Cdc42 FRET constructs. The expressed large protein is a single polypeptide chain that consists of four domains: the YFP domain and CFP domain at the termini, the Rac1 or Cdc42 GTPase domain, and the Ras-binding domain. The Ras-binding domain can only bind to small GTPase domain in its active form, i.e., when it is GTP bound. The interaction of the Ras-binding domain with the small GTPase domain results in conformational changes in the whole protein when the small GTPase is active. This interaction between the two central domains will then lead to conformational changes of the protein, and bring the CFP and YFP domains into close proximity and allow for the FRET effect to take place. We measured the activation of Rac1 and Cdc42 in ED cells in response to exposure with UV-inactivated EHV-1, using the FRET-based biosensors. ED cells expressing

the FRET biosensors were imaged with 2HZ frequency with two sensors, allowing for the simultaneous collection of the signals emitted by donor (CFP) and FRET (YFP), with an imaging duration of 20-25 minutes. At two minutes after the start of the imaging sequence, UV-inactivated EHV-1 was added to the cells. The mean intensity for the region of interest was measured, and the ratio of FRET/CFP was calculated and plotted as a moving average of 20 points. The measurement was repeated three times for each of the biosensors. We observed the activation of both (Rac1 and Cdc42) small GTPases in cells shortly after exposure to EHV-1 (Figure 3).

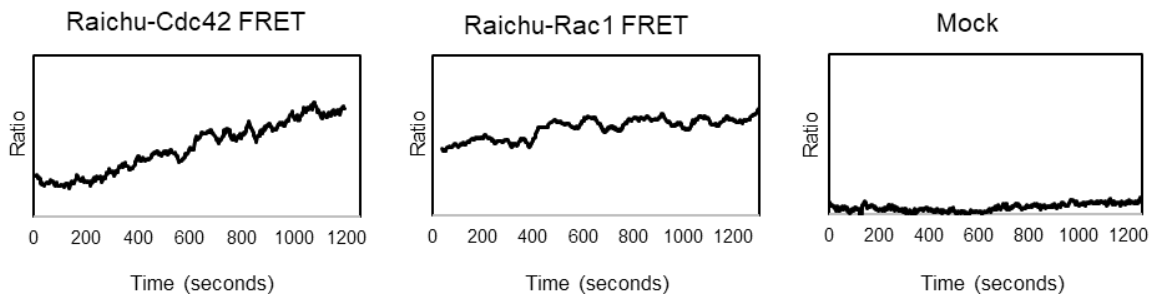


Figure 3.3. Small GTPase activation with ratiometric FRET in response to EHV-1 infection. Raichu-FRET biosensors were used to examine the activation status of small GTPases. ED cells were transfected with pRaichu-Rac1- or pRaichu-Cdc42-biosensor expressing plasmids. Twenty-four hours after transfection, EHV-1 RFP was added to ED cells and emissions of donor and acceptor was simultaneously measured and later analyzed. The ratio of FRET/CFP (acceptor/donor) was calculated for the selected region of interest (transfected cell) and plotted as a moving average of 20 frames.

3.4.4 Tracking of Virus Transport in Cells

The entry of EHV-1 into equine ED cells can either be through direct fusion with the plasma membrane, or after interaction with the $\alpha 4\beta 1$ integrins that induce a signaling cascade, triggering the fusion process. Alternatively, if integrin binding is altered and the signaling cascade abrogated, EHV-1 is redirected to the endosomal pathway [15]. Virus particles are then transported inside the cell to the nucleus along microtubules [35], where replication takes place. We investigated whether small GTPases play a role in the virus transport that might lead to a reduction of infection, as seen in Figure 1. The transient effects of GTPase inhibitors on EHV-1 infection (Figure 2) indicated that GTPases play a role at steps of infection after cell entry. In a time-resolved fashion, we investigated three loci for the presence of virus particles after infection: (i) the plasma membrane at 30 minutes post infection, (ii) endosomes at three hours post infection, and (iii) nucleus or cytoplasm at six hours post infection. ED cells were treated with chemical inhibitors of small GTPases for three hours, then infected with EHV-1, and fixed after 30 minutes, 3 or 6 hpi. One-hundred virus particles were counted manually in a blinded fashion in three replicates for each setup. For the 30-minute setup, each particle was counted as on cell borders (colocalized with the plasma membrane), as visualized by FITC-labeled lectin. The treatment of cells with Cdc42 inhibitors resulted in a small, yet significant, increase in the number of virus particles that were colocalized with the plasma membrane when compared to mock-treated cells (Figure 4A). A decrease in colocalization with the plasma membrane was determined after treatment of cells with Rho/Rac/Cdc42 Activator (Figure 4A). We did not observe a change in numbers of plasma membrane-localizing viruses after treatment with Rac1 or Rho inhibitors (Figure 4A). Additionally, we did not record any increase in virus colocalization with endosomes, lysosomes, or caveolae at 3 hpi in inhibitor-treated cells when compared to mock-treated cells (Figure 4C-E). We further investigated the efficiency of virion delivery to the nucleus in the inhibitor-treated ED cells, by counting the number of virus particles in the perinuclear zone and the cytoplasm. Both Cdc42 and Rac1 inhibitors resulted in a significant delay of virus transport to the nucleus when compared to virus transport in mock-treated cells: a significantly smaller number of virus particles reached the nucleus, and the majority remained in the cytoplasm at 6 hpi (Figure 4B). Taken together, these findings

indicated that the small GTPases, Cdc42 and Rac1, play a role in the transport of the virus particles to the cell nucleus.

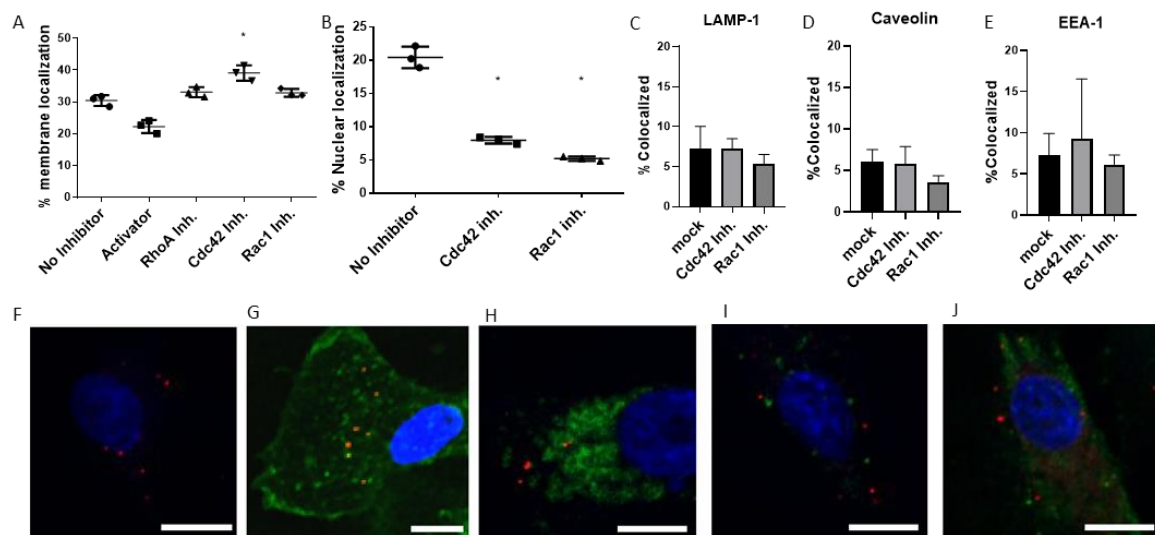


Figure 3.4. Effects of small GTPase inhibitors on virus transport. Inhibitor-treated ED cells were infected with EHV-1 at a MOI of 1, fixed at 30 minutes, 3 or 6 hours after infection, and stained in one of the following ways. (A) ED cells fixed at 30 minutes post infection were stained with FITC-lectin, and the number of particles localizing with the plasma membrane was counted manually. (B) At 6 hpi, ED cells were fixed and stained with DAPI. (C-E) Colocalization of EHV-1 with endosomal markers in ED cells treated with inhibitors of the small GTPases Cdc42 and Rac1. Colocalization of EHV-1 with cellular compartments: cells were stained with only DAPI at 6 hpi. Exemplary images following staining: (F) DAPI stain at 6 hpi. (G) FITC-lectin 30 minutes after infection, (H) anti-LAMP-1 antibodies 3 hpi, (I) anti-EEA-1 antibodies 3 hpi, (J) or anti-caveolin antibodies 3 hpi. Scale bars represent 10 μ m. DAPI is pseudocolored blue, EHV-1 particles as red, staining target (Lectin, LAMP-1, EEA-1, or Caveolin-1) as green. Data are presented as means with S.D. of three independent experiments and normalized to the mean (with S.D.) of the control (virus infection without inhibitor treatment). One-way ANOVA was employed, followed by Dunnett's multiple comparisons correction; * $p < 0.05$.

3.4.5 *Rac1 and Cdc42 Activation Is Required for EHV-1-Induced Tubulin Acetylation*

Alphaherpesviruses utilize microtubule transport to reach the nucleus [36]. EHV-1, in particular, is transported by dynein motor proteins to the cell nucleus [28]. The acetylation of lysine 40 (K40) is an important posttranslational modification of α -tubulin that stabilizes microtubule structure [37–39] and increases dynein binding and motility [40]. EHV-1, as well as HSV-1, were described to induce microtubule acetylation, as the inhibition of acetylation resulted in reduced virus infectivity of both viruses [28,41]. To investigate whether small GTPases play a role in microtubule acetylation, we treated cells with small GTPases inhibitors prior to infection and determined tubulin acetylation levels with monoclonal antibodies by immunoblot analysis. We confirmed that EHV-1 induces microtubule acetylation at 1 hpi in 293T cells, through a mechanism that might involve the activation of Rac1 and Cdc42. We further found that both Rac1 and Cdc42 inhibitors significantly prevented the acetylation of the α -tubulin when compared to EHV-1-infected cells (Figure 5).

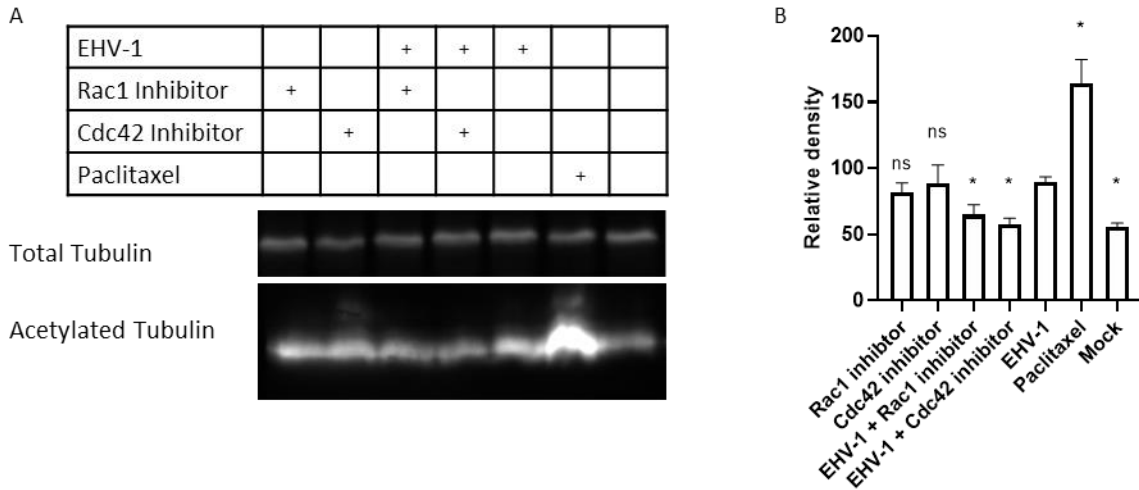


Figure 3.5. Tubulin acetylation by EHV-1 requires virus-activated GTPases. (A) Human 293T cells were treated with inhibitors or mock-treated for 3 hours and infected for 60 minutes with EHV-1. Paclitaxel, a chemical inducing microtubule acetylation, was used to treat cells for one hour as a positive control. Cell lysates were used for immunoblotting with anti-total tubulin, and an antibody that is specific for acetylated tubulin. (B) Densitometry of the bands in (A) was done using ImageJ. The experiment was repeated three times. Data are presented as means with S.D. of three independent experiments and normalized to the mean (with S.D.) of the control (EHV-1 virus infection without inhibitor treatment); One-way ANOVA test followed by Dunnett's multiple comparisons correction (each sample vs EHV-1); * $p < 0.05$.

3.4.6 EHV-1-Induced Cell-to-Cell Fusion Is Dependent on Rac1 and Cdc42 Activation

EHV-1 has the ability to trigger the fusion of infected with non-infected cells. The viral glycoproteins gB, gD and gH/gL that are expressed in infected cells mediate cell-to-cell fusion [42]. Small GTPases play a role in membrane remodeling, as well as the cytoskeletal rearrangements in infected cells [43,44] that govern the cell motility and transport efficacy inside the cell. To test whether small GTPases play a role in cell-to-cell fusion, luciferase-based cell-to-cell fusion assays were performed. To investigate the role of small GTPases on cell-to-cell fusion in an experimental infection set-up with chemical inhibitors, it was necessary to establish similar levels of infections first, since we already know that small GTPase inhibitors significantly reduce EHV-1 infection in ED cells. Thus, comparison of cell-to-cell fusion in a group of cells that have different infection levels would produce biased results. With the purpose of having inhibitor-treated cells with similar infection rates, we first infected ED cells with EHV-1 for three hours, before the inhibitors were added for another three hours. Levels of infection, as measured by eGFP expression at 6 hpi, were determined and showed no influence of the inhibitors on infection rates; these conditions were chosen for the cell-to-cell fusion assay. In this assay, two groups of ED cells were independently nucleofected with (i) a plasmid vector encoding luciferase under the control of T7 promoter, and (ii) a plasmid vector encoding T7 polymerase. In this experiment, the expression of luciferase will only occur in cells that also express T7 polymerase protein. In other words, the levels of luciferase expressed are functions of the number of cells that undergo cell-to-cell fusion. At 24 hours after nucleofection, ED cells nucleofected with the luciferase carrying plasmid were infected with EHV-1 at a MOI of 1 for 3 hours, and subsequently subjected to inhibitor treatment for another 3 hours. Afterwards, the infected luciferase carrying cells and T7 polymerase-expressing uninfected cells were gently detached, mixed, and incubated for 24 hours, in the presence or absence of inhibitors. At 24 hours after mixing, cells were lysed, and the level of luciferase produced was measured via the chemiluminescence intensity of the lysate for each treatment. We found that the treatment of cells with either Rac1 or Cdc42 inhibitors led to a significant decrease in cell-to-cell fusion (Figure 6).

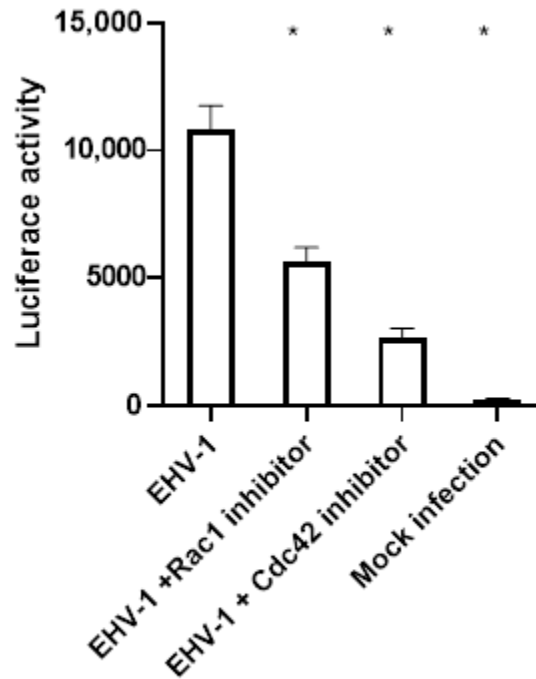


Figure 3.6. Small GTPases influence cell-to-cell fusion after infection. ED cells were nucleofected with pT7-EMC-Luc or T7 polymerase-expressing plasmid pCAGT7. pT7-EMC-Luc-nucleofected cells were infected with EHV-1 for three hours and then treated with inhibitors, or mock treated, for three hours. Both pT7-EMC-Luc-nucleofected infected-cells and pCAGT7-nucleofected non-infected cells were mixed and incubated for 24 hours. Cells were lysed, and the levels of luciferase protein produced were measured as intensity of chemiluminescence. Data are presented as means with S.D. of three independent experiments (one-way ANOVA under assumption of normal distribution). All values were compared to the control (EHV-1 infection without inhibitor treatment), and Duntett's correction for multiple comparisons was used; * $p < 0.0001$.

3.5 Discussion

Cellular processes are tightly regulated through intracellular signaling events. Small GTPases are signaling molecules that are known to play a role in large variety of cellular processes, including cytoskeleton remodeling, cell cycle regulation, motility, and other regulatory functions [3,6]. Furthermore, it has been shown that small GTPases are implicated in facilitating the entry and infection of several viruses [10–12]. Binding of EHV-1 gH to $\alpha\beta 1$ integrins can induce signaling cascades inside the cell that lead to virus fusion with the plasma membrane [15]. In the current study, we have investigated the role of small GTPases during EHV-1 entry and throughout the infection cycle. Our data show that the small GTPases Cdc42 and Rac1 facilitate virus entry and promote efficient virus replication by (i) facilitating virion transport inside the cells through the regulation of α -tubulin acetylation and (ii) regulating the direct fusion of infected with uninfected cells, thereby enhancing the cell-to-cell spread. EHV-1 was able to induce Rac1 and Cdc42 activation, as demonstrated by a FRET analysis.

Rac1 and Cdc42 inhibitors had a strong inhibitory effect on EHV-1 infection. To investigate at which step of the replication cycle the virus was affected, we monitored virus trafficking inside the cell, starting from entry, microtubule transport to the nucleus, and ending with direct virus spread from the infected to uninfected cells. The inhibition of Cdc42 led to a moderate, but significant, increase in virus particles at the plasma membrane, indicating a delay in cellular entry. The inhibition of Rac1, on the other hand, had no effect on virus entry. In a previous study, Hoppe and coworkers reported that there was no effect on the cell entry of HSV-1 in MDCKII cells with inhibited Rac1 or Cdc42 GTPases [12]. On the other hand, the

activation of Rac1 and Cdc42 was shown to be essential for the entry of dengue virus type-2 (DENV-2), since it relies on the formation of filopodia [45] and for the entry of pseudorabies virus via micropinocytosis in HeLa cells [46]. In contrast, one study of HSV-1 in keratinocytes showed that Rac1 and Cdc42 signaling pathways were not important [47]. However, Rac1 and Cdc42 are generally considered to be required for HSV-1 infection [12,48]. Both filopodia formation and virus fusion at the plasma membrane rely on actin remodeling, which in turn is regulated via small GTPases [49,50].

We also investigated if EHV-1 was redirected towards the endosomal pathway [51]. In the absence of Rac1 or Cdc42 signaling, there were no significant changes in virion localization in the endosomes, suggesting that Rac1 and Cdc42 play no role in the choice of entry pathway. Investigation of virion localization to the nucleus revealed that a smaller proportion of virions was present in the nucleus of cells treated with either Cdc42 or Rac1 inhibitors. These findings are consistent with the infection assay results (Figure 1) that also showed that the inhibition of Rac1 or Cdc42 led to a decrease in overall production of infectious EHV-1. Presumably, virus particles that cannot reach the nucleus are degraded in the cytoplasm by the proteasome, or are re-directed to lysosomes [36,52]. Alternatively, they may be sequestered in the cytoplasm in a quiescent state [53]. It was described for the vesicular stomatitis virus (VSV) that under conditions with reduced Cdc42 activation, the trafficking of viral particles from the ER to the Golgi was blocked, and the majority of VSV particles were trapped in the ER [54]. In the case of Kaposi's sarcoma-associated herpesvirus (KSHV), the virus is able to activate cellular signaling and the acetylation of microtubules. The disruption of the small GTPase signaling cascade and the consequent absence of microtubule acetylation led to the reduction of virion transport, as measured by the presence of viral DNA in the nucleus [55]. We, therefore, surmise that the main reason for reduced infection rates by blocking Cdc42 or Rac1 is reduced virion trafficking in the host cell, caused by the inability of EHV-1 to induce α -tubulin acetylation.

The observation that cells treated with Cdc42 or Rac1 inhibitors were able to internalize similar numbers of viruses compared to mock-treated cells and produce similar numbers of plaques in inhibitor-free media (Figure 2) suggests that the activation of small GTPases is not essential for cell entry. However, it was clear that virions require the activation of these GTPases to efficiently reach the nucleus for replication [55]. It seems likely that GTPases affect virion transport in the cytoplasm, most likely by interfering with proper microtubule function.

Alphaherpesviruses are known to be transported along microtubules to the nucleus [36,56]. We, therefore, investigated the acetylation of microtubules during infection, and the possible role of GTPases in this step. The acetylation of microtubules is considered an indication of their stability and kinesin and dynein motility [37,38,40,57]. We showed that the inhibition of Cdc42 and Rac1 reduced the virus-induced acetylation of α -tubulin. Similar effects were reported for EHV-1, where the activation of ROCK1 is required for the acetylation of α -tubulin [28]. In the case of influenza A virus (IAV) infection, the activation of the RhoA small GTPase was reported to induce tubulin acetylation, which is presumably required for trafficking of IAV particle components [58]. Similarly, KSHV was able to induce RhoA activation, which leads to the acetylation of tubulin in endothelial cells [55]. The HSV-1 VP22 protein was previously reported to be responsible for tubulin acetylation and microtubule bundling, even in the context of transient transfection [59]. An impaired ability of virus particles to induce α -tubulin acetylation in the presence of GTPase inhibitors might explain the accumulation of virus particles in the cytoplasm, due to the reduced transport in infected cells under such conditions.

Herpesviruses induce cell-to-cell fusion to facilitate virus spread [60,61]. We found that the small GTPases Cdc42 and Rac1 play a role in the post-replicative stages of EHV-1 infection by facilitating cell-to-cell spread. Inhibition of both GTPases, reduced virus cell-to-cell spread and the ability of virus-infected cells to induce cell-to-cell fusion. This reduction of the fusogenic activity of infected cells could also be a direct consequence of the decrease in acetylation of tubulin, which has been shown to play a role in cell motility and cell-to-cell fusion [62,63], or reduce the formation of cytoplasm extensions that serve for viral transport to neighboring cells, or the ability of the microtubules to transport infectious particles across the cytoplasmic extension [64]. Additionally, small GTPase inhibitors can affect cell-to-cell fusion through other mechanisms, that were not investigated in this study, such as (i) the modification

of intracellular trafficking may result in reduced gB and gH-gL (virus fusion machinery) presence in the plasma membrane, and thus reduced cell to cell spread [6,42]; (ii) changes in the rates of polymerization of actin filaments can lead to reduced cell-to-cell contact [65,66]; (iii) or even change aspects of the cell physiology independent of viral infection [48].

The infection of EHV-4 and the other recombinant EHV-1 that are unable to bind to integrins (EHV-1 gH4 and EHV-1 gHS440A) was also affected in a fashion similar to that recorded for EHV-1, which we showed binds to integrins. These data suggested that the activation of the small GTPases play a role in a the signaling cascade independent of that induced by integrins [51]. Further studies will be needed to investigate the exact mechanistic role of small GTPases in EHV-1 and EHV-4 infection. Of specific interest is our observation that while the plaque number of EHV-4 was strongly reduced, the reduction of plaque size was less pronounced.

In conclusion, we have shown that EHV-1 activates small GTPases to facilitate the stabilization of α -tubulin and promote virion transport inside the cell and to neighboring cells via cell-to-cell fusion. Chemical inhibitors of the small GTPases Rac1 and Cdc42 precluded the virus-induced activation of small GTPases and ultimately resulted in impaired virus trafficking to the nucleus of infected cell. Furthermore, the reduced acetylation of the microtubules is likely the main reason of the observed phenomena. A deeper understanding of the mechanisms of the virus-host interactions of EHV-1 and its relatives in the Alphaherpesvirinae may provide the basis for the rational development of therapeutics or preventive measures against this important group of human and animal pathogens.

3.6 Author Contributions

Conceptualization, W.A.; Formal analysis, O.K.; Funding acquisition, N.O. and W.A.; Methodology, O.K. and M.A.K.; Project administration, W.A.; Supervision, N.O. and W.A.; Validation, W.A.; Visualization, O.K.; Writing—original draft, O.K.; Writing—review and editing, M.A.K., N.O. and W.A. All authors have read and agreed to the published version of the manuscript.

3.7 Funding

This work was supported by grants from the Deutsche Forschungsgemeinschaft (DFG AZ 97/3-2) to WA and the Morris Animal Foundation (D19EQ-003) to WA and NO, and unrestricted funds made available by Dr. Manfred Semmer to the Equine Herpesvirus Program at Freie Universität Berlin. OK was supported by a stipend from DAAD (Deutscher Akademischer Austauschdienst), and his graduate studies were completed with support from ZIBI (Zentrum für Infektionsbiologie und Immunologie) and DRS (Dahlem Research School).

3.8 Acknowledgments

We are grateful to Yoshizaki and Matsuda from Osaka University for providing the FRET-based biosensor plasmids. The pT7EMCLuc plasmid, which expresses the firefly luciferase reporter gene under the control of T7 promoter, and pCAGT7 plasmid, which expresses T7 RNA polymerase, were generously provided by Richard Longnecker, Northwestern University. We thank Michaela Zeitlow and Selvaraj Pavulraj for their technical assistance and methodological support. We thank Katharina Achazi, core facility of Freie Universität Berlin BioSupraMol, for providing training and use of the equipment. The publication of this article was funded by Freie Universität Berlin.

3.9 Conflicts of Interest

The authors declare no conflict of interest.

3.10 References

1. Alberts, B.; Johnson, A.; Lewis, J.; Raff, M.; Roberts, K.; Walter, P. *Molecular Biology of the Cell*, 4th ed.; Garland Science: New York, NY, USA, 2002; ISBN 978-0-8153-3218-3.
2. Haga, R.B.; Ridley, A.J. *Rho GTPases: Regulation and roles in*

- cancer cell biology. *Small GTPases* 2016, 7, 207–221, doi:10.1080/21541248.2016.1232583.
3. Hall, A. Rho GTPases and the control of cell behaviour. *Biochem. Soc. Trans.* 2005, 33, 891–895, doi:10.1042/BST0330891.
 4. Kötting, C.; Gerwert, K. The dynamics of the catalytic site in small GTPases, variations on a common motif. *FEBS Lett.* 2013, 587, 2025–2027, doi:10.1016/j.febslet.2013.05.021.
 5. Aslan, J.E.; McCarty, O.J.T. Rho GTPases in Platelet Function. *J. Thromb. Haemost. JTH* 2013, 11, 35–46, doi:10.1111/jth.12051.
 6. Nobes, C.D.; Hall, A. Rho GTPases Control Polarity, Protrusion, and Adhesion during Cell Movement. *J. Cell Biol.* 1999, 144, 1235–1244, doi:10.1083/jcb.144.6.1235.
 7. Madaule, P.; Axel, R. A novel ras-related gene family. *Cell* 1985, 41, 31–40, doi:10.1016/0092-8674(85)90058-3.
 8. Boettner, B.; Van Aelst, L. The role of Rho GTPases in disease development. *Gene* 2002, 286, 155–174, doi:10.1016/s0378-1119(02)00426-2.
 9. Ellenbroek, S.I.J.; Collard, J.G. Rho GTPases: Functions and association with cancer. *Clin. Exp. Metastasis* 2007, 24, 657–672, doi:10.1007/s10585-007-9119-1.
 10. Fujioka, Y.; Tsuda, M.; Nanbo, A.; Hattori, T.; Sasaki, J.; Sasaki, T.; Miyazaki, T.; Ohba, Y. A Ca²⁺-dependent signalling circuit regulates influenza A virus internalization and infection. *Nat. Commun.* 2013, 4, 1–13, doi:10.1038/ncomms3763.
 11. Wang, J.-L.; Zhang, J.-L.; Chen, W.; Xu, X.-F.; Gao, N.; Fan, D.-Y.; An, J. Roles of Small GTPase Rac1 in the Regulation of Actin Cytoskeleton during Dengue Virus Infection. *PLoS Negl. Trop. Dis.* 2010, 4, e809, doi:10.1371/journal.pntd.0000809.
 12. Hoppe, S.; Schelhaas, M.; Jaeger, V.; Liebig, T.; Petermann, P.; Knebel-Mörsdorf, D. Early herpes simplex virus type 1 infection is dependent on regulated Rac1/Cdc42 signalling in epithelial MDCKII cells. *J. Gen. Virol.* 2006, 87, 3483–3494, doi:10.1099/vir.0.82231-0.
 13. Kurtz, B.M.; Singletary, L.B.; Kelly, S.D.; Frampton, A.R. Equus caballus Major Histocompatibility Complex Class I Is an Entry Receptor for Equine Herpesvirus Type 1. *J. Virol.* 2010, 84, 9027–9034, doi:10.1128/JVI.00287-10.
 14. Azab, W.; Osterrieder, N. Glycoproteins D of Equine Herpesvirus Type 1 (EHV-1) and EHV-4 Determine Cellular Tropism Independently of Integrins. *J. Virol.* 2012, 86, 2031–2044, doi:10.1128/JVI.06555-11.
 15. Azab, W.; Gramatica, A.; Herrmann, A.; Osterrieder, N. Binding of Alphaherpesvirus Glycoprotein H to Surface $\alpha 4\beta 1$ -Integrins Activates Calcium-Signaling Pathways and Induces Phosphatidylserine Exposure on the Plasma Membrane. *mBio* 2015, 6, e01552-15, doi:10.1128/mBio.01552-15.
 16. Price, L.S.; Langeslag, M.; ten Klooster, J.P.; Hordijk, P.L.; Jalink, K.; Collard, J.G. Calcium signaling regulates translocation and activation of Rac. *J. Biol. Chem.* 2003, 278, 39413–39421, doi:10.1074/jbc.M302083200.
 17. Saneyoshi, T.; Hayashi, Y. The Ca²⁺ and Rho GTPase signaling pathways underlying activity-dependent actin remodeling at dendritic spines. *Cytoskelet. Hoboken NJ* 2012, 69, 545–554, doi:10.1002/cm.21037.
 18. Wilk-Blaszczak, M.A.; Singer, W.D.; Quill, T.; Miller, B.; Frost, J.A.; Sternweis, P.C.; Belardetti, F. The monomeric G-proteins Rac1 and/or Cdc42 are required for the inhibition of voltage-dependent calcium current by bradykinin. *J. Neurosci. Off. J. Soc. Neurosci.* 1997, 17, 4094–4100.
 19. Azab, W.; Zajic, L.; Osterrieder, N. The role of glycoprotein H of equine herpesviruses 1 and 4 (EHV-1 and EHV-4) in cellular host range and integrin binding. *Vet. Res.* 2012, 43, 61, doi:10.1186/1297-9716-43-61.
 20. Azab, W.; Kato, K.; Arii, J.; Tsujimura, K.; Yamane, D.; Tohya, Y.; Matsumura, T.; Akashi, H. Cloning of the genome of equine herpesvirus 4

- strain TH20p as an infectious bacterial artificial chromosome. *Arch. Virol.* 2009, 154, 833–842, doi:10.1007/s00705-009-0382-0.
21. Rauth, A.M. The Physical State of Viral Nucleic Acid and the Sensitivity of Viruses to Ultraviolet Light. *Biophys. J.* 1965, 5, 257–273, doi:10.1016/S0006-3495(65)86715-7.
 22. Surviladze, Z.; Waller, A.; Strouse, J.J.; Bologa, C.; Ursu, O.; Salas, V.; Parkinson, J.F.; Phillips, G.K.; Romero, E.; Wandinger-Ness, A.; et al. A Potent and Selective Inhibitor of Cdc42 GTPase. In *Probe Reports from the NIH Molecular Libraries Program; National Center for Biotechnology Information (US): Bethesda, MD, USA, 2010.*
 23. Aguilar, J.; Roy, D.; Ghazal, P.; Wagner, E. Dimethyl sulfoxide blocks herpes simplex virus-1 productive infection in vitro acting at different stages with positive cooperativity. Application of micro-array analysis. *BMC Infect. Dis.* 2002, 2, 9, doi:10.1186/1471-2334-2-9.
 24. Ngamwongsatit, P.; Banada, P.P.; Panbangred, W.; Bhunia, A.K. WST-1-based cell cytotoxicity assay as a substitute for MTT-based assay for rapid detection of toxigenic *Bacillus* species using CHO cell line. *J. Microbiol. Methods* 2008, 73, 211–215, doi:10.1016/j.mimet.2008.03.002.
 25. Dey, P.; Bergmann, T.; Cuellar-Camacho, J.L.; Ehrmann, S.; Chowdhury, M.S.; Zhang, M.; Dahmani, I.; Haag, R.; Azab, W. Multivalent Flexible Nanogels Exhibit Broad-Spectrum Antiviral Activity by Blocking Virus Entry. *ACS Nano* 2018, 12, 6429–6442, doi:10.1021/acsnano.8b01616.
 26. Mochizuki, N.; Yamashita, S.; Kurokawa, K.; Ohba, Y.; Nagai, T.; Miyawaki, A.; Matsuda, M. Spatio-temporal images of growth-factor-induced activation of Ras and Rap1. *Nature* 2001, 411, 1065–1068, doi:10.1038/35082594.
 27. Yoshizaki, H.; Ohba, Y.; Kurokawa, K.; Itoh, R.E.; Nakamura, T.; Mochizuki, N.; Nagashima, K.; Matsuda, M. Activity of Rho-family GTPases during cell division as visualized with FRET-based probes. *J. Cell Biol.* 2003, 162, 223–232, doi:10.1083/jcb.200212049.
 28. Frampton, A.R.; Uchida, H.; von Einem, J.; Goins, W.F.; Grandi, P.; Cohen, J.B.; Osterrieder, N.; Glorioso, J.C. Equine herpesvirus type 1 (EHV-1) utilizes microtubules, dynein, and ROCK1 to productively infect cells. *Vet. Microbiol.* 2010, 141, 12–21, doi:10.1016/j.vetmic.2009.07.035.
 29. Ji, H. Lysis of Cultured Cells for Immunoprecipitation. *Cold Spring Harb. Protoc.* 2010, 2010, pdb.prot5466, doi:10.1101/pdb.prot5466.
 30. Method 9: Semi-Dry Blotting of Proteins. In *Electrophoresis in Practice; John Wiley & Sons Ltd.: London, UK, 2005; pp. 247–255, ISBN 978-3-527-60346-6.*
 31. Using ImageJ to Quantify Blots. Available online: <https://di.uq.edu.au/community-and-alumni/sparq-ed/sparq-ed-services/using-imagej-quantify-blots> (accessed on 11 March 2020).
 32. Sorem, J.; Longnecker, R. Cleavage of Epstein-Barr Virus Glycoprotein B is required for Full Function in Cell:Cell Fusion with both Epithelial and B Cells. *J. Gen. Virol.* 2009, 90, 591–595, doi:10.1099/vir.0.007237-0.
 33. Distler, J.H.W.; Jüngel, A.; Kurowska-Stolarska, M.; Michel, B.A.; Gay, R.E.; Gay, S.; Distler, O. Nucleofection: A new, highly efficient transfection method for primary human keratinocytes*. *Exp. Dermatol.* 2005, 14, 315–320, doi:10.1111/j.0906-6705.2005.00276.x.
 34. Fleming, I.N.; Elliott, C.M.; Buchanan, F.G.; Downes, C.P.; Exton, J.H. Ca²⁺/calmodulin-dependent protein kinase II regulates Tiam1 by reversible protein phosphorylation. *J. Biol. Chem.* 1999, 274, 12753–12758, doi:10.1074/jbc.274.18.12753.
 35. Lyman, M.G.; Enquist, L.W. Herpesvirus Interactions with the Host Cytoskeleton. *J. Virol.* 2009, 83, 2058–2066, doi:10.1128/JVI.01718-08.
 36. Sodeik, B.; Ebersold, M.W.; Helenius, A. Microtubule-mediated transport of incoming herpes simplex virus 1

- capsids to the nucleus. *J. Cell Biol.* 1997, 136, 1007–1021, doi:10.1083/jcb.136.5.1007.
37. Schulze, E.; Asai, D.J.; Bulinski, J.C.; Kirschner, M. Posttranslational modification and microtubule stability. *J. Cell Biol.* 1987, 105, 2167–2177, doi:10.1083/jcb.105.5.2167.
 38. Takemura, R.; Okabe, S.; Umeyama, T.; Kanai, Y.; Cowan, N.J.; Hirokawa, N. Increased microtubule stability and alpha tubulin acetylation in cells transfected with microtubule-associated proteins MAP1B, MAP2 or tau. *J. Cell Sci.* 1992, 103, 953–964.
 39. Bulinski, J.C.; Richards, J.E.; Piperno, G. Posttranslational modifications of alpha tubulin: Detyrosination and acetylation differentiate populations of interphase microtubules in cultured cells. *J. Cell Biol.* 1988, 106, 1213–1220, doi:10.1083/jcb.106.4.1213.
 40. Reed, N.A.; Cai, D.; Blasius, T.L.; Jih, G.T.; Meyhofer, E.; Gaertig, J.; Verhey, K.J. Microtubule Acetylation Promotes Kinesin-1 Binding and Transport. *Curr. Biol.* 2006, 16, 2166–2172, doi:10.1016/j.cub.2006.09.014.
 41. Zhong, M.; Zheng, K.; Chen, M.; Xiang, Y.; Jin, F.; Ma, K.; Qiu, X.; Wang, Q.; Peng, T.; Kitazato, K.; et al. Heat-Shock Protein 90 Promotes Nuclear Transport of Herpes Simplex Virus 1 Capsid Protein by Interacting with Acetylated Tubulin. *PLoS ONE* 2014, 9, e99425, doi:10.1371/journal.pone.0099425.
 42. Turner, A.; Bruun, B.; Minson, T.; Browne, H. Glycoproteins gB, gD, and gHgL of Herpes Simplex Virus Type 1 Are Necessary and Sufficient to Mediate Membrane Fusion in a Cos Cell Transfection System. *J. Virol.* 1998, 72, 873–875.
 43. Wittmann, T.; Waterman-Storer, C.M. Cell motility: Can Rho GTPases and microtubules point the way? *J. Cell Sci.* 2001, 114, 3795–3803.
 44. Csellner, H.; Walker, C.; Wellington, J.E.; McLure, L.E.; Love, D.N.; Whalley, J.M. EHV-1 glycoprotein D (EHV-1 gD) is required for virus entry and cell-cell fusion, and an EHV-1 gD deletion mutant induces a protective immune response in mice. *Arch. Virol.* 2000, 145, 2371–2385, doi:10.1007/s007050070027.
 45. Zamudio-Meza, H.; Castillo-Alvarez, A.; González-Bonilla, C.; Meza, I. Cross-talk between Rac1 and Cdc42 GTPases regulates formation of filopodia required for dengue virus type-2 entry into HMEC-1 cells. *J. Gen. Virol.* 2009, 90, 2902–2911, doi:10.1099/vir.0.014159-0.
 46. Lv, C.; Lin, Y.; Sun, E.-Z.; Tang, B.; Ao, J.; Wang, J.-J.; Zhang, Z.-L.; Zheng, Z.; Wang, H.; Pang, D.-W. Internalization of the pseudorabies virus via macropinocytosis analyzed by quantum dot-based single-virus tracking. *Chem. Commun.* 2018, 54, 11184–11187, doi:10.1039/C8CC05614E.
 47. Petermann, P.; Haase, I.; Knebel-Mörsdorf, D. Impact of Rac1 and Cdc42 Signaling during Early Herpes Simplex Virus Type 1 Infection of Keratinocytes. *J. Virol.* 2009, 83, 9759–9772, doi:10.1128/JVI.00835-09.
 48. O'Donnell, C.D.; Shukla, D. A novel function of heparan sulfate in the regulation of cell-cell fusion. *J. Biol. Chem.* 2009, 284, 29654–29665, doi:10.1074/jbc.M109.037960.
 49. Eitzen, G. Actin remodeling to facilitate membrane fusion. *Biochim. Biophys. Acta BBA Mol. Cell Res.* 2003, 1641, 175–181, doi:10.1016/S0167-4889(03)00087-9.
 50. Ellis, S.; Mellor, H. The novel Rho-family GTPase Rif regulates coordinated actin-based membrane rearrangements. *Curr. Biol.* 2000, 10, 1387–1390, doi:10.1016/S0960-9822(00)00777-6.
 51. Azab, W.; Lehmann, M.J.; Osterrieder, N. Glycoprotein H and $\alpha 4\beta 1$ integrins determine the entry pathway of alphaherpesviruses. *J. Virol.* 2013, 87, 5937–5948, doi:10.1128/JVI.03522-12.
 52. Reszka, N.; Zhou, C.; Song, B.; Sodroski, J.G.; Knipe, D.M. Simian TRIM5 α Proteins Reduce Replication of Herpes Simplex Virus. *Virology* 2010, 398, 243–250, doi:10.1016/j.virol.2009.11.041.

53. Cohen, E.M.; Avital, N.; Shamay, M.; Kobilier, O. Abortive herpes simplex virus infection of nonneuronal cells results in quiescent viral genomes that can reactivate. *Proc. Natl. Acad. Sci. USA* 2020, 117, 635–640, doi:10.1073/pnas.1910537117.
54. Wu, W.J.; Erickson, J.W.; Lin, R.; Cerione, R.A. The γ -subunit of the coatomer complex binds Cdc42 to mediate transformation. *Nature* 2000, 405, 800–804, doi:10.1038/35015585.
55. Raghu, H.; Sharma-Walia, N.; Veettil, M.V.; Sadagopan, S.; Caballero, A.; Sivakumar, R.; Varga, L.; Bottero, V.; Chandran, B. Lipid rafts of primary endothelial cells are essential for Kaposi's sarcoma-associated herpesvirus/human herpesvirus 8-induced phosphatidylinositol 3-kinase and RhoA-GTPases critical for microtubule dynamics and nuclear delivery of viral DNA but dispensable for binding and entry. *J. Virol.* 2007, 81, 7941–7959, doi:10.1128/JVI.02848-06.
56. Döhner, K.; Nagel, C.-H.; Sodeik, B. Viral stop-and-go along microtubules: Taking a ride with dynein and kinesins. *Trends Microbiol.* 2005, 13, 320–327, doi:10.1016/j.tim.2005.05.010.
57. Alper, J.D.; Decker, F.; Agana, B.; Howard, J. The Motility of Axonemal Dynein Is Regulated by the Tubulin Code. *Biophys. J.* 2014, 107, 2872–2880, doi:10.1016/j.bpj.2014.10.061.
58. Husain, M.; Harrod, K.S. Enhanced acetylation of alpha-tubulin in influenza A virus infected epithelial cells. *FEBS Lett.* 2011, 585, 128–132, doi:10.1016/j.febslet.2010.11.023.
59. Elliott, G.; O'Hare, P. Herpes Simplex Virus Type 1 Tegument Protein VP22 Induces the Stabilization and Hyperacetylation of Microtubules. *J. Virol.* 1998, 72, 6448–6455.
60. Atanasiu, D.; Saw, W.T.; Cohen, G.H.; Eisenberg, R.J. Cascade of Events Governing Cell-Cell Fusion Induced by Herpes Simplex Virus Glycoproteins gD, gH/gL, and gB. *J. Virol.* 2010, 84, 12292–12299, doi:10.1128/JVI.01700-10.
61. Atanasiu, D.; Saw, W.T.; Eisenberg, R.J.; Cohen, G.H. Regulation of Herpes Simplex Virus Glycoprotein-Induced Cascade of Events Governing Cell-Cell Fusion. *J. Virol.* 2016, 90, 10535–10544, doi:10.1128/JVI.01501-16.
62. Palazzo, A.; Ackerman, B.; Gundersen, G.G. Cell biology: Tubulin acetylation and cell motility. *Nature* 2003, 421, 230, doi:10.1038/421230a.
63. Naghavi, M.H.; Walsh, D. Microtubule Regulation and Function during Virus Infection. *J. Virol.* 2017, 91, doi:10.1128/JVI.00538-17.
64. Baghi, H.B.; Laval, K.; Favoreel, H.; Nauwynck, H.J. Isolation and characterization of equine nasal mucosal CD172a+ cells. *Vet. Immunol. Immunopathol.* 2014, 157, 155–163, doi:10.1016/j.vetimm.2013.12.001.
65. Nakamichi, K.; Matsumoto, Y.; Otsuka, H. Bovine Herpesvirus 1 Glycoprotein G Is Necessary for Maintaining Cell-to-Cell Junctional Adherence among Infected Cells. *Virology* 2002, 294, 22–30, doi:10.1006/viro.2001.1264.
66. Haller, C.; Tibroni, N.; Rudolph, J.M.; Grosse, R.; Fackler, O.T. Nef does not inhibit F-actin remodelling and HIV-1 cell–cell transmission at the T lymphocyte virological synapse. *Eur. J. Cell Biol.* 2011, 90, 913–921, doi:10.1016/j.ejcb.2010.09.010.

Chapter 4

4.1 General discussion

EHV-1 is an important pathogen, and that is closely related to the EHV-4 [1–3], they present a unique model among Alpha herpesviruses to study virus-host interactions, since they vary in the pathogenic manifestations with EHV-1 causing systemic infection and equine herpesviral myeloencephalopathy, pneumonia, abortions, ataxia paralysis and death, while EHV-4 is limited to respiratory manifestations [4–6]. The difference is also present in the specifics of infection at the cellular level, EHV-4 infection is limited to fusion within the endocytic pathway, while EHV-1 is additionally capable of fusion at the plasma membrane utilizing the signaling cascade that involves activation of PIP3, PLSCR-1 and release of Ca²⁺ from ER resulting in increase in cytosolic Ca²⁺ concentration and exposure of PS to the outer leaflet of the plasma membrane [7]. However, the specific role that PS plays in EHV-1 infection, or what the function is of EHV-1 induced signaling cascade in infection has not yet been described. For this dissertation, I therefore aimed to explore the roles of PS and intracellular signaling in EHV-1 infection.

4.2 Importance of phospholipids in EHV-1 entry

EHV-1 is enveloped virus and its entry into the host cell is mediated by a few host factors such as attachment factors heparan sulfate proteoglycans (HSPG) and chondroitin sulfate proteoglycans (CSPG) [8,9]. EHV-1 infection induced exposure of PS through activation of PLSCR-1 to the outer leaflet of the plasma membrane [7]. PS is seldomly exposed in normal cells [10] that leads to suspicion that PS plays role in virus infection, perhaps facilitating the attachment similar to what was found for hepatitis C virus [11]. Another distinct possibility is that PS exposure plays role in masking the infected cell from the host immune system in the process known as apoptotic mimicry [12,13], since PS exposure on the outer leaflet of the plasma membrane is associated with the apoptotic states of the cells [14]. However, EHV-1-induced PS exposure is a characteristic of an early stage of infection [7], and it is likely to be localized to the virus attachment site suggesting that exposure of PS is playing role in the virus attachment or entry. Another potential role that PS exposure at the point of virus attachment can play is modulation of the plasma membrane fluidity since it is highly dependent on the phospholipid composition [15,16]. Physical properties of the membrane, including the fluidity determine the likelihood of the fusion [17–19]. The process of fusion is essential in order to release nucleocapsid into the cytoplasm and the infection process to continue.

4.3 EHV-1 inhibition with charged lipids

In the course of this work we have identified that PS and DOTAP both inhibit the infection of Equine dermal (ED) cells by EHV-1. Inhibition of the viral infection with the charged phospholipids added to the infection media in the form of vesicles was immediate, reversible, dose dependent and seems not to rely on the integration of the phospholipids into the plasma membrane of the host cell, but rather to interact with the virus. Biophysical examination of interaction between PS or DOTAP with EHV-1, as measured by the surface plasmon resonance showed that both PS and DOTAP are interacting with the viral particles. Additionally, microscopic examination showed strong viral preference to binding to the PS and DOTAP GUVs. In both cases interaction with the DOTAP was stronger.

EHV-1 can interact with both cationic (DOTAP) and anionic (PS) lipids. The finding that during EHV-1 infection there is a scramblase mediated exposure of PS to the outer leaflet of the plasma membrane suggest that PS is utilized by the EHV-1. Findings that EHV-1 is inhibited both by positively and negatively charged lipids is interesting in itself, DOTAP seems to have much stronger interactions with the EHV-1 particle on SPR and under microscopical examinations. It appears that DOTAP vesicles enclose the viral particle and perhaps preventing the virus from getting in to proximity of the cell. This strong interaction with the DOTAP can be explained through overall charge interactions between the viral particle and the lipids [106]. Interactions of EHV-1 with PS are not as strong as with DOTAP, while the inhibition

of infection is about equal, this suggests that mechanism through which PS is inhibiting EHV-1 infection is more specific. The viral interactions partners and the role that PS plays in the context of cell entry during EHV-1 infection remains to be studied.

Another potential application of the interaction and inhibition that we found charged phospholipids have, is potential future development of antiviral or therapeutic strategies. Phosphatidylserine liposomes were already used as a drug delivery vehicle and shown to have beneficial effects on their own. However, effects of on Phosphatidylserine liposomes on EHV-1 or EHV-4 infections in-vivo have not been investigated [107–109].

4.4 Role of Rac1 and Cdc42 in EHV-1 infection

Infection of ED cells with EHV-1 and EHV-4 involves activation of small GTPases. Inhibition of the small GTPases Rac1 and Cdc42 leads to reduction of infection. This effect is transient, and affects early stages of infection. In the experiment where virus was allowed to penetrate cells prior to inhibition of small GTPases, the infection was not affected. We found activation of the Rac1 and Cdc42 small GTPases in a 20-minute time window after contact with inactivated viral particles in a FRET assay.

We present some evidence to suggest that activation of small GTPase RhoA is involved in EHV-4 entry, but not in EHV-1 entry. We found that RhoA inhibitor had no effect on the ability of EHV-1 to establish the infection, while EHV-1 gH4, and EHV-1 gHS440A, both mutants that cannot fuse at the plasma membrane, had their infection rates significantly reduced. RhoA, has been described playing important role in endocytic pathway, that is utilized by the EHV-1 gH4, EHV-1 gHS440A and EHV-4 viruses [28,110].

4.5 Small GTPases activation is independent from integrin interaction

Inhibition of small GTPases affected infections of both integrin binding EHV-1, and EHV-1 mutants that cannot bind to the integrins EHV-1 gH4, EHV-1 gHS440A [20] and EHV-4 [21]. Signaling cascade that starts with EHV-1 gH interactions with $\alpha 4\beta 1$ -Integrins and activates calcium release from endoplasmic reticulum and is essential for EHV-1 fusion at the plasma membrane may involve small GTPases although this topic will require further investigation [7].

4.6 Role of small GTPases in EHV-1 transport

We have identified that small GTPases Cdc42 and Rac1 play role in the viral transport, inhibition of Cdc42 and Rac1 small GTPases had prevented EHV-1 induces acetylation of the tubulin, similar to effect described previously for ROCK1 small GTPase [22]. Effects on the EHV-1 transport can be detected in the decreased infections rates as early as 3 HPI and increased number of viral particles present at the cytoplasm while reducing number of viral particles that reached the nucleus. While the EHV-1 cell entry, does not seem to require activation of Cdc42 and Rac1. EHV-1 was able to enter Rac1 and Cdc42 inhibitor treated cells, effectively avoiding the low pH treatment, so that infection can be rescued if the inhibitors were removed from the media.

4.7 Role of small GTPases in EHV-4 infection

EHV-4 infection was reduced under conditions of Cdc42 and Rac1 inhibition. Interestingly in case of EHV-4 small GTPase inhibition resulted in reduction of both plaque number and plaque diameter. Observation is interesting, in this study the number of plaques developed under Cdc42 inhibition was low. However, the few EHV-4 plaques that developed under the condition of Cdc42 inhibition were much closer to the typical diameter, than EHV-1 plaques. The exact role of Cdc42 in EHV-4 infection, particularly in cell-to-cell spread remains to be studied.

Inhibition of small GTPases can have number of effects on the cell, in our experiments, we utilized non-cytotoxic concentration of the inhibitors, and observed some specificity for

example inhibitor of RhoA small GTPase, that is primarily described as a cytoskeleton regulator [111], had no statistically significant effect on the EHV-1 establishing infection, while Rac1 and Cdc42 inhibitors has led to strong reduction of the infection. RhoA inhibitor, has led to reduction in cell-to-cell spread of the virus, as suggested by the plaque size assay. Testing role of the small GTPases on EHV-1 infection with the other approaches, such as dominant negative or constitutively active mutants of the small GTPases, would grant higher confidence to our findings [67,68]. Over the course of this work, we have attempted to utilize mutant forms of small GTPases, but these approaches have not yielded consistent outcomes and were not included in the results. ED cells used in this study are primary cells, transfection of ED cells has very low efficacy. Transfection of GTPase mutant expressing plasmids was out of the question, as this would yield low double digits of the number of transfected cells. Nucleofection of ED cells, while producing workable amounts of successfully nucleofected cells, seemingly resulted in high amounts of cell stress response [112], we found cellular signaling under such conditions to be inconsistent. Another alternative approach that we have tried was to infect the ED cells with the lentivirus, to establish cell lines that would express desired small GTPase mutant. This lentivirus-based approach met a number of obstacles and was unsuccessful in the end as well. Rates of lentivirus infection of the ED cells was low, and comparable to the transfection rates, thus creating a small bottle neck for the progeny cells, the progeny cells had slow generation times, and morphology of the cells was similar to very high passage number ED cells, at the point where their number would allow to perform an experiment. Constant expression of the cell-cycle involved GTPase mutants, presumably also had an effect on the selection of the cells, potentially resulting in cells that were able to readjust cell signaling to overcome the effects of expressed small GTPase mutant. As a consequence of such limitations, Lentivirus-based approach to expression of small GTPases did not yield an interpretable result.

4.8 Final remarks and outlook

We found that under the conditions of Cdc42 or Rac1 inhibition, there was no significant accumulation of the virus particles near the plasma membrane, neither there was an increased colocalization with the endosomal markers, while we found increase in cytoplasmically localized virus particles, proportional to decrease of viral particles that was found at the nucleus. This suggests that EHV-1 infection in such conditions was not redirected towards the endocytic pathways, and fusion at the plasma membrane was undisturbed, while the trafficking of the virus particles to the perinuclear space was affected. This is consistent with the finding that Cdc42 and Rac1 inhibitors are preventing EHV-1 induced stabilization microtubules through K-40 acetylation and that the infection of the Cdc42 and Rac1 inhibited cells could be rescued, if the inhibitors were removed post virus entry. However, some aspects of this study could be further improved, for example acetylation status of tubulin, was examined in the human 293-T embryonic kidney cell line due to non-reactivity of the monoclonal antibodies to ED cells K-40 acetylated α -tubulin, despite this reactivity being previously reported [64]. Additionally, low selection and quality of horse specific antibodies, did not allow to quantify the amount of activated GTPases in infected cells with a commonly used pulldown assay, followed by an immunoblotting analysis, nor to measure the changes in localization of PLSCR-1 in response cell-virus interactions. With techniques such as artificial in-vitro selection of nanobodies [113] in combination with expression of the required fragments, would theoretically allow to produce high-quality antibodies in house, however this technique would require costly upfront investment, that was beyond the scope of the current work. FRET analysis could be further improved with the utilization of the two-photon approach [114] or near infrared imaging [115] to reduce the phototoxicity during the imaging process, and increase the resolution, allowing to observe the kinetics of the viral particle in the cell under different treatments.

In conclusion our data suggest the model where EHV-1 infection is inducing activation of small GTPases Cdc42 and Rac1, activation is required for viral transport to the nucleus, and cell-to-cell spread but not for cell entry. Activation of Cdc42 and Rac1 is needed for the EHV-1 induced stabilization of microtubules, that is achieved through acetylation of α -tubulin.

4.9 Reference

1. Rodrigues, R.; Danskog, K.; Överby, A.K.; Arnberg, N. Characterizing the Cellular Attachment Receptor for Langkat Virus. *PLOS ONE* **2019**, *14*, e0217359, doi:10.1371/journal.pone.0217359.
2. Ugolini, S.; Mondor, I.; Sattentau, Q.J. HIV-1 Attachment: Another Look. *Trends Microbiol.* **1999**, *7*, 144–149, doi:10.1016/s0966-842x(99)01474-2.
3. Vlasak, M.; Goesler, I.; Blaas, D. Human Rhinovirus Type 89 Variants Use Heparan Sulfate Proteoglycan for Cell Attachment. *J. Virol.* **2005**, *79*, 5963–5970, doi:10.1128/JVI.79.10.5963-5970.2005.
4. Fields, B.N.; Knipe, D.M.; Howley, P.M.; Griffin, D.E. *Fields Virology*; Lippincott Williams & Wilkins: Philadelphia, 2001; ISBN 978-0-7817-1832-5.
5. Di Lorenzo, C.; Angus, A.G.N.; Patel, A.H. Hepatitis C Virus Evasion Mechanisms from Neutralizing Antibodies. *Viruses* **2011**, *3*, 2280–2300, doi:10.3390/v3112280.
6. Mondor, I.; Ugolini, S.; Sattentau, Q.J. Human Immunodeficiency Virus Type 1 Attachment to HeLa CD4 Cells Is CD4 Independent and Gp120 Dependent and Requires Cell Surface Heparans. *J. Virol.* **1998**, *72*, 3623–3634, doi:10.1128/JVI.72.5.3623-3634.1998.
7. Osterrieder, N. Construction and Characterization of an Equine Herpesvirus 1 Glycoprotein C Negative Mutant. *Virus Res.* **1999**, *59*, 165–177, doi:10.1016/S0168-1702(98)00134-8.
8. Chandran, B. Early Events in Kaposi's Sarcoma-Associated Herpesvirus Infection of Target Cells. *J. Virol.* **2010**, *84*, 2188–2199, doi:10.1128/JVI.01334-09.
9. Xiong, X.; Zhao, Y.; Zhuge, S.; Zhou, H.; Cui, Y. Small Interfering RNA-Mediated Inhibition of Respiratory Syncytial Virus Infections in Hela Cells. *Int. J. Clin. Exp. Med.* **2019**, *12*, 12264–12270.
10. Nicola, A.V.; Hou, J.; Major, E.O.; Straus, S.E. Herpes Simplex Virus Type 1 Enters Human Epidermal Keratinocytes, but Not Neurons, via a PH-Dependent Endocytic Pathway. *J. Virol.* **2005**, *79*, 7609–7616, doi:10.1128/JVI.79.12.7609-7616.2005.
11. Ward, A.E.; Dryden, K.A.; Tamm, L.K.; Ganser-Pornillos, B.K. Catching HIV in the Act of Fusion: Insight from Cryo-Et Intermediates of HIV Membrane Fusion. *Biophys. J.* **2019**, *116*, 180a.
12. Moss, B. Membrane Fusion during Poxvirus Entry. *Semin. Cell Dev. Biol.* **2016**, *60*, 89–96, doi:10.1016/j.semcdb.2016.07.015.
13. Theerawatanasirikul, S.; Phecharat, N.; Prawetongsopon, C.; Chaicumpa, W.; Lekcharoensuk, P. Dynein Light Chain DYNLL1 Subunit Facilitates Porcine Circovirus Type 2 Intracellular Transports along Microtubules. *Arch. Virol.* **2017**, *162*, 677–686, doi:10.1007/s00705-016-3140-0.
14. Döhner, K.; Nagel, C.-H.; Sodeik, B. Viral Stop-and-Go along Microtubules: Taking a Ride with Dynein and Kinesins. *Trends Microbiol.* **2005**, *13*, 320–327, doi:10.1016/j.tim.2005.05.010.
15. Wen, L.; Zheng, Z.-H.; Liu, A.-A.; Lv, C.; Zhang, L.-J.; Ao, J.; Zhang, Z.-L.; Wang, H.-Z.; Lin, Y.; Pang, D.-W. Tracking Single Baculovirus Retrograde Transportation in Host Cell via Quantum Dot-Labeling of Virus Internal Component. *J. Nanobiotechnology* **2017**, *15*, 37, doi:10.1186/s12951-017-0270-9.
16. Greber, U.F.; Way, M. A Superhighway to Virus Infection. *Cell* **2006**, *124*, 741–754, doi:10.1016/j.cell.2006.02.018.
17. Lyman, M.G.; Enquist, L.W. Herpesvirus Interactions with the Host Cytoskeleton. *J. Virol.* **2009**, *83*, 2058–2066, doi:10.1128/JVI.01718-08.
18. Davison, A.J.; Eberle, R.; Ehlers, B.; Hayward, G.S.; McGeoch, D.J.; Minson, A.C.; Pellett, P.E.; Roizman, B.; Studdert, M.J.; Thiry, E. The Order Herpesvirales. *Arch. Virol.* **2009**, *154*,

- 171–177, doi:10.1007/s00705-008-0278-4.
19. Ma, G.; Azab, W.; Osterrieder, N. Equine Herpesviruses Type 1 (EHV-1) and 4 (EHV-4)—Masters of Co-Evolution and a Constant Threat to Equids and Beyond. *Vet. Microbiol.* **2013**, *167*, 123–134, doi:10.1016/j.vetmic.2013.06.018.
 20. Azab, W.; Tsujimura, K.; Maeda, K.; Kobayashi, K.; Mohamed, Y.M.; Kato, K.; Matsumura, T.; Akashi, H. Glycoprotein C of Equine Herpesvirus 4 Plays a Role in Viral Binding to Cell Surface Heparan Sulfate. *Virus Res.* **2010**, *151*, 1–9, doi:10.1016/j.virusres.2010.03.003.
 21. Banfield, B.W.; Leduc, Y.; Esford, L.; Schubert, K.; Tufaro, F. Sequential Isolation of Proteoglycan Synthesis Mutants by Using Herpes Simplex Virus as a Selective Agent: Evidence for a Proteoglycan-Independent Virus Entry Pathway. *J. Virol.* **1995**, *69*, 3290–3298.
 22. Spear, P.G.; Longnecker, R. Herpesvirus Entry: An Update. *J. Virol.* **2003**, *77*, 10179–10185, doi:10.1128/JVI.77.19.10179-10185.2003.
 23. Kurtz, B.M.; Singletary, L.B.; Kelly, S.D.; Frampton, A.R. Equus Caballus Major Histocompatibility Complex Class I Is an Entry Receptor for Equine Herpesvirus Type 1. *J. Virol.* **2010**, *84*, 9027–9034, doi:10.1128/JVI.00287-10.
 24. Sasaki, M.; Hasebe, R.; Makino, Y.; Suzuki, T.; Fukushi, H.; Okamoto, M.; Matsuda, K.; Taniyama, H.; Sawa, H.; Kimura, T. Equine Major Histocompatibility Complex Class I Molecules Act as Entry Receptors That Bind to Equine Herpesvirus-1 Glycoprotein D. *Genes Cells* **2011**, *16*, 343–357, doi:10.1111/j.1365-2443.2011.01491.x.
 25. Azab, W.; Harman, R.; Miller, D.; Tallmadge, R.; Frampton, A.R.; Antczak, D.F.; Osterrieder, N. Equid Herpesvirus Type 4 Uses a Restricted Set of Equine Major Histocompatibility Complex Class I Proteins as Entry Receptors. *J. Gen. Virol.* **2014**, *95*, 1554–1563, doi:10.1099/vir.0.066407-0.
 26. Azab, W.; Lehmann, M.J.; Osterrieder, N. Glycoprotein H and A4 β 1 Integrins Determine the Entry Pathway of Alphaherpesviruses. *J. Virol.* **2013**, *87*, 5937–5948, doi:10.1128/JVI.03522-12.
 27. Azab, W.; Gramatica, A.; Herrmann, A.; Osterrieder, N. Binding of Alphaherpesvirus Glycoprotein H to Surface A4 β 1-Integrins Activates Calcium-Signaling Pathways and Induces Phosphatidylserine Exposure on the Plasma Membrane. *mBio* **2015**, *6*, e01552-15, doi:10.1128/mBio.01552-15.
 28. Azab, W.; Zajic, L.; Osterrieder, N. The Role of Glycoprotein H of Equine Herpesviruses 1 and 4 (EHV-1 and EHV-4) in Cellular Host Range and Integrin Binding. *Vet. Res.* **2012**, *43*, 61, doi:10.1186/1297-9716-43-61.
 29. Nobes, C.D.; Hall, A. Rho GTPases Control Polarity, Protrusion, and Adhesion during Cell Movement. *J. Cell Biol.* **1999**, *144*, 1235–1244, doi:10.1083/jcb.144.6.1235.
 30. Kötting, C.; Gerwert, K. The Dynamics of the Catalytic Site in Small GTPases, Variations on a Common Motif. *FEBS Lett.* **2013**, *587*, 2025–2027, doi:10.1016/j.febslet.2013.05.021.
 31. Cherfils, J.; Zeghouf, M. Regulation of Small GTPases by GEFs, GAPs, and GDIs. *Physiol. Rev.* **2013**, *93*, 269–309, doi:10.1152/physrev.00003.2012.
 32. Harvey, J.J. AN UNIDENTIFIED VIRUS WHICH CAUSES THE RAPID PRODUCTION OF TUMOURS IN MICE. *Nature* **1964**, *204*, 1104–1105, doi:10.1038/2041104b0.
 33. Willingham, M.C.; Pastan, I.; Shih, T.Y.; Scolnick, E.M. Localization of the Src Gene Product of the Harvey Strain of MSV to Plasma Membrane of Transformed Cells by Electron Microscopic Immunocytochemistry. *Cell* **1980**, *19*, 1005–1014, doi:10.1016/0092-8674(80)90091-4.
 34. Shih, T.Y.; Weeks, M.O.; Young, H.A.; Scholnick, E.M. Identification of a Sarcoma Virus-Coded Phosphoprotein in Nonproducer Cells Transformed by Kirsten or Harvey Murine Sarcoma

- Virus. *Virology* **1979**, *96*, 64–79, doi:10.1016/0042-6822(79)90173-9.
35. Scolnick, E.M.; Papageorge, A.G.; Shih, T.Y. Guanine Nucleotide-Binding Activity as an Assay for Src Protein of Rat-Derived Murine Sarcoma Viruses. *Proc. Natl. Acad. Sci.* **1979**, *76*, 5355–5359, doi:10.1073/pnas.76.10.5355.
 36. Chang, E.H.; Gonda, M.A.; Ellis, R.W.; Scolnick, E.M.; Lowy, D.R. Human Genome Contains Four Genes Homologous to Transforming Genes of Harvey and Kirsten Murine Sarcoma Viruses. *Proc. Natl. Acad. Sci. U. S. A.* **1982**, *79*, 4848–4852.
 37. Parada, L.F.; Weinberg, R.A. Presence of a Kirsten Murine Sarcoma Virus Ras Oncogene in Cells Transformed by 3-Methylcholanthrene. *Mol. Cell. Biol.* **1983**, *3*, 2298–2301.
 38. Santos, E.; Martin-Zanca, D.; Reddy, E.P.; Pierotti, M.A.; Della Porta, G.; Barbacid, M. Malignant Activation of a K-Ras Oncogene in Lung Carcinoma but Not in Normal Tissue of the Same Patient. *Science* **1984**, *223*, 661–664, doi:10.1126/science.6695174.
 39. Gibbs, J.B.; Sigal, I.S.; Poe, M.; Scolnick, E.M. Intrinsic GTPase Activity Distinguishes Normal and Oncogenic Ras P21 Molecules. *Proc. Natl. Acad. Sci. U. S. A.* **1984**, *81*, 5704–5708, doi:10.1073/pnas.81.18.5704.
 40. Scheffzek, K.; Ahmadian, M.R.; Kabsch, W.; Wiesmüller, L.; Lautwein, A.; Schmitz, F.; Wittinghofer, A. The Ras-RasGAP Complex: Structural Basis for GTPase Activation and Its Loss in Oncogenic Ras Mutants. *Science* **1997**, *277*, 333–339, doi:10.1126/science.277.5324.333.
 41. Trahey, M.; Wong, G.; Halenbeck, R.; Rubinfeld, B.; Martin, G.A.; Ladner, M.; Long, C.M.; Crosier, W.J.; Watt, K.; Kohts, K. Molecular Cloning of Two Types of GAP Complementary DNA from Human Placenta. *Science* **1988**, *242*, 1697–1700, doi:10.1126/science.3201259.
 42. Trahey, M.; McCormick, F. A Cytoplasmic Protein Stimulates Normal N-Ras P21 GTPase, but Does Not Affect Oncogenic Mutants. *Science* **1987**, *238*, 542–545, doi:10.1126/science.2821624.
 43. Bos, J.L.; Fearon, E.R.; Hamilton, S.R.; Verlaan-de Vries, M.; van Boom, J.H.; van der Eb, A.J.; Vogelstein, B. Prevalence of Ras Gene Mutations in Human Colorectal Cancers. *Nature* **1987**, *327*, 293–297, doi:10.1038/327293a0.
 44. Ras Oncogenes in Human Cancer: A Review | Cancer Research Available online: <https://cancerres.aacrjournals.org/content/49/17/4682.short> (accessed on 12 June 2020).
 45. de Vos, A.M.; Tong, L.; Milburn, M.V.; Matias, P.M.; Jancarik, J.; Noguchi, S.; Nishimura, S.; Miura, K.; Ohtsuka, E.; Kim, S.H. Three-Dimensional Structure of an Oncogene Protein: Catalytic Domain of Human c-H-Ras P21. *Science* **1988**, *239*, 888–893, doi:10.1126/science.2448879.
 46. Schlichting, I.; Almo, S.C.; Rapp, G.; Wilson, K.; Petratos, K.; Lentfer, A.; Wittinghofer, A.; Kabsch, W.; Pai, E.F.; Petsko, G.A.; et al. Time-Resolved X-Ray Crystallographic Study of the Conformational Change in Ha-Ras P21 Protein on GTP Hydrolysis. *Nature* **1990**, *345*, 309–315, doi:10.1038/345309a0.
 47. Downward, J.; Riehl, R.; Wu, L.; Weinberg, R.A. Identification of a Nucleotide Exchange-Promoting Activity for P21ras. *Proc. Natl. Acad. Sci. U. S. A.* **1990**, *87*, 5998–6002, doi:10.1073/pnas.87.15.5998.
 48. Rodriguez-Viciana, P.; Warne, P.H.; Dhand, R.; Vanhaesebroeck, B.; Gout, I.; Fry, M.J.; Waterfield, M.D.; Downward, J. Phosphatidylinositol-3-OH Kinase Direct Target of Ras. *Nature* **1994**, *370*, 527–532, doi:10.1038/370527a0.
 49. Warne, P.H.; Vician, P.R.; Downward, J. Direct Interaction of Ras and the Amino-Terminal Region of Raf-1 in Vitro. *Nature* **1993**, *364*, 352–355, doi:10.1038/364352a0.
 50. Chin, L.; Tam, A.; Pomerantz, J.; Wong, M.; Holash, J.; Bardeesy, N.; Shen, Q.; O'Hagan, R.; Pantginis, J.; Zhou, H.; et al. Essential Role for Oncogenic Ras in Tumour

- Maintenance. *Nature* **1999**, *400*, 468–472, doi:10.1038/22788.
51. Johnson, L.; Greenbaum, D.; Cichowski, K.; Mercer, K.; Murphy, E.; Schmitt, E.; Bronson, R.T.; Umanoff, H.; Edelman, W.; Kucherlapati, R.; et al. K-Ras Is an Essential Gene in the Mouse with Partial Functional Overlap with N-Ras. *Genes Dev.* **1997**, *11*, 2468–2481.
 52. Koera, K.; Nakamura, K.; Nakao, K.; Miyoshi, J.; Toyoshima, K.; Hatta, T.; Otani, H.; Aiba, A.; Katsuki, M. K-Ras Is Essential for the Development of the Mouse Embryo. *Oncogene* **1997**, *15*, 1151–1159, doi:10.1038/sj.onc.1201284.
 53. Colicelli, J. Human RAS Superfamily Proteins and Related GTPases. *Sci. STKE* **2004**, *2004*, re13–re13, doi:10.1126/stke.2502004re13.
 54. Bourne, H.R.; Sanders, D.A.; McCormick, F. The GTPase Superfamily: Conserved Structure and Molecular Mechanism. *Nature* **1991**, *349*, 117–127, doi:10.1038/349117a0.
 55. Seabra, M.C.; Wasmeier, C. Controlling the Location and Activation of Rab GTPases. *Curr. Opin. Cell Biol.* **2004**, *16*, 451–457, doi:10.1016/j.ceb.2004.06.014.
 56. Bishop, A.L.; Hall, A. Rho GTPases and Their Effector Proteins. *Biochem. J.* **2000**, *348 Pt 2*, 241–255.
 57. Hall, A. Rho GTPases and the Control of Cell Behaviour. *Biochem. Soc. Trans.* **2005**, *33*, 891–895, doi:10.1042/BST0330891.
 58. Ridley, A.J. Rho Family Proteins: Coordinating Cell Responses. *Trends Cell Biol.* **2001**, *11*, 471–477, doi:10.1016/s0962-8924(01)02153-5.
 59. Haga, R.B.; Ridley, A.J. Rho GTPases: Regulation and Roles in Cancer Cell Biology. *Small GTPases* **2016**, *7*, 207–221, doi:10.1080/21541248.2016.1232583.
 60. Etienne-Manneville, S.; Hall, A. Rho GTPases in Cell Biology. *Nature* **2002**, *420*, 629–635, doi:10.1038/nature01148.
 61. Fujioka, Y.; Tsuda, M.; Nanbo, A.; Hattori, T.; Sasaki, J.; Sasaki, T.; Miyazaki, T.; Ohba, Y. A Ca²⁺-Dependent Signalling Circuit Regulates Influenza A Virus Internalization and Infection. *Nat. Commun.* **2013**, *4*, 1–13, doi:10.1038/ncomms3763.
 62. Hoppe, S.; Schelhaas, M.; Jaeger, V.; Liebig, T.; Petermann, P.; Knebel-Mörsdorf, D. Early Herpes Simplex Virus Type 1 Infection Is Dependent on Regulated Rac1/Cdc42 Signalling in Epithelial MDCKII Cells. *J. Gen. Virol.* **2006**, *87*, 3483–3494, doi:10.1099/vir.0.82231-0.
 63. Zamudio-Meza, H.; Castillo-Alvarez, A.; González-Bonilla, C.; Meza, I. Cross-Talk between Rac1 and Cdc42 GTPases Regulates Formation of Filopodia Required for Dengue Virus Type-2 Entry into HMEC-1 Cells. *J. Gen. Virol.* **2009**, *90*, 2902–2911, doi:10.1099/vir.0.014159-0.
 64. Frampton, A.R.; Uchida, H.; von Einem, J.; Goins, W.F.; Grandi, P.; Cohen, J.B.; Osterrieder, N.; Glorioso, J.C. Equine Herpesvirus Type 1 (EHV-1) Utilizes Microtubules, Dynein, and ROCK1 to Productively Infect Cells. *Vet. Microbiol.* **2010**, *141*, 12–21, doi:10.1016/j.vetmic.2009.07.035.
 65. Wang, J.-L.; Zhang, J.-L.; Chen, W.; Xu, X.-F.; Gao, N.; Fan, D.-Y.; An, J. Roles of Small GTPase Rac1 in the Regulation of Actin Cytoskeleton during Dengue Virus Infection. *PLoS Negl. Trop. Dis.* **2010**, *4*, e809, doi:10.1371/journal.pntd.0000809.
 66. Zhang, J.; Wu, N.; Gao, N.; Yan, W.; Sheng, Z.; Fan, D.; An, J. Small G Rac1 Is Involved in Replication Cycle of Dengue Serotype 2 Virus in EAhy926 Cells via the Regulation of Actin Cytoskeleton. *Sci. China Life Sci.* **2016**, *59*, 487–494, doi:10.1007/s11427-016-5042-5.
 67. Fernandes, J.J.; Atreya, K.B.; Desai, K.M.; Hall, R.E.; Patel, M.D.; Desai, A.A.; Benham, A.E.; Mable, J.L.; Straessle, J.L. A Dominant Negative Form of Rac1 Affects Myogenesis of Adult Thoracic Muscles in *Drosophila*. *Dev. Biol.* **2005**, *285*, 11–27, doi:10.1016/j.ydbio.2005.05.040.
 68. Akeda, Y.; Kodama, T.; Kashimoto, T.; Cantarelli, V.; Horiguchi, Y.; Nagayama, K.; Iida, T.; Honda, T. Dominant-Negative Rho, Rac, and

- Cdc42 Facilitate the Invasion Process of *Vibrio Parahaemolyticus* into Caco-2 Cells. *Infect. Immun.* **2002**, *70*, 970–973, doi:10.1128/IAI.70.2.970-973.2002.
69. Cuartas-López, A.M.; Hernández-Cuellar, C.E.; Gallego-Gómez, J.C. Disentangling the Role of PI3K/Akt, Rho GTPase and the Actin Cytoskeleton on Dengue Virus Infection. *Virus Res.* **2018**, *256*, 153–165, doi:10.1016/j.virusres.2018.08.013.
 70. Johnson, F.B.; Fenn, L.B.; Owens, T.J.; Faucheux, L.J.; Blackburn, S.D. Attachment of Bovine Parvovirus to Sialic Acids on Bovine Cell Membranes. *J. Gen. Virol.* **2004**, *85*, 2199–2207, doi:10.1099/vir.0.79899-0.
 71. Summerford, C.; Bartlett, J.S.; Samulski, R.J. AVβ5 Integrin: A Co-Receptor for Adeno-Associated Virus Type 2 Infection. *Nat. Med.* **1999**, *5*, 78–82, doi:10.1038/4768.
 72. Sanlioglu, S.; Benson, P.K.; Yang, J.; Atkinson, E.M.; Reynolds, T.; Engelhardt, J.F. Endocytosis and Nuclear Trafficking of Adeno-Associated Virus Type 2 Are Controlled by Rac1 and Phosphatidylinositol-3 Kinase Activation. *J. Virol.* **2000**, *74*, 9184–9196, doi:10.1128/JVI.74.19.9184-9196.2000.
 73. Ueda, M.; Daidoji, T.; Du, A.; Yang, C.-S.; Ibrahim, M.S.; Ikuta, K.; Nakaya, T. Highly Pathogenic H5N1 Avian Influenza Virus Induces Extracellular Ca²⁺ Influx, Leading to Apoptosis in Avian Cells. *J. Virol.* **2010**, *84*, 3068–3078, doi:10.1128/JVI.01923-09.
 74. Vanhaesebroeck, B.; Stephens, L.; Hawkins, P. PI3K Signalling: The Path to Discovery and Understanding. *Nat. Rev. Mol. Cell Biol.* **2012**, *13*, 195–203, doi:10.1038/nrm3290.
 75. Alberts, B.; Johnson, A.; Lewis, J.; Raff, M.; Roberts, K.; Walter, P. *Molecular Biology of the Cell*, 4th ed.; Garland Science, 2002; ISBN 978-0-8153-3218-3.
 76. van Meer, G.; Voelker, D.R.; Feigenson, G.W. Membrane Lipids: Where They Are and How They Behave. *Nat. Rev. Mol. Cell Biol.* **2008**, *9*, 112–124, doi:10.1038/nrm2330.
 77. Doherty, G.J.; McMahon, H.T. Mechanisms of Endocytosis. *Annu. Rev. Biochem.* **2009**, *78*, 857–902, doi:10.1146/annurev.biochem.78.0813.07.110540.
 78. Chen, E.H.; Olson, E.N. Unveiling the Mechanisms of Cell-Cell Fusion. *Science* **2005**, *308*, 369–373, doi:10.1126/science.1104799.
 79. Eitzen, G. Actin Remodeling to Facilitate Membrane Fusion. *Biochim. Biophys. Acta BBA - Mol. Cell Res.* **2003**, *1641*, 175–181, doi:10.1016/S0167-4889(03)00087-9.
 80. Zhang, C.; Zhu, S.; Wei, L.; Yan, X.; Wang, J.; Quan, R.; She, R.; Hu, F.; Liu, J. Recombinant Flagellin-Porcine Circovirus Type 2 Cap Fusion Protein Promotes Protective Immune Responses in Mice. *PLoS ONE* **2015**, *10*, e0129617, doi:10.1371/journal.pone.0129617.
 81. Mercer, J. Viral Apoptotic Mimicry Party: P.S. Bring Your Own Gas6. *Cell Host Microbe* **2011**, *9*, 255–257, doi:10.1016/j.chom.2011.04.002.
 82. de Freitas Balanco, J.M.; Costa Moreira, M.E.; Bonomo, A.; Bozza, P.T.; Amarante-Mendes, G.; Pirmez, C.; Barcinski, M.A. Apoptotic Mimicry by an Obligate Intracellular Parasite Downregulates Macrophage Microbicidal Activity. *Curr. Biol.* **2001**, *11*, 1870–1873, doi:10.1016/S0960-9822(01)00563-2.
 83. Amara, A.; Mercer, J. Viral Apoptotic Mimicry. *Nat. Rev. Microbiol.* **2015**, *13*, 461–469, doi:10.1038/nrmicro3469.
 84. Buchmann, J.P.; Holmes, E.C. Cell Walls and the Convergent Evolution of the Viral Envelope. *Microbiol. Mol. Biol. Rev.* **2015**, *79*, 403–418, doi:10.1128/MMBR.00017-15.
 85. Zimmerberg, J.; Chernomordik, L.V. Membrane Fusion. *Adv. Drug Deliv. Rev.* **1999**, *38*, 197–205, doi:10.1016/S0169-409X(99)00029-0.
 86. Leikin, S.L.; Kozlov, M.M.; Chernomordik, L.V.; Markin, V.S.; Chizmadzhev, Y.A. Membrane Fusion: Overcoming of the Hydration Barrier and Local Restructuring. *J. Theor.*

- Biol.* **1987**, *129*, 411–425, doi:10.1016/S0022-5193(87)80021-8.
87. White, J.M.; Whittaker, G.R. Fusion of Enveloped Viruses in Endosomes. *Traffic* **2016**, *17*, 593–614, doi:10.1111/tra.12389.
 88. Harrison, S.C. Viral Membrane Fusion. *Nat. Struct. Mol. Biol.* **2008**, *15*, 690–698, doi:10.1038/nsmb.1456.
 89. Harrison, S.C. Viral Membrane Fusion. *Virology* **2015**, *479–480*, 498–507, doi:10.1016/j.virol.2015.03.043.
 90. Shmulevitz, M.; Duncan, R. A New Class of Fusion-Associated Small Transmembrane (FAST) Proteins Encoded by the Non-Enveloped Fusogenic Reoviruses. *EMBO J.* **2000**, *19*, 902–912, doi:10.1093/emboj/19.5.902.
 91. Weed, D.J.; Nicola, A.V. Herpes Simplex Virus Membrane Fusion. *Adv. Anat. Embryol. Cell Biol.* **2017**, *223*, 29–47, doi:10.1007/978-3-319-53168-7_2.
 92. Cole, N.L.; Grose, C. Membrane Fusion Mediated by Herpesvirus Glycoproteins: The Paradigm of Varicella-Zoster Virus. *Rev. Med. Virol.* **2003**, *13*, 207–222, doi:10.1002/rmv.377.
 93. Markosyan, R.M.; Miao, C.; Zheng, Y.-M.; Melikyan, G.B.; Liu, S.-L.; Cohen, F.S. Induction of Cell-Cell Fusion by Ebola Virus Glycoprotein: Low PH Is Not a Trigger. *PLOS Pathog.* **2016**, *12*, e1005373, doi:10.1371/journal.ppat.1005373.
 94. Bornholdt, Z.A.; Ndungo, E.; Fusco, M.L.; Bale, S.; Flyak, A.I.; Crowe, J.E.; Chandran, K.; Saphire, E.O. Host-Primed Ebola Virus GP Exposes a Hydrophobic NPC1 Receptor-Binding Pocket, Revealing a Target for Broadly Neutralizing Antibodies. *mBio* **2016**, *7*, doi:10.1128/mBio.02154-15.
 95. Podbilewicz, B. Virus and Cell Fusion Mechanisms. *Annu. Rev. Cell Dev. Biol.* **2014**, *30*, 111–139, doi:10.1146/annurev-cellbio-101512-122422.
 96. Raghu, H.; Sharma-Walia, N.; Veettil, M.V.; Sadagopan, S.; Caballero, A.; Sivakumar, R.; Varga, L.; Bottero, V.; Chandran, B. Lipid Rafts of Primary Endothelial Cells Are Essential for Kaposi's Sarcoma-Associated Herpesvirus/Human Herpesvirus 8-Induced Phosphatidylinositol 3-Kinase and RhoA-GTPases Critical for Microtubule Dynamics and Nuclear Delivery of Viral DNA but Dispensable for Binding and Entry. *J. Virol.* **2007**, *81*, 7941–7959, doi:10.1128/JVI.02848-06.
 97. Lingwood, D.; Simons, K. Lipid Rafts As a Membrane-Organizing Principle. *Science* **2010**, *327*, 46–50, doi:10.1126/science.1174621.
 98. Simons, K.; Toomre, D. Lipid Rafts and Signal Transduction. *Nat. Rev. Mol. Cell Biol.* **2000**, *1*, 31–39, doi:10.1038/35036052.
 99. Erwig, L.-P.; Henson, P.M. Clearance of Apoptotic Cells by Phagocytes. *Cell Death Differ.* **2008**, *15*, 243–250, doi:10.1038/sj.cdd.4402184.
 100. Wood, W.; Turmaine, M.; Weber, R.; Camp, V.; Maki, R.A.; McKercher, S.R.; Martin, P. Mesenchymal Cells Engulf and Clear Apoptotic Footplate Cells in Macrophageless PU.1 Null Mouse Embryos. *Development* **2000**, *127*, 5245–5252.
 101. Zaitseva, E.; Zaitsev, E.; Melikov, K.; Arakelyan, A.; Marin, M.; Villasmil, R.; Margolis, L.B.; Melikyan, G.B.; Chernomordik, L.V. Fusion Stage of HIV-1 Entry Depends on Virus-Induced Cell Surface Exposure of Phosphatidylserine. *Cell Host Microbe* **2017**, *22*, 99-110.e7, doi:10.1016/j.chom.2017.06.012.
 102. Maitani, Y.; Ishigaki, K.; Nakazawa, Y.; Aragane, D.; Akimoto, T.; Iwamizu, M.; Kai, T.; Hayashi, K. Polyethylenimine Combined with Liposomes and with Decreased Numbers of Primary Amine Residues Strongly Enhanced Therapeutic Antiviral Efficiency against Herpes Simplex Virus Type 2 in a Mouse Model. *J. Controlled Release* **2013**, *166*, 139–146, doi:10.1016/j.jconrel.2012.12.027.
 103. Tahara, K.; Kobayashi, M.; Yoshida, S.; Onodera, R.; Inoue, N.; Takeuchi, H. Effects of Cationic Liposomes with Stearylamine against Virus Infection. *Int. J. Pharm.* **2018**,

- 543, 311–317,
doi:10.1016/j.ijpharm.2018.04.001.
104. Ellis, S.; Mellor, H. The Novel Rho-Family GTPase Rif Regulates Coordinated Actin-Based Membrane Rearrangements. *Curr. Biol.* **2000**, *10*, 1387–1390, doi:10.1016/S0960-9822(00)00777-6.
105. Jin, M.; Guan, C.; Jiang, Y.; Chen, G.; Zhao, C.; Cui, K.; Song, Y.; Wu, C.; Poo, M.; Yuan, X. Ca²⁺-Dependent Regulation of Rho GTPases Triggers Turning of Nerve Growth Cones. *J. Neurosci.* **2005**, *25*, 2338–2347, doi:10.1523/JNEUROSCI.4889-04.2005.
106. Kreuger, J.; Spillmann, D.; Li, J.; Lindahl, U. Interactions between Heparan Sulfate and Proteins: The Concept of Specificity. *J. Cell Biol.* **2006**, *174*, 323–327, doi:10.1083/jcb.200604035.
107. Eskandarynasab, M.; Doustimotlagh, A.H.; Takzaree, N.; Etemad-Moghadam, S.; Alaeddini, M.; Dehpour, A.R.; Goudarzi, R.; Partoazar, A. Phosphatidylserine Nanoliposomes Inhibit Glucocorticoid-Induced Osteoporosis: A Potential Combination Therapy with Alendronate. *Life Sci.* **2020**, *257*, 118033, doi:10.1016/j.lfs.2020.118033.
108. Fan, D.; Bucana, C.D.; O'Brian, C.A.; Zwelling, L.A.; Seid, C.; Fidler, I.J. Enhancement of Murine Tumor Cell Sensitivity to Adriamycin by Presentation of the Drug in Phosphatidylcholine-Phosphatidylserine Liposomes. *Cancer Res.* **1990**, *50*, 3619–3626.
109. Tomizawa, H.; Aramaki, Y.; Fujii, Y.; Kara, T.; Suzuki, N.; Yachi, K.; Kikuchi, H.; Tsuchiya, S. Uptake of Phosphatidylserine Liposomes by Rat Peyer's Patches Following Intraluminal Administration. *Pharm. Res.* **1993**, *10*, 549–552, doi:10.1023/A:1018945902276.
110. Veettil, M.V.; Sharma-Walia, N.; Sadagopan, S.; Raghu, H.; Sivakumar, R.; Naranatt, P.P.; Chandran, B. RhoA-GTPase Facilitates Entry of Kaposi's Sarcoma-Associated Herpesvirus into Adherent Target Cells in a Src-Dependent Manner. *J. Virol.* **2006**, *80*, 11432–11446, doi:10.1128/JVI.01342-06.
111. Kumar, D.; Lassar, A.B. The Transcriptional Activity of Sox9 in Chondrocytes Is Regulated by RhoA Signaling and Actin Polymerization. *Mol. Cell. Biol.* **2009**, *29*, 4262–4273, doi:10.1128/MCB.01779-08.
112. Anderson, B.R.; Karikó, K.; Weissman, D. Nucleofection Induces Transient EIF2 α Phosphorylation by GCN2 and PERK. *Gene Ther.* **2013**, *20*, 136–142, doi:10.1038/gt.2012.5.
113. McMahon, C.; Baier, A.S.; Pascolutti, R.; Wegrecki, M.; Zheng, S.; Ong, J.X.; Erlandson, S.C.; Hilger, D.; Rasmussen, S.G.F.; Ring, A.M.; et al. Yeast Surface Display Platform for Rapid Discovery of Conformationally Selective Nanobodies. *Nat. Struct. Mol. Biol.* **2018**, *25*, 289–296, doi:10.1038/s41594-018-0028-6.
114. Yang, S.; Guo, C.; Li, Y.; Guo, J.; Xiao, J.; Qing, Z.; Li, J.; Yang, R. A Ratiometric Two-Photon Fluorescent Cysteine Probe with Well-Resolved Dual Emissions Based on Intramolecular Charge Transfer-Mediated Two-Photon-FRET Integration Mechanism. *ACS Sens.* **2018**, *3*, 2415–2422, doi:10.1021/acssensors.8b00919.
115. Shcherbakova, D.M.; Cox Cammer, N.; Huisman, T.M.; Verkhusha, V.V.; Hodgson, L. Direct Multiplex Imaging and Optogenetics of Rho GTPases Enabled by Near-Infrared FRET. *Nat. Chem. Biol.* **2018**, *14*, 591–600, doi:10.1038/s41589-018-0044-1.

Zusammenfassung

Neue Erkenntnisse über die Rolle von Phospholipiden und kleinen GTPasen in der molekularen Pathogenese von equinen Herpesviren

Die Equinen Herpesviren Typ 1 (EHV-1) und Typ 4 (EHV-4) sind eng verwandte Viren, die wichtige Unterschiede in den wichtigsten molekularen Aspekten der Infektion aufweisen. EHV-1 kann im Gegensatz zu EHV-4 nach einer gH-Integrin-Wechselwirkung eine Signalkaskade in der Wirtszelle induzieren, die zur Exposition von Phosphatidylserin (PS) auf der extraplasmatischen Seite der Plasmamembran führt und für die Fusion an der Plasmamembran erforderlich ist. Um zu bewerten, welche Rolle die Exposition von PS auf der extraplasmatischen Seite der Plasmamembran im Falle einer EHV-1-Infektion spielt, haben wir untersucht, welche Auswirkungen Lipide mit positiver, natürlicher oder negativer Ladung auf die EHV-1-Infektion in der Zellkultur haben. Wir fanden heraus, dass Liposomen, die negativ geladenes PS oder positiv geladenes DOTAP enthielten, die EHV-1-Infektion hemmten, während neutrales Phosphatidylcholin (PC) keine Wirkung hatte. Die Hemmung der Infektion durch PS ist dosisabhängig und vorübergehend. Eine Verringerung der Infektion kann auf die Wechselwirkung zwischen den Lipidvesikeln und dem Viruspartikel selbst zurückgeführt werden. Die starke Virusinteraktion wurde sowohl mit DOTAP als auch mit PS identifiziert, gemessen durch Mikroskopie mit großen unilamellaren Vesikeln (LUVs) und riesigen unilamellaren Vesikeln (GUVs) sowie durch Oberflächenplasmonresonanz (SPR) -Analyse von EHV-1-Wechselwirkungen mit Liposomen aus neutralen, kationischen oder anionischen Phospholipiden, in beiden Fällen war die Wechselwirkung mit kationischem DOTAP stärker als mit PS. Dies legt nahe, dass die PS-induzierte Hemmung der Infektion spezifischer ist als die von DOTAP. Möglicherweise wird die PS-Hemmung durch spezifische Wechselwirkung mit den viralen Glykoproteinen gH / gL und gB vermittelt, während DOTAP auf weniger spezifische Weise wirken kann, indem es die viralen Partikel umgibt und abschirmt.

Kleine GTPasen sind allgegenwärtige Signalproteine, die stromabwärts der EHV-1-induzierten Calciumfreisetzung aktiviert werden könnten. Um zu untersuchen, ob kleine GTPasen eine Rolle bei der EHV-1-Infektion spielen, infizierten wir mit kleinen GTPase-Inhibitoren behandelte Zellen. Wir fanden heraus, dass die Aktivierung kleiner GTPasen für die EHV-1-Infektion bei den Schritten nach dem Eintritt unter Verwendung des Fluoreszenzresonanzenergietransfers (FRET) erforderlich ist identifizierten, dass EHV-1 in der Lage ist, die Aktivierung von Rac1 und Cdc42 in wenigen Minuten nach Kontakt mit der Zelle zu induzieren, obwohl diese Hypothese aufgrund technischer Einschränkungen mit alternativen Experimenten nicht bestätigt werden konnte. Die Feststellung, dass EHV-1 mit Inhibitor behandelten Zellen eindringen kann und dass eine Infektion durch Verdünnung des Inhibitormediums gerettet werden kann, zeigt, dass kleine GTPasen für den Viruseintritt selbst nicht essentiell sind. Es wurde festgestellt, dass kleine GTPasen Rac1 und Cdc42 für die EHV-1-induzierte Acetylierung von Tubulin erforderlich sind, was mit der Feststellung übereinstimmt, dass mit Rac1- oder Cdc42-Inhibitor behandelte Zellen das Virus schlechter an den Zellkern abgeben und verringerte Zellraten aufweisen Zellfusion, gemessen durch Plaquedurchmesser-Assay und Luciferase-Fusionsassay. Um zu untersuchen, ob die kleinen GTPasen stromabwärts des durch gH-Integration induzierten Weges aktiviert werden, wurde eine Anzahl von nicht mit Integrin interagierenden Viren wie EHV-4, EHV-1 gH4 und EHV-1 gHS440A durch kleine GTPase beeinflusst Inhibitoren, was darauf hindeutet, dass kleine GTPasen Rac1 und Cdc42 auf irgendeine Weise orthogonal zum zuvor beschriebenen gH-Integrationsweg aktiviert werden.

Zusammengenommen legen die Daten nahe, dass PS eine spezifische Rolle bei der EHV-1-Infektion spielen könnte und dass die Aktivierung der kleinen GTPasen Rac1 und Cdc42 für die Infektion von EHV-1 und EHV-4 wichtig ist. In EHV-1 spielen Rac1 und Cdc42 eine Rolle beim intrazellulären Transport des Viruspartikels durch Acetylierung von Tubulin und erleichtern die Ausbreitung von Zelle zu Zelle, ohne den Viruseintritt zu beeinflussen.

Summary

Equine herpesvirus type 1 (EHV-1) and equine herpesvirus type 4 (EHV-4) are closely related viruses that have important differences in the key molecular aspects of infection. EHV-1 unlike EHV-4, can induce signaling cascade inside the host cell following gH-integrin interaction, that leads to exposure of phosphatidylserine (PS) in the outer leaflet of the plasma membrane, and is required for fusion at the plasma membrane. To evaluate what role exposure of PS to the outer leaflet of the plasma membrane plays in case of EHV-1 infection we investigated what effects lipids with positive, natural or negative charge had on EHV-1 infection in cell culture. We found that liposomes containing negatively charged PS or positively charged DOTAP inhibited EHV-1 infection, while neutral phosphatidylcholine (PC) had no effect. Inhibition of infection with PS was dose dependent, decreased with time, and transient. Reduction in infection can be attributed to the interaction between the lipid vesicles and the virus particle itself. The strong virus interaction was identified with both DOTAP and PS, as measured with microscopy with large unilamellar vesicles (LUVs) and giant unilamellar vesicles (GUVs) as well as Surface plasmon resonance (SPR) analysis of EHV-1 interactions with model membrane composed of neutral, cationic, or anionic phospholipids, in both cases interaction with cationic DOTAP was stronger than with PS. This suggests that PS induced inhibition of infection is more specific, than that of DOTAP. Perhaps PS inhibition is mediated through specific interaction with viral glycoproteins gH/gL and gB, while DOTAP can act in a less specific manner, by surrounding and shielding the viral particle.

Small GTPases are ubiquitous signaling proteins, that could be activated downstream of EHV-1 induced calcium release. To investigate whether small GTPases play role in EHV-1 infection we infected cell treated with small GTPase inhibitors, we found that activation of small GTPases is required for EHV-1 infection at the post entry steps, using fluorescence resonance energy transfer (FRET) we identified that EHV-1 is activating Rac1 and Cdc42 in a few minutes after contact with the cell, although due to technical limitations this hypothesis could not be confirmed with alternative experiments. The finding that EHV-1 can penetrate inhibitor treated cells and that infection can be rescued through dilution of the inhibitor media, indicates that small GTPases are not essential for the virus entry itself. It was identified that small GTPases Rac1 and Cdc42 are required for EHV-1 induced acetylation of tubulin, which is consistent with the finding that Rac1 or Cdc42 inhibitor treated cells are worse at delivering the virus to the nucleus, and have reduced rates of cell-to-cell fusion, as measured by plaque diameter assay, and luciferase fusion assay. In order to examine if the small GTPases are being activated downstream from gH integrin induced pathway, number of non-integrin interacting viruses were employed, such as EHV-4, EHV-1 gH4 and EHV-1 gHS440A, were affected by small GTPase inhibitors, suggesting that small GTPases Rac1 and Cdc42 are activated in some way orthogonal from previously described gH integrin pathway.

Taken together, the data suggests that PS could play a specific role in the EHV-1 infection, and that activation of small GTPases Rac1 and Cdc42 is important for infection of both EHV-1 and EHV-4. In EHV-1 Rac1 and Cdc42 play role in intracellular transport of the virus particle through acetylation of tubulin, and facilitate cell to cell spread, while not affecting the virus entry.

Publication List

Kolyvushko O, Latzke J, Dahmani I, Osterrieder N, Chiantia S, Azab W

Differentially-Charged Liposomes Interact with Alphaherpesviruses and Interfere with Virus Entry.

Pathogens **2020**, 9(5), 359

<https://doi.org/10.3390/pathogens9050359>

Kolyvushko O, Kelch MA, Osterrieder N, Azab W

Equine Alphaherpesviruses Require Activation of the Small GTPases Rac1 and Cdc42 for Intracellular Transport.

Microorganisms **2020**, 8(7), 1013

<https://doi.org/10.3390/microorganisms8071013>

Details of funding sources

The work was financially supported by Deutscher Akademischer Austauschdienst and Deutsche Forschungsgemeinschaft.

There is no conflict of interest due to financial support of the work.

Acknowledgments

I am deeply grateful to Prof. Dr. Klaus Osterrieder, the head of Institute of Virology, for giving me his supervision and the opportunity to work in his lab as a PhD student and as part of ZIBI graduate school to complete my study. Your inordinate experience always allowed to find the weak points in the argumentation or the methods chosen, which in turn helped us to strive for and achieve the best possible work we could do.

I would like to express special gratitude to my supervisor Dr. Walid Azab, who helped me to navigate the field of research in many ways.

I would like to thank Dr. Thorsten Wolff who generously agreed to be the part of my supervisory committee, for bringing external critical view to the supervision of my project and for reviewing and evaluating my thesis.

I would like to thank Ismail Dahmani and Salvatore Chiantia for our productive collaboration, Dr. Katharina Achazi from core facilities for her assistance and training on the CLSM SP8. Dr. Ankur Midha for kind support and proofreading the thesis.

My friends and colleges who have helped me tremendously through my work Ankur, Oleksandr, Pavul, Vivi, Mariia, Juliane, Mohamed, Sky, Vlad, Kolya, Shaal, Jador, Zalo, Michi and other people at the institute who contributed to creating productive, rigorous and comfortable environment at our meetings and in the labs in general. My loving family and all artist, workers and scientist who contributed to the development of civilization and science.

Selbständigkeitserklärung

Hiermit bestätige ich, dass ich die vorliegende Arbeit selbstständig angefertigt habe. Ich versichere, dass ich ausschließlich die angegebenen Quellen und Hilfen in Anspruch genommen habe.

Berlin, den 16.09.2020

Oleksandr Kolyvushko